

Fall 2000

# Glacial Chronology and Paleoclimatic Significance of Cirque Moraines near Mts Baker and Shuksan, North Cascade Range, WA

Robert A. (Robert Allen) Burrows  
*Western Washington University*

Follow this and additional works at: <https://cedar.wwu.edu/wwuet>



Part of the [Geology Commons](#)

---

## Recommended Citation

Burrows, Robert A. (Robert Allen), "Glacial Chronology and Paleoclimatic Significance of Cirque Moraines near Mts Baker and Shuksan, North Cascade Range, WA" (2000). *WWU Graduate School Collection*. 826.  
<https://cedar.wwu.edu/wwuet/826>

This Masters Thesis is brought to you for free and open access by the WWU Graduate and Undergraduate Scholarship at Western CEDAR. It has been accepted for inclusion in WWU Graduate School Collection by an authorized administrator of Western CEDAR. For more information, please contact [westerncedar@wwu.edu](mailto:westerncedar@wwu.edu).

**GLACIAL CHRONOLOGY AND PALEOCLIMATIC SIGNIFICANCE  
OF CIRQUE MORAINES NEAR MTS BAKER AND SHUKSAN,  
NORTH CASCADE RANGE, WA**

BY

ROBERT A. BURROWS

Accepted in Partial Completion  
of the Requirements for the Degree  
Master of Science

---

Moheb A. Ghali, Dean of the Graduate School

**ADVISORY COMMITTEE**

---

Chair, Dr. Douglas H. Clark

---

Director, Dr. Don J. Easterbrook

---

Dr. Andrew J. Bach

---

Dr. Thor A. Hansen

### MASTER'S THESIS

In presenting this thesis in partial fulfillment of the requirements for a master's degree at Western Washington University, I agree that the Library shall make its copies freely available for inspection. I further agree that copying of this thesis in whole or in part is allowable only for scholarly purposes. It is understood however, that any copying or publication of this thesis for commercial purposes, or for financial gain, shall not be allowed without my written permission.

Signature 

Date November 17, 2000

## MASTER'S THESIS

In presenting this thesis in partial fulfillment of the requirements for a master's degree at Western Washington University, I grant to Western Washington University the non-exclusive royalty-free right to archive, reproduce, distribute, and display the thesis in any and all forms, including electronic format, via any digital library mechanisms maintained by WWU.

I represent and warrant this is my original work and does not infringe or violate any rights of others. I warrant that I have obtained written permissions from the owner of any third party copyrighted material included in these files.

I acknowledge that I retain ownership rights to the copyright of this work, including but not limited to the right to use all or part of this work in future works, such as articles or books.

Library users are granted permission for individual, research and non-commercial reproduction of this work for educational purposes only. Any further digital posting of this document requires specific permission from the author.

Any copying or publication of this thesis for commercial purposes, or for financial gain, is not allowed without my written permission.

Name: Robert A. Burrows

Signature: \_\_\_\_\_

Date: 6/19/2018

**GLACIAL CHRONOLOGY AND PALEOCLIMATIC  
SIGNIFICANCE OF CIRQUE MORAINES NEAR MTS BAKER AND  
SHUKSAN, NORTH CASCADE RANGE, WA**

A Thesis  
Presented to  
The Faculty of  
Western Washington University

In Partial Fulfillment  
of the Requirements for the Degree  
Master of Science

by  
Robert A. Burrows  
November 2000

## Abstract

Moraines of at least two ages occur in alpine cirques near the Mt. Baker volcano in the North Cascades Range, WA. The south Swift Creek cirque preserves a distinct sequence of moraines representing the two primary age groups. In south Swift Creek cirque, the upper group of moraines (1450-1550 m) has little soil development and vegetation. Increment borings of the oldest trees growing on the upper moraines suggest that they were formed between the late 1800s and early 1900s. This age range correlates with numerous late Little Ice Age (LIA) moraines elsewhere in the Cascade Range. The south Swift Creek cirque Little Ice Age moraines have a reconstructed equilibrium line altitude (ELA) of 1550 m.

The lower moraines in south Swift Creek cirque are overlain by and older than Mazama ash (6800  $^{14}\text{C}$  yrs B.P.). In addition, a date of  $9560 \pm 50$   $^{14}\text{C}$  yrs B.P. on charcoal from the base of a bog just outside the lowermost moraine provides a closer minimum limiting age. A date of  $9350 \pm 180$   $^{14}\text{C}$  yrs B.P. from a branch near the base of a bog behind the uppermost pre-Mazama moraine indicates that trees were growing at the edge of the cirque by that time. Other cirque moraines in Swift Creek and Shuksan Creek, which are similar in extent to the older group of south Swift Creek cirque moraines, are constrained only as older than Mazama ash.

Moraines several kilometers distant and similar in altitude and geomorphic position to the pre-Mazama moraines of south Swift Creek cirque occupy the mouth of Bagley Creek cirque and dam Highwood Lake. A basal radiocarbon date from a Highwood Lake sediment core demonstrates that deglaciation occurred before  $9410 \pm 50$   $^{14}\text{C}$  yrs B.P.

The similar limiting radiocarbon dates and similar reconstructed equilibrium line altitudes (ELAs) of  $\sim 1400$  m for pre-Mazama moraines in both Bagley Creek cirque and south Swift Creek cirque indicates that they are correlative. Two dates with a mean of  $\sim 10,700$   $^{14}\text{C}$  yrs B.P. from charcoal layers in outwash associated with moraines 40 km down the North Fork Nooksack valley provide a maximum limiting age, constraining the Swift Creek and Bagley Creek moraines to the early Holocene or late Pleistocene (Kovanen and Easterbrook, 2001).

The minimum ages indicate that Bagley Creek cirque and south Swift Creek cirque moraines predate most of the early Holocene moraines on the south flank of Mt. Baker and probably correlate to the similar-scale McNeely II moraines near Mt. Rainier (Heine, 1998). However, the range of limiting dates (10,700 – 9600 <sup>14</sup>C yrs B.P.) allows an alternative correlation with the youngest Sumas moraines (younger than 10,250 <sup>14</sup>C yrs B.P.) from the remnant of the Cordilleran Ice Sheet on the Fraser Lowland (Kovanen and Easterbrook, in review-a).

The modern local ELA is estimated at 1640 m from small existing glaciers at the heads of south Swift Creek cirque and Bagley Creek cirque and a regional ELA of 1890 m based on northeast-to-northwest facing, modern glaciers near the study area. The difference ( $\Delta$ ELA) between the modern local and the south Swift Creek Little Ice Age ELAs is 75 m. The local ELA is used because local topographic effects that strongly influence mass balance and the ELA today probably also influenced the LIA glacier. The  $\Delta$ ELA between the regional ELA and the late-Pleistocene/early Holocene ELA in Swift Creek and Bagley Creek is ~ 490 m. The mean regional ELA is a more appropriate comparison for the earlier glacier positions because the glaciers were large enough at that time to have substantially reduced local topographic effects on mass balance and ELA.

Simple comparisons of modern climate at reconstructed ELAs with modern glacier ELA climate conditions suggest that in order to build the oldest moraines in south Swift Creek cirque and Bagley Creek cirque, ablation season temperature would have to decrease by 1.6-degrees C or winter precipitation would have to increase by 870 mm. Similarly, building the oldest LIA moraine in south Swift Creek cirque would require a 0.85-degree C decrease in ablation season temperature or a 440-mm accumulation season precipitation increase.

## **Acknowledgements**

I would like to wholeheartedly thank the following people who assisted in all aspects of the work that culminated in this thesis: My thesis committee; Doug Clark, Don Easterbrook, Andy Bach, and Thor Hansen; All the people that helped me in the field and office and just provided moral support; Jeff Laub, Sharon Gelinias, Anna Lookabill, Ryan Kopp, Richard Navus, Don and Nancy Burrows, Matt Burgess, Geoff Landis, Ingrid Enschede, Dylan Taylor, Holly Riffe, Brandie Theisen, Megan Demers, Joanie Lawrence, Tammy Fawcett, Eric Bilderback, Alex Feldy, Dori Kovanen, Paul Thomas, Bernie Housen, Rod Redfern, Denny O'brien, Mike Brown, Phyllis Gregoire, Kris Addis, Andrew Greene, Ann Buckley, Steve Schindler, Jeff Campbell, and Jon Riedel.

In addition I would like to acknowledge the following organizations that provided funding: National Science Foundation (through Don Easterbrook), Geological Society of America, GSA Quaternary and Geomorphology Division, The Mazamas, Western Washington University Graduate School and Department of Geology, and Sigma Xi.

## Table of Contents

Abstract .....	iv
Acknowledgements .....	vi
List of Figures and Tables .....	ix
Chapter 1 Introduction .....	1
The Study Area .....	1
Introduction to Research Problem.....	5
General Glacial History of Northwestern Washington .....	5
An early Holocene glacial advance in the North American Cordillera?.....	8
Climatic Setting.....	9
Vegetation .....	10
Chapter 2 Methods .....	11
Glacial Landform Mapping.....	11
Dendrochronology.....	11
Bog and Lake Coring .....	12
Radiocarbon Dating .....	13
Tephrochronology .....	13
Equilibrium Line Altitude and Paleoclimate Reconstruction Methods .....	14
Chapter 3 Swift Creek and Shuksan Creek Glacial Geology.....	15
Moraine Morphology and Stratigraphy.....	15
Sediment Cores and Basal Radiocarbon Dates .....	25
Radiocarbon Date Inconsistencies .....	30
Limiting Dates for the Cathedral Crag Tephra .....	33
Chapter 4 Bagley Creek .....	34
Moraine Morphology and Stratigraphy.....	39
Sediment Cores .....	42
Chapter 5 Interpretation and Chronology .....	52
Swift Creek and Shuksan Creek Glacial Chronology .....	52
Bagley Creek Glacial Chronology .....	56
Summary of Morainal Evidence .....	58
Chapter 6 Equilibrium Line Altitudes (ELAs) and Paleoclimatic Reconstructions .	60
The Modern ELA .....	61
ELA Reconstructions .....	65
$\Delta$ ELAs .....	65
Climate at Modern Glacier ELAs .....	70
Modern Climate at Calculated ELAs for Past Glaciers in the Study Area ...	74
Climate Shifts to Reestablish Reconstructed Glaciers .....	75

Chapter 7 Comparison with Other Studies.....	77
Little Ice Age.....	77
Early Holocene/Late Pleistocene .....	78
Chapter 8 Summary.....	80
The Moraine Record and Limiting Ages .....	80
ELA Reconstructions and $\Delta$ ELA .....	81
Paleoclimate Significance of Moraines.....	82
Comparison with Other Studies .....	82
References .....	84

## List of Figures and Tables

Chapter 1 Introduction	
Figure 1.1 Locator map and study area vicinity.....	2
Figure 1.2 Study area map showing cirques that were investigated by this study.....	3
Table 1.1 Late-Pleistocene and Holocene stratigraphy for western Washington and southwestern British Columbia.....	7
Chapter 3 Swift Creek and Shuksan Creek Glacial Geology	
Figure 3.1 Glacial deposit map for upper Swift Creek and upper Shuksan Creek.....	16
Figure 3.2 Air photo of upper Swift Creek and upper Shuksan Creek .....	17
Figure 3.3 View looking northeast into south Swift Creek Cirque .....	18
Figure 3.4 SSC glacier in the late summer.....	20
Figure 3.5 North Swift Creek Cirque .....	20
Figure 3.6 View looking southeast to HSC from Huntoon Point.....	23
Figure 3.7 View looking down at the HSC moraines from above .....	23
Figure 3.8 View looking south at LAC and NShC from Shuksan Arm.....	23
Figure 3.9 The esker on the floor of north Shuksan Creek Cirque .....	24
Figure 3.10 The view southeast looking down South Shuksan Creek Cirque .....	24
Figure 3.11 Swift Creek cores stratigraphy and fence diagrams.....	26
Table 3.1 Swift Creek cores radiocarbon dates.....	28
Figure 3.12 Core SC-7 site.....	29
Figure 3.13 Core SC-8 site.....	29
Table 3.2 Age differences between root fibers and those of charcoal and plant macrofossils .....	32
Chapter 4 Bagley Creek	
Figure 4.1 Glacial deposit and landform map of the Bagley Creek trough.....	35
Figure 4.2 Aerial oblique view of Heather Meadows and Bagley Creek looking up the valley to the southwest .....	36
Figure 4.3 Vertical air photo showing Bagley Creek and Heather Meadows .....	37
Figure 4.4 View looking west of Bagley Creek Cirque from Austin Pass.....	38
Figure 4.5 View looking northwest on lower Bagley Creek trench and end moraine complex .....	38
Figure 4.6 A whaleback on the valley floor of Bagley Creek trench.....	40
Figure 4.7 Road cut of upper Galena Camp lateral moraine.....	40
Figure 4.8 The pocket of drift below the Galena Camp moraines.....	41
Figure 4.9 The diamicton of the Picture Lake road cut.....	41
Figure 4.10 A road cut of till at the hairpin curve.....	43
Figure 4.11 Road cut of the Austin Pass moraine .....	43
Figure 4.12 The pocket of drift below Austin Pass.....	44
Figure 4.13 Highwood Lake, looking north .....	44
Figure 4.14 Highwood Lake core stratigraphy, magnetic susceptibility, and important radiocarbon dates from cores HL-6 and HL-7 .....	47

Figure 4.15 Comparison of magnetic susceptibility and loss on ignition results for core HL-3 .....	48
Table 4.1 Highwood Lake core radiocarbon dates.....	49
 Chapter 5 Interpretation and Chronology	
Figure 5.1 Swift Creek and Shuksan Creek glacier reconstructions .....	53
Figure 5.2 Correlation of Swift Creek cores and Highwood Lake core.....	55
Figure 5.3 Glacier reconstructions for Bagley Creek trough .....	57
 Chapter 6 Equilibrium Line Altitudes (ELAs) and Paleoclimatic Reconstructions	
Table 6.1 Modern ELAs of glaciers in the vicinity of the study area .....	64
Table 6.2 Calculated paleo-ELAs for the study area.....	64
Table 6.3 $\Delta$ ELAs for Swift Creek and Bagley Creek Glaciers .....	64
Figure 6.1 Swift Creek Little Ice Age glacier reconstruction .....	66
Figure 6.2 Swift Creek and Shuksan Creek glacier reconstructions based on the outermost moraines .....	67
Figure 6.3 Swift Creek Phase minimum glacier reconstruction.....	68
Figure 6.4 Bagley Creek Glacier Reconstruction for the Picture Lake moraines with a minimum limiting radiocarbon age of 9410 years B.P. ....	69
Table 6.4 Some ELAs and climatic parameters of glaciers that may serve as models for the reconstructed glaciers of this study .....	72
Table 6.5 Table showing modern climate conditions for various altitudes, which correspond to calculated past and modern ELAs .....	72
Figure 6.5 A comparison of modern glacier ELA climates (measured and estimated) with modern climates .....	73
Table 6.6 Ablation season temperature and accumulation season precipitation shifts from modern climate at past ELAs to a glacial climate.....	76

## Chapter 1 Introduction

### *The Study Area*

The North Cascade Range provides an excellent location to investigate recent alpine glaciation. The range occupies northwestern Washington and a small part of southwestern British Columbia and extends from Snoqualmie Pass in the south to the Fraser River in the north. High relief, rugged topography, and modest modern glaciation characterize the North Cascade Range. Precipitation decreases markedly across the range from west to east. High precipitation and thick forests and brush occur on the wet, west side of the range where the study area is located.

The study area lies in northwestern Washington between Mt. Baker (3287 m (10,781 ft)), a Quaternary stratovolcano, and Mt. Shuksan (2784 m (9131 ft)), a prominent thrust-sheet massif (Figure 1.1). The topography of the study area is dominated by the east-west trending ridges of Shuksan arm and Table Mountain and lesser, variably trending, subalpine/alpine ridges between 1070 and 1980 m altitude (3500 to 6500 feet) (Figure 1.2). The ridges and lower peaks were inundated to an upper altitude of ~2000 m (6600 feet) by the Cordilleran Ice Sheet during glacial maxima of the Pleistocene. Inundation by the Cordilleran ice sheet is indicated by numerous erratics from the last maximum (Easterbrook, 1963). Rounded ridges below ~2000 m are likely a result of repeated ice sheet glaciations. Well-developed cirques have been cut into the ridges and U-shaped valleys have been carved by past valley glacier erosion.

This study focuses on the glacial geomorphology in the eastern most headwaters of upper Swift Creek, upper Shuksan Creek, and upper Bagley Creek (Figure 1.2). Upper Swift Creek and upper Shuksan Creek are compound cirques. Each sub-cirque of the compound cirques is given a name (additionally, some are given acronyms, which are used in the figures and tables) based on its position within the drainage (Figure 1.2). In order to make the discussion easier for the reader to follow, full names of each cirque are used in the text with acronyms in parenthesis, because acronyms are used on figures. Swift Creek has four sub-cirques identified in this study: south Swift Creek cirque (SSC); north Swift Creek cirque (NSC); high Swift Creek cirque (HSC); and Austin Pass cirque. Shuksan Creek has

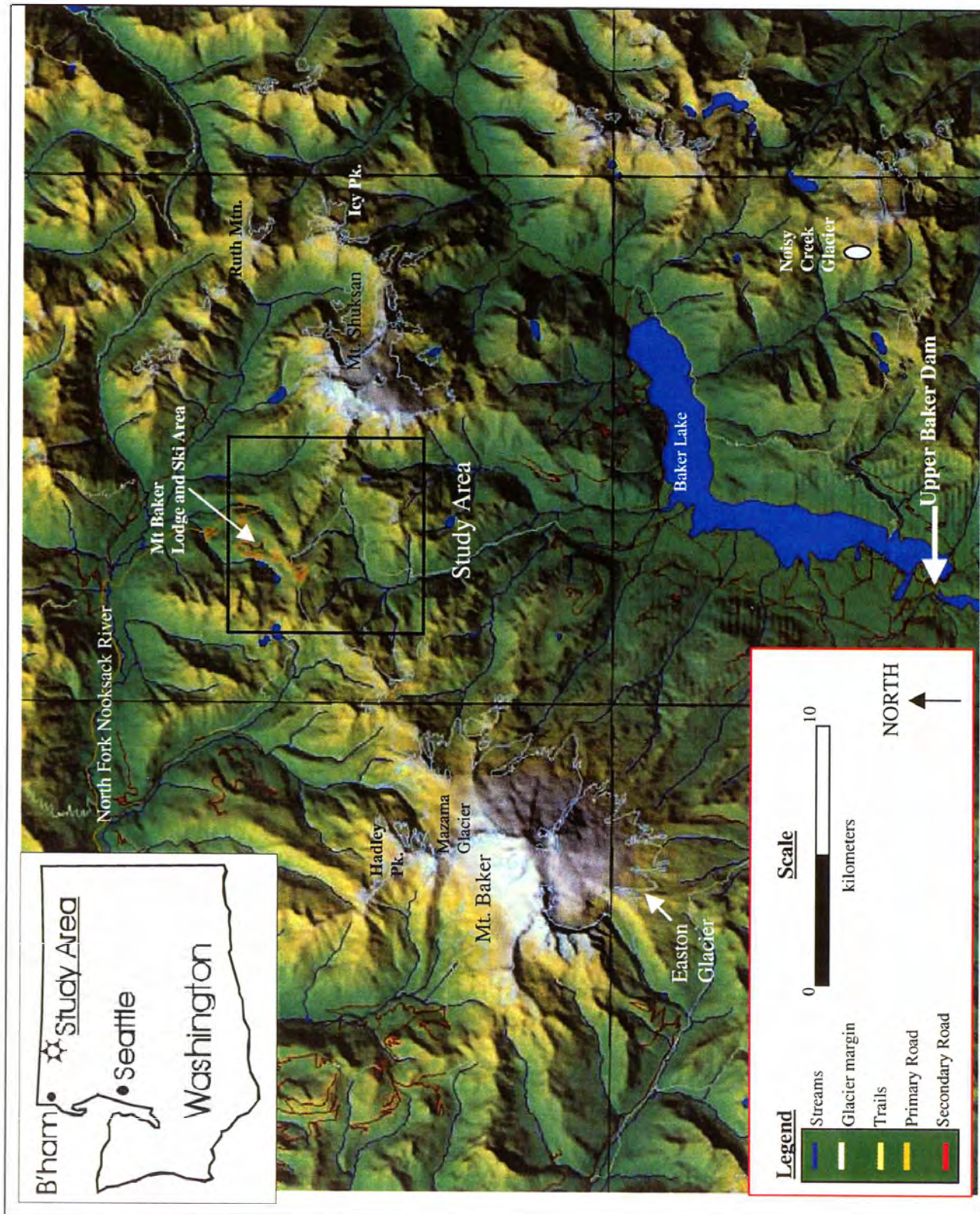


Figure 1.1 Locator map and study area and vicinity. Map rendering courtesy Donald Burrows from USGS DEM data.

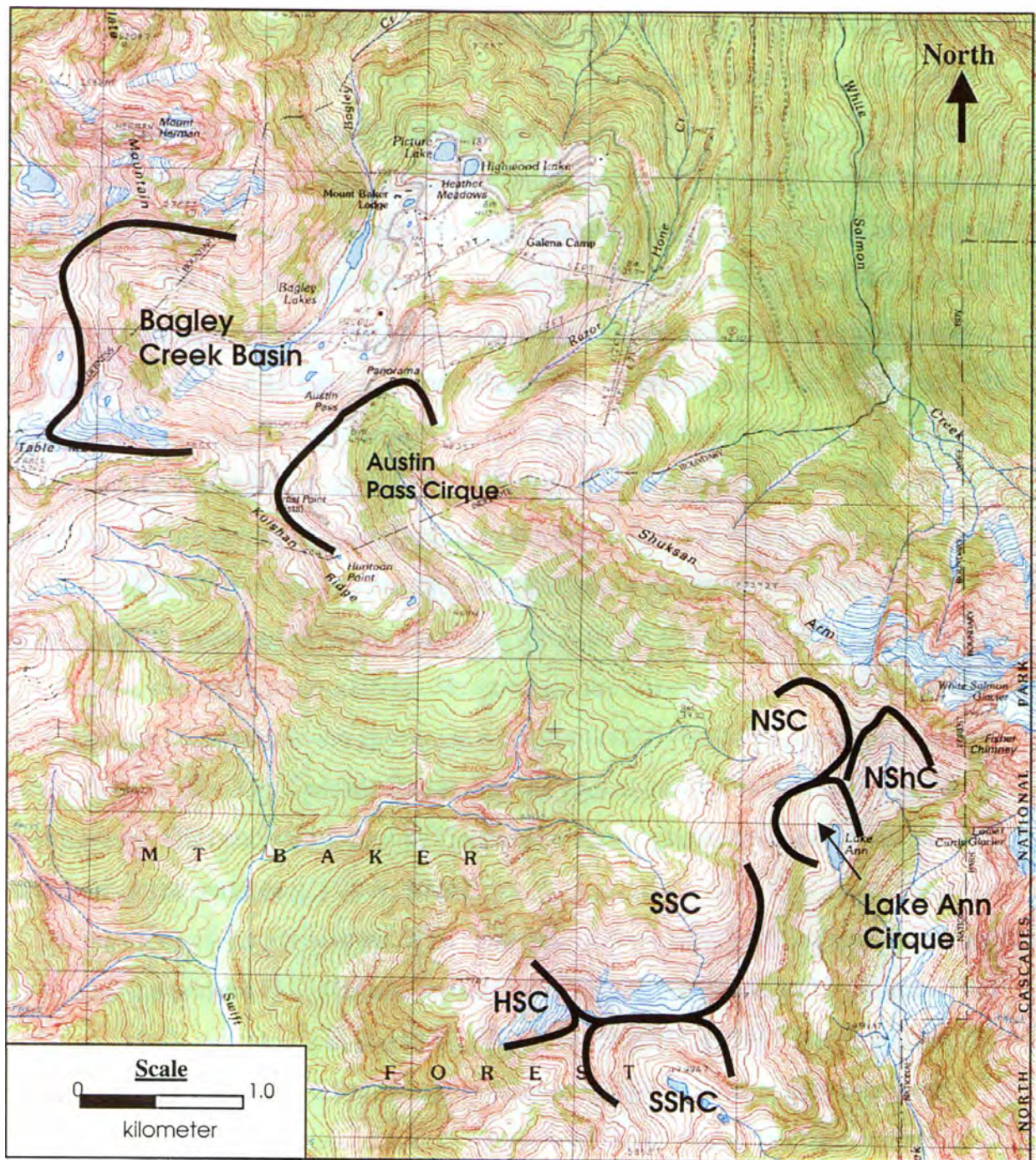


Figure 1.2 Study area map showing cirques that were investigated in this study. Cirque walls are outlined in black. NSC = north Swift Creek cirque, SSC = south Swift Creek cirque, HSC = high Swift Creek cirque, NShC = north Shuksan Creek cirque, SShC = south Shuksan Creek cirque. Source: Shuksan Arm USGS 7.5 minute Quadrangle 1989.

three sub-cirques identified in this study: north Shuksan Creek cirque (NShC); Lake Ann cirque; and south Shuksan Creek cirque (SShC). The cirque and upper valley of Bagley Creek is simply referred to as Bagley Creek cirque.

North Cascades glaciers and associated landforms are important for understanding late-Pleistocene and Holocene glacial history and climate change. The glaciers are close to the Pacific coast and therefore sensitive to weather patterns originating in the North Pacific (McCabe and Fountain, 1995). This study adds to the understanding of correlations and variability of the glacial history of the North Cascades and North American Cordillera. The North Cascades are unique in the western Cordillera of North America because of their relationship to the Pleistocene Cordilleran Ice Sheet. Although much of the range was inundated by Cordilleran ice at glacial maxima, the North Cascade Range was not a major source area for Cordilleran ice as were the Coast Ranges to the north. The western North Cascades preserve moraines of valley glaciation after retreat of the ice sheet (Kovanen, 1996; J. Riedel, personal comm., 1998). However, in the eastern North Cascades (the Methow drainage) Cordilleran ice appears to have downwasted with no subsequent valley glaciers (Waitt, 1972). The Cascade Range was not inundated by Cordilleran ice to the south of Cascade Pass and so a record of Pleistocene valley glaciation is preserved in the southern part of the range (e.g. Porter, 1976).

At the close of the Pleistocene, a last remnant of the Cordilleran ice sheet readvanced briefly to near the present U.S.-Canada border during the Sumas Stade and Younger Dryas (Easterbrook, 1963; Armstrong et al., 1965; Clague et al., 1997, 1998; Easterbrook and Kovanen, 1998; Kovanen and Easterbrook, in review-a). Climatic changes during the Sumas Stade, in which ice advanced almost to sea level in the Fraser lowland, probably influenced the timing and pattern of late Pleistocene alpine glaciation in the adjacent northwest North Cascades and the study area (Kovanen and Easterbrook, 2001).

### *Introduction to Research Problem*

The discovery of a set of striking moraines on aerial photographs in the upper Swift Creek valley initiated this thesis. These moraines and similar ones in Bagley Creek and Shuksan Creek valleys provide a distinct record of landscape and climate change since the last glacial maximum in the area. The moraines provide a means to compare the timing and extent of these changes with those elsewhere in the Cascade Range. Specifically, the six main goals of this study are:

- (1) to identify and map glacial landforms in the study area (concentrating on depositional landforms);
- (2) to determine close limiting ages for formation of moraines in the study area using dendrochronology and radiocarbon dating of organic matter in sediment cores of lakes and bogs adjacent to the moraines;
- (3) to determine if an early Holocene advance occurred in the study area.
- (4) to compare the glacial history of this area with the glacial history elsewhere in the Cascade Range;
- (5) to reconstruct margins and calculate the former equilibrium line altitudes (ELAs) of past glaciers in the study area (from map and field evidence) and compare reconstructed ELAs with modern ELAs;
- (6) to estimate past climate deviations (from modern climate) related to these glacial events, based on changes of ELA.

### *General Glacial History of Northwestern Washington*

Studies of glacial geology and analyses of pollen from all over the world first shaped concepts of climate change. Recently, ice cores from Antarctica and Greenland have yielded high-resolution paleoclimate records, which most notably show the variability and rapidity of past climate change (eg. Bender et al., 1994; Johnson et al., 1997; Meese et al., 1994; White et al., 1997). Paleoclimate in the Pacific Northwest generally fits into the global

framework (e.g. Mullineaux et al., 1965; Heller 1980; Easterbrook, 1992; Thomas, 1997; Porter and Swanson, 1998; Walker et al., 1999) (Table 1.1). The last glacial maximum of the region, named the Vashon Stade, was marked by the maximum extent of the Puget Lobe of the Cordilleran Ice Sheet (CIS). Soon after the maximum (~14,500 <sup>14</sup>C years B.P), the ice sheet abruptly and rapidly retreated (Mullineaux et al., 1965; Easterbrook, 1992; Porter and Swanson, 1998) and climate ameliorated during the Everson Interstade during which the northern Puget Lowland was flooded by marine water. The marine water floated the remaining ice, at which time the Everson glaciomarine drift was deposited (Armstrong et al., 1965). Multiple moraines and associated deposits of the Sumas Stade of the CIS in the Pacific Northwest indicate that the warming climate at the end of the Pleistocene was interrupted by a brief, return to near-glacial conditions. A piedmont glacier readvanced in the late Pleistocene on the Fraser Lowland of southwestern British Columbia and northwestern Washington, and deposited several large moraine and drift complexes (Kovanen and Easterbrook, in review-a). The readvance is known as the Sumas Stade of the Vashon Glaciation (Armstrong et al. 1965). Kovanen and Easterbrook (in review-a) recognize three primary moraine-building events of the Sumas Stade, the first between ~11,600 and ~11,400 <sup>14</sup>C years B.P., the second between ~ 11,400 and 10,250 <sup>14</sup>C years B.P., and the third after 10,250 <sup>14</sup>C years B.P. The last two events correlate to the Younger Dryas event of the North Atlantic region (11,000-10,000 <sup>14</sup>C years B. P.) and other similarly dated cool events around the world (Rutter et al., 2000). In addition, a large alpine valley glacier system that occupied the North, Middle, and South Forks of the Nooksack River drainage may correlate with the Sumas Stade (Kovanen and Easterbrook, 2001).

Based on pollen studies in the Pacific Northwest, the early-to-mid-Holocene has generally been thought of as a period of warm and dry conditions (e.g. Whitlock, 1992), included in the Hypsithermal (defined by Deevy and Flint (1957) between ~10,000 and 2500 <sup>14</sup>C years B.P.). The Neoglacial period, which overlaps with the Hypsithermal, is commonly used for the period of glacier expansion after warm dry conditions (Porter and Denton, 1967). The start of the Neoglacial period varies regionally from 5000 to 8000 <sup>14</sup>C years B.P. (Denton and Porter, 1970).

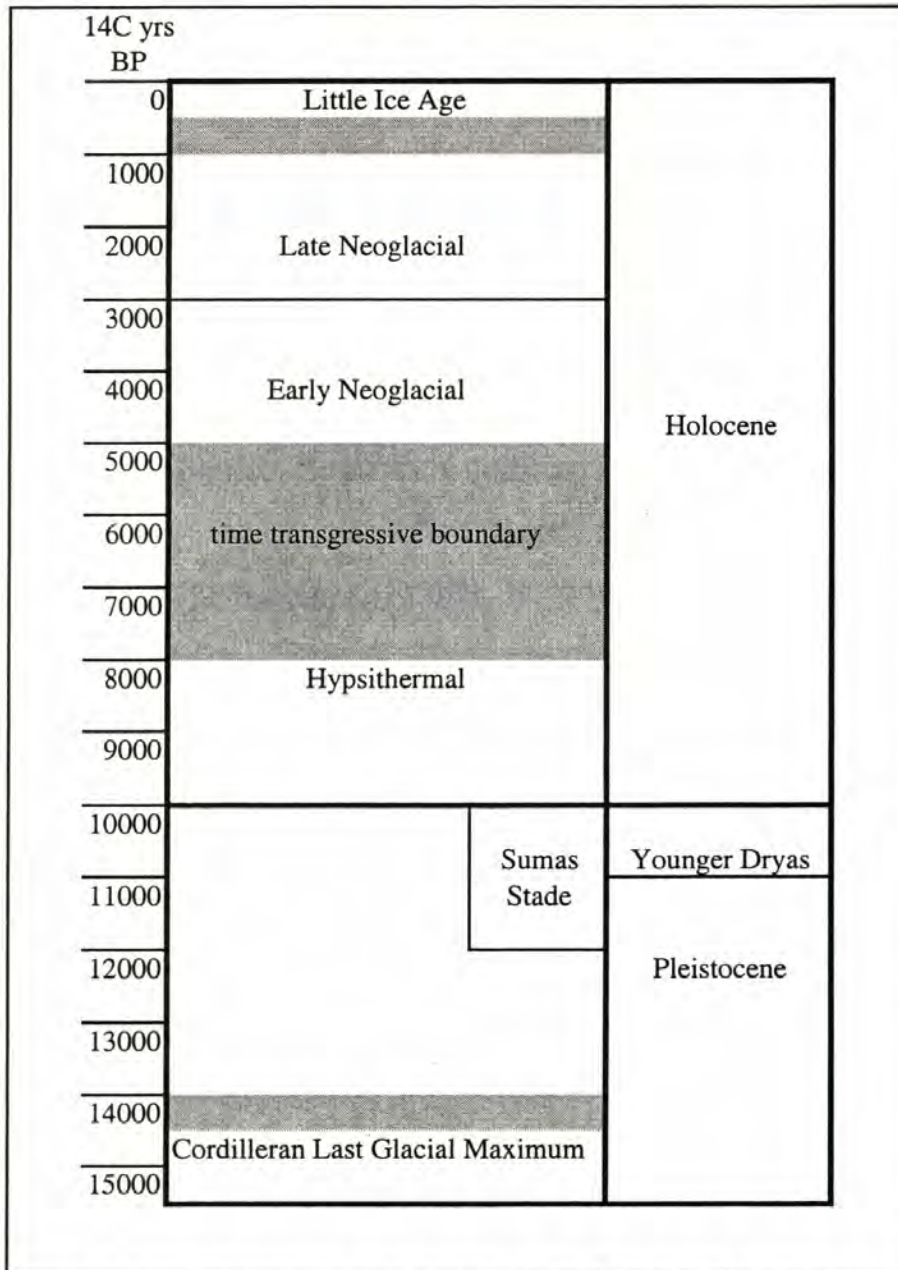


Table 1.1 Late-Pleistocene and Holocene stratigraphy for western Washington and southwestern British Columbia. Sources: Mullineaux et al., 1965; Heller 1980; Easterbrook, 1992; Clague et al. 1997; Kovanen and Easterbrook 1997; Thomas 1997; Easterbrook and Kovanen, 1998; Porter and Swanson, 1998.

Thus, the boundary between the Hypsithermal and Neoglacial is considered time transgressive. Mathes (1939) first coined the term “Little Ice Age”(LIA) for the same period as Neoglaciation. More recently Little Ice Age has come to mean the time of glacier expansion during the past ~ 700 years within and at the end of the Neoglacial (late Neoglacial). The end of the LIA (and the Neoglacial) and the beginning of warmer, modern conditions are generally considered to have started at the end of the 19<sup>th</sup> Century.

#### *An early Holocene glacial advance in the North American Cordillera?*

Most glaciers in the North American Cordillera reached their Holocene maximum extents during the Neoglacial period. However, a number of pre-Neoglacial moraines, some assigned early Holocene ages, have been identified (Beget, 1981; 1988; Easterbrook and Burke, 1972; Easterbrook, 1975; Waitt et al., 1983). Because of the long-held view of prevalent, warm and dry conditions during the Hypsithermal and lack of rigorous dating control on many of these moraines, substantial early Holocene glacial advances have been viewed with skepticism by some (Davis and Osborn, 1987; Luckman, 1998).

In the Cascade Range, cirque moraines mantled by Mazama ash (~6800 <sup>14</sup>C years B.P.) near the south side of Mt. Baker provided an early indication of an early Holocene glacier advance (Easterbrook and Burke, 1972; Easterbrook, 1975). More recently, charcoal from one of these moraines has been dated at ~8500 <sup>14</sup>C years B.P. (Easterbrook and Kovanen, 1999). Thomas (1997; Thomas et al., 2000) documented evidence for an extended position of the Easton Shelf Glacier on the south flank of Mt. Baker between 6800 and 8400 <sup>14</sup>C years B.P. Beget (1981) provided evidence for an early Holocene advance near Glacier Peak between about 8300 to 8400 <sup>14</sup>C years B.P. In a reexamination of Beget's field area, Davis and Osborn (1987) concluded that Beget's dates are from colluvium rather than till, but Beget (1988) maintained that an early Holocene advance did occur there. Waitt et al. (1983) suggested an early Holocene advance in the southern North Cascades marked by moraines mantled with Mazama Ash (older than ~6800 <sup>14</sup>C years B.P.). However, the age of

these moraines is poorly constrained with a maximum limiting age of ~13,000 <sup>14</sup>C years B.P. (Waite et al., 1983).

Heine (1998) dated the McNeely I and II advances of Crandell and Miller (1964) near Mt. Rainier. Based on radiocarbon dates from lake and bog sediment and tephrochronology, the McNeely I advance occurred before 11,300 <sup>14</sup>C years B.P., and the McNeely II advance occurred at the beginning of the Holocene, between 9800 and 8950 <sup>14</sup>C years B.P. Thus, the only well-dated evidence for an early Holocene glacier advance in the Cascade Range and in the North American Cordillera comes from the vicinities of Mt. Baker and Mt. Rainier. Some moraines in the study area appear to be good candidates for early Holocene age. They are similar in extent, are covered by Mazama ash, and their position relative to Little Ice Age moraines is similar to those near Mt. Baker and Mt. Rainier.

### *Climatic Setting*

The North Cascades lie within a highland maritime climate zone characterized by cool, wet winters and relatively dry, warm summers. The average annual temperature at Mt. Baker Lodge (near the mouth of Bagley Creek cirque) is 4.4 deg. C (39.9 deg. F), and the average annual precipitation is 279 cm (110 inches) (Porter, 1977; Douglas, 1969). Approximately 80 percent of the annual precipitation in the study area falls between October and April, most of which falls as snow. Frequent winter storms and orographic lifting are responsible for the large amounts of winter snowfall. Storms commonly come from the west and southwest off the Pacific Ocean. During the winter, an atmospheric low-pressure pattern (the Aleutian Low) dominates the northeast Pacific directing storms onto the northwest coast of North America. During the summer, a high-pressure pattern (the Pacific High) shifts northward and dominates the northwest coast, causing drier conditions to prevail (Ahrens, 1994). The North Cascade Range is distinct from the South Cascade Range in that the North Cascades receive occasional blasts of arctic air from the north during the winter, lowering temperatures and freezing levels in the mountains.

### *Vegetation*

The study area occurs mostly in the subalpine vegetation zone. This zone is patchy forest parkland of heather/huckleberry, wetland meadows, and stands of mountain hemlock and fir. The subalpine vegetation zone is defined as the area above closed (montane) forest but below the limits of krummholz and alpine tundra (Douglas, 1969). In the North Cascades, these limits typically are between 1280 m (4200 ft) and 1820 m (5970 ft) on north-facing slopes and 1580 m (5180 ft) to 1980 m (6490 ft) on south-facing slopes (Douglas, 1969). The primary non-altitudinal controls on vegetation patterns in the study area are duration of summer snow cover, age of recent deglaciation, soil drainage, and substrate type.

## Chapter 2 Methods

### *Glacial Landform Mapping*

Landforms were mapped from stereo air photos and topographic maps. Black and white (USDA, Mt Baker-Snoqualmie National Forest, 1963) and color air photos (USDA, Mt Baker-Snoqualmie National Forest, 1985) at a scale of 1:12,000 were used in conjunction with the USGS, 7.5-minute Shuksan Arm quadrangle (1989). Field sites suitable for investigation were identified on the photos, which were later used to compile maps of glacial deposits in upper Swift Creek, Shuksan Creek (Figure 3.1) and Bagley Creek (Figure 4.1). However, ground exploration proved to be the most accurate method of mapping.

Field mapping in upper Swift Creek and Shuksan Creek was conducted from July to October, 1998. Reconnaissance field mapping in Bagley Creek was completed in September, 1999. The main goal of the field mapping was to distinguish primary moraine crests. Both sparsely vegetated Neoglacial moraines and densely vegetated pre-Neoglacial moraine crests were distinct on air photos and in the field. Where available, exposures of till in stream cuts, trail cuts, and tree throws allowed moraines to be distinguished from bedrock ridges. Where till exposures were lacking, interpretations were based on surface morphology as well as the presence and provenance of surface clasts.

### *Dendrochronology*

The ages of Neoglacial moraines were estimated using dendrochronology (Lawrence, 1950). Few trees occur on the Neoglacial moraines and those that do are quite small (1-3 m tall) mountain hemlock or subalpine fir. The oldest were readily recognized by their size and were sampled. A 12-inch long increment borer was used to obtain cores as close to the base of the tree trunk as possible. A small number of trees occur on each moraine so no problems were encountered in distinguishing the oldest.

From several studies in the North Cascades, the estimated time to establish trees on moraines after glacier retreat (ecesis) is between 15 and 35 years (Long, 1953; Miller, 1969; Leonard, 1974; Heikkinen, 1984). However, estimates of ecesis from studies on Mt. Rainier

vary from 5 years (Sigafos and Hendricks, 1961) to 50 years (Harrison, 1956) to 100 years (Burbank, 1981). Recent observations by the author of a ~20 year-old moraine from the nearby Coleman Glacier (on Mt. Baker) noted numerous tree seedlings already established. The lowest estimate of 15 to 35 years is used in this study.

### *Bog and Lake Coring*

Sediment records and radiocarbon dates from bogs and lakes associated with moraines have been used successfully to determine close limiting ages to glacier advances (e.g., Surgenor, 1978; Davis et al., 1979; Leonard 1986b; Clark and Gillespie, 1997; Heine, 1998). A number of bogs in Swift Creek were cored in October 1998; Highwood Lake was cored during February, July, and September 1999; and several attempts were made to core Lake Ann from June to August 1999. Three types of coring systems were utilized in this study:

- (1) A simple PVC pipe percussion corer was utilized to obtain shallow (1.0-1.5 m) bog cores in Swift Creek basin. Two-inch diameter, schedule 40, PVC pipe in 1.0 and 1.5 meter lengths, beveled at one end (a cutting edge), were driven into the ground with a hammer and wooden block. The PVC pipe was then extracted from the ground by digging around the pipe.
- (2) Highwood Lake and Lake Ann cores were obtained using a modified Livingstone piston sampler (Livingstone, 1955; Vallentyne, 1955; Wright, 1984).
- (3) A lightweight, percussion core sampler (Reasoner, 1993) was used in Lake Ann. This system proved problematic. One partial core was obtained, but much of the device was lost in the bottom of the lake when the main support rope was accidentally cut. With some modifications this system could be an effective alternative to the modified Livingstone sampler and would be better suited for transport into and use in deep, remote lakes. The modifications should include using a piston to create suction in extracting the core instead of a core catcher with fingers at the sharp end of the corer (Reasoner, 1993; P. Bierman, personal comm., 1999).

All cores were split, measured, and the stratigraphy sketched and photographed. Charcoal, wood, plant fragments, and peat were sampled for radiocarbon dating and any tephra present was sampled for identification. Before the Highwood Lake cores were split, bulk magnetic susceptibility was measured every 2 cm using a Bartington MS2c analyzer.

### *Radiocarbon Dating*

Samples large enough for conventional radiocarbon analysis (a few grams) were submitted to Beta Analytic, Inc. Smaller samples were dated by accelerator mass spectrometry (AMS) methods at the Arizona AMS radiocarbon laboratory (AAMS) and at the Center for Accelerator Mass Spectrometry (CAMS) at Lawrence Livermore National Laboratory.

Radiocarbon ages were calibrated using the world wide web-based calibration program, HTML CALIB 4.2 (<http://depts.washington.edu/qil/calib/>) (Stuiver and Reimer, 1993). This program uses 1998 international calibration data sets, summarized in Stuiver et al. (1998). Two-sigma calibrated age ranges are reported in this thesis.

### *Tephrochronology*

The presence of tephtras on moraines provides minimum age markers. Tephtras in bog and lake sediments are useful in correlating stratigraphic horizons. Two ubiquitous tephtras are present in the field area, Mazama ash (Bacon, 1983; Easterbrook, 1975) and the tephtra first referred to informally as black sandy tephtra by Hyde and Crandell (1978) then as Cathedral Crag tephtra (Kovanen and Easterbrook, in review-b).

Mazama ash is silt-sized, white to orange, and up to 25 cm in thickness in the study area and well dated at  $6850 \pm 50$   $^{14}\text{C}$  years B.P. (7590-7760 and 7780 cal. years) (Bacon 1983) and  $6730 \pm 40$   $^{14}\text{C}$  years (7510-7530 and 7560-7670 cal. years) (Hallet et al., 1997). Although the two radiocarbon ages are different at 1 sigma, the calibrated age ranges for each is not, with overlap between 7590 and 7670 cal. years B.P. (at the 2-sigma range of uncertainty).

Cathedral Crag tephra is predominantly sand-sized, black and gray in color, and originated from nearby Mt. Baker. Maximum estimates of its age vary from 6400 to 5800 <sup>14</sup>C years (7420 – 6450 cal. years B.P.) from radiocarbon dates on charcoal, peat, and plant macrofossils (this thesis; Kovanen and Easterbrook, in review-b). Bob Mierendorf (Personal Communication, 1999) obtained a date of 6040 ± 80 <sup>14</sup>C years B.P. from charcoal embedded within the tephra from a site on Copper Ridge, several kilometers to the northeast of the study area. At several locations on the south flank of Mt Baker, Cathedral Crag tephra directly overlies the Rocky Creek tephra. The Rocky Creek tephra is directly overlain by a lahar deposit and peat. The lahar deposit is dated at ~5700 <sup>14</sup>C years B.P. and the peat beds are dated between 5730 and 5965 <sup>14</sup>C-yrs B. P. Thereby providing a minimum limiting ages for the Cathedral Crag tephra.

Other sediment collected from cores and trail cuts suspected to be tephra layers but not readily identified were submitted to Nick Foit at Washington State University for microprobe analysis and correlation. Analyzed sediments were identified as Mazama ash, Cathedral Crag tephra, and one sample was concluded not to be a tephra (See Chapter 4).

#### *Equilibrium Line Altitude and Paleoclimate Reconstruction Methods*

Equilibrium line altitudes (ELAs) are calculated from modern and reconstructed past glaciers using the 0.65 accumulation area ratio (AAR) method (Meier and Post, 1962). Modern climate is estimated at these past and present equilibrium line altitudes in the study area using lapse rates from lower altitude stations. The modern climate at an ELA is then compared with the possible range of documented climates at modern glaciers (these are used as an estimate for climate of the past glacier ELA) in order to determine a deviation from modern conditions. This approach follows Leonard (1989) and is covered in more detail in Chapter 6.

### Chapter 3 Swift Creek and Shuksan Creek Glacial Geology

The headwaters of Swift Creek and Shuksan Creek occur in compound cirques. Each sub-cirque is named according to its position within the compound cirque. Upper Swift Creek is comprised of three sub-cirques: north Swift Creek Cirque (NSC); south Swift Creek cirque (SSC); and high Swift Creek cirque (HSC) (Figure 3.1). Upper Shuksan Creek has four sub-cirques: north Shuksan Creek cirque (NShC); Lake Ann Cirque; south Shuksan Creek cirque (SShC); and lower Curtis glacier cirque (this cirque is not shown on Figure 3.1). Organic material from sediment cores collected near moraines associated with south Swift Creek cirque (SSC) provided age control for the moraines. Dendrochronology provided age control for younger moraines in south Swift Creek cirque (SSC) and high Swift Creek cirque.

#### *Moraine Morphology and Stratigraphy*

Moraines in Swift Creek were identified and mapped from 1:12,000 scale black and white and color air photos and in the field during the summer of 1998 (Figures 3.1 and 3.2). “Undifferentiated drift” in Figure 3.1 includes hummocky ground or ablation moraine, small moraine crests, and outwash. Bedrock, talus, colluvium, and alluvium are not mapped. Moraine crests are grouped according to presence or absence of a mantle of Mazama ash (“pre-Mazama” or “post-Mazama” respectively). Purple stars indicate ponds and bogs cored during this study. Black stars indicate other sites not cored but could be lucrative for future coring. These ponds and bogs were not cored because of time constraints.

South Swift Creek cirque (SSC), a two-tiered cirque, is the largest (~1 km<sup>2</sup> area) and best-developed cirque of the Swift Creek sub-cirques (Figure 3.1, 3.2, and 3.3). The upper, north-facing tier is poorly developed and hosts a small unnamed glacier (0.07 km<sup>2</sup> area), which lies between 1550-1680 m altitude (5100-5500 feet) (Figure 3.4). This glacier, identified in the Post et al. (1971) glacier inventory (0.10-km<sup>2</sup> area), has a few poorly developed crevasses and no obvious modern moraine. The upper set of moraines, consisting of discontinuous lateral and end moraines, lies at the edge of the upper cirque between 1340 and 1580 m altitude (4400 and 5200 feet) (Figure 3.1). The lower, well-developed,

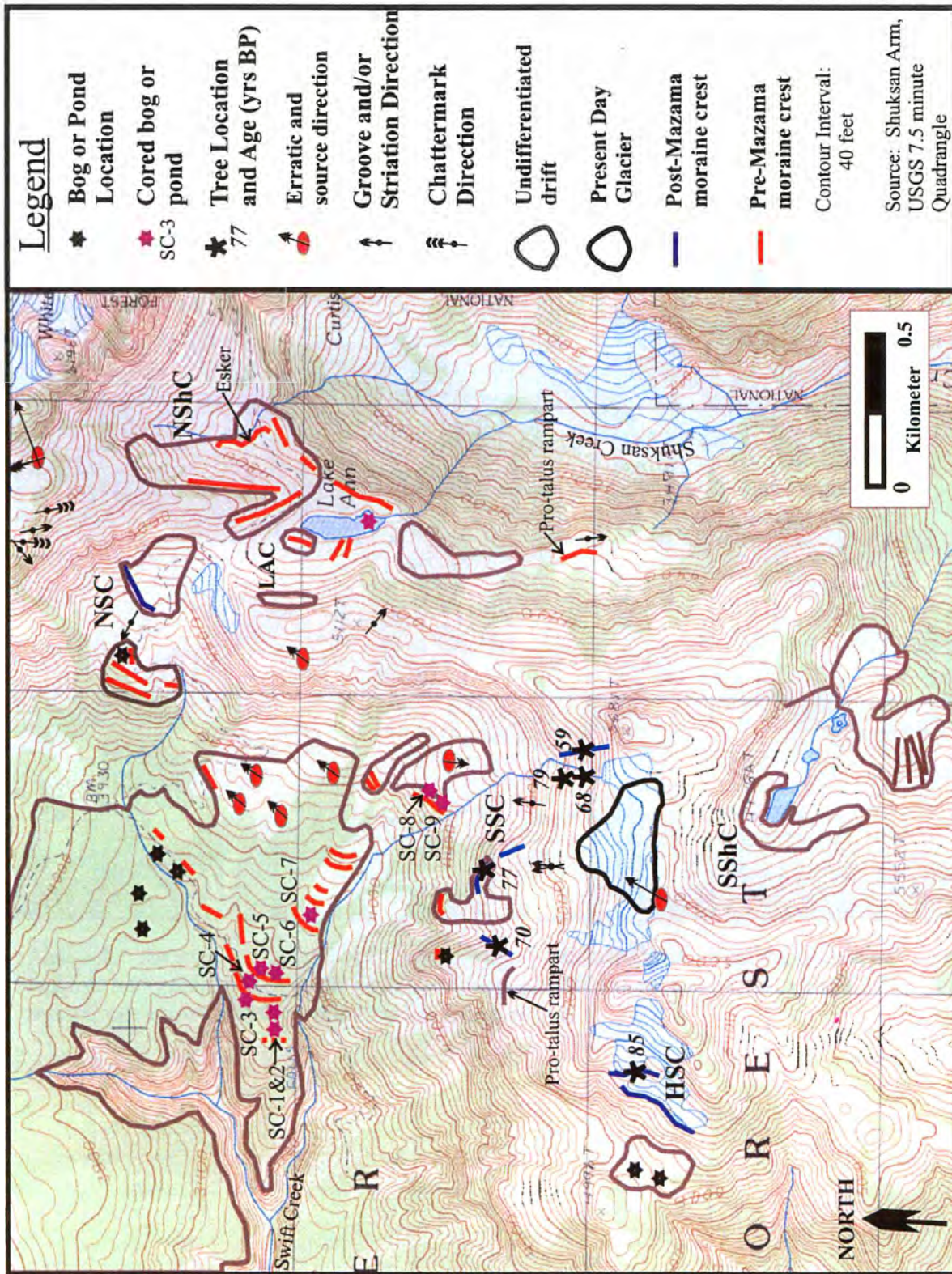
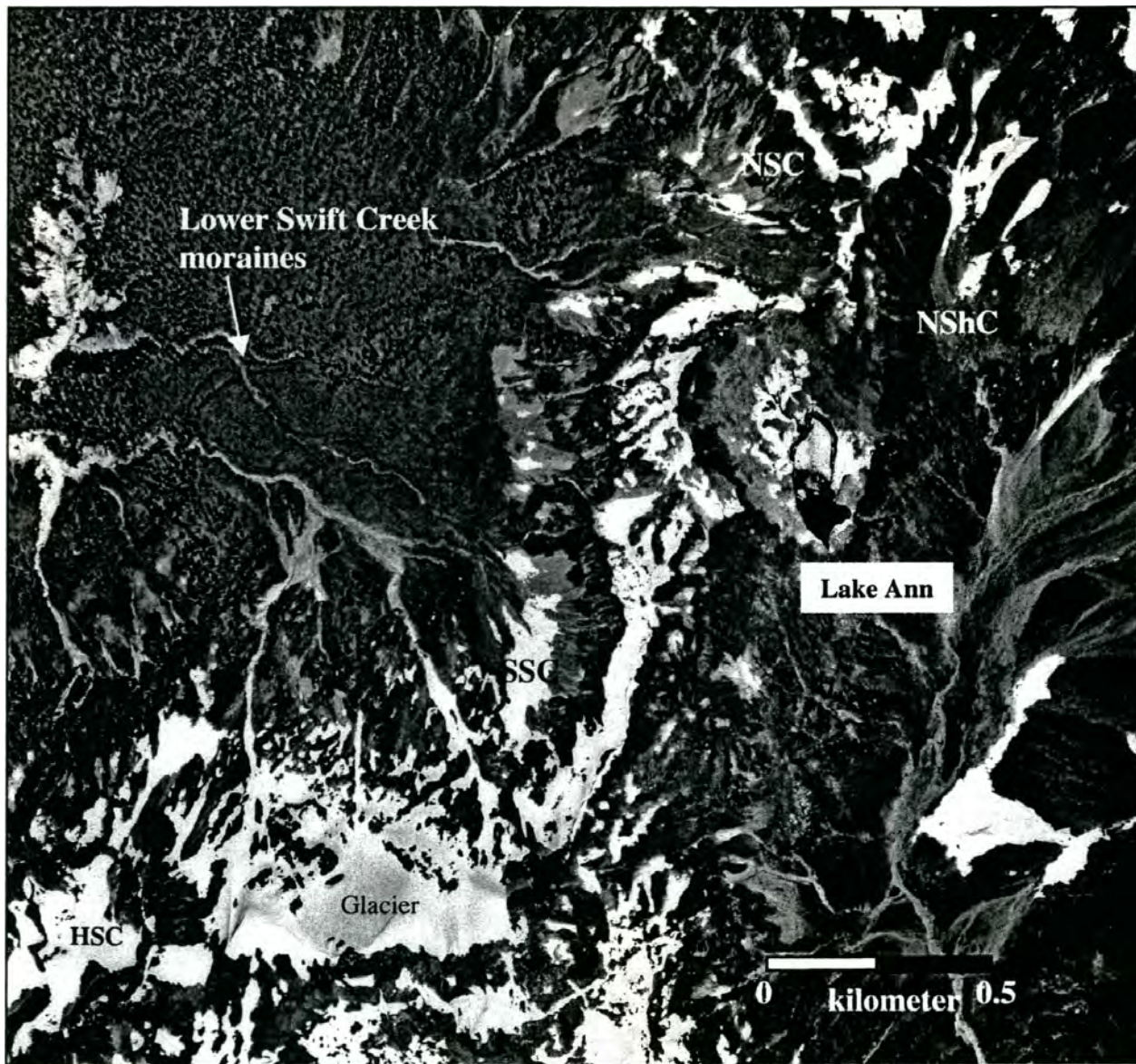


Figure 3.1 Glacial deposit map for upper Swift Creek and upper Shuksan Creek. Key to cirque acronyms: NSC = north Swift Creek cirque; SSC = south Swift Creek cirque; HSC = high Swift Creek cirque; ShCC = north Shuksan Creek cirque; LAC = Lake Ann cirque; SShC = south Shuksan Creek cirque.



*Figure 3.2* Air photo of upper Swift Creek and upper Shuksan Creek. Note the arcuate end moraines in upper left center. SSC = south Swift Creek cirque, NSC = north Swift Creek cirque, HSC = high Swift Creek cirque, NShC = north Shuksan Creek cirque.

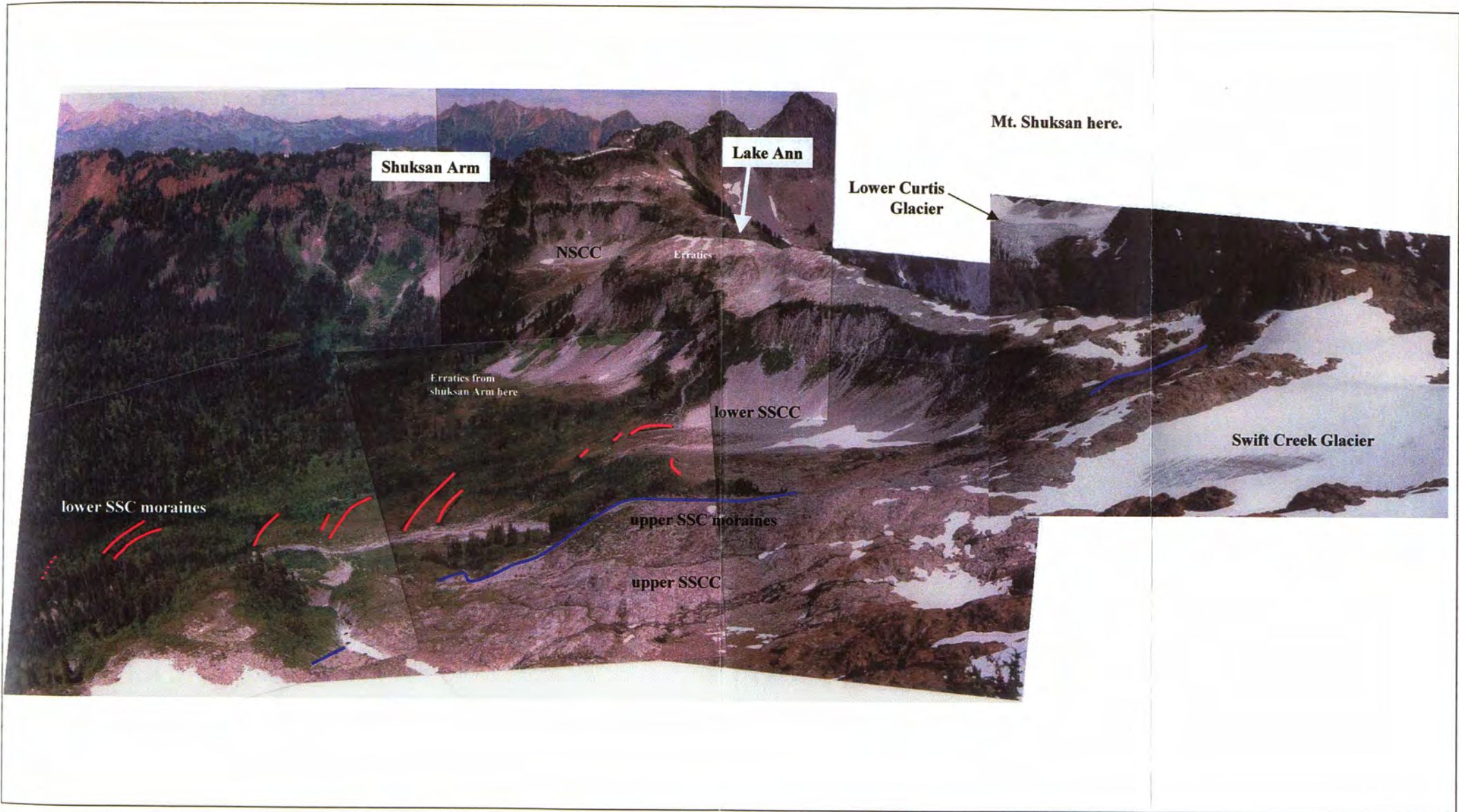


Figure 3.3 View looking northeast into south Swift Creek cirque (SSCC). South Swift Creek Cirque lower moraines are in red and upper moraines are blue. North Swift Creek cirque (NSCC) is in the background and Lake Ann is behind the rounded bedrock ridge where the arrow points. Note the intervening slopes between north Swift Creek cirque and south Swift Creek cirque, drift on these slopes contains erratics from Shuksan Arm to the north. Photographed from the west peak of the south ridge above south Swift Creek cirque in August 1998.

northwest-facing cirque has an average floor altitude of 1370 m (4500 feet). It is floored with sculpted bedrock and till and has several discontinuous but distinct moraine crests at the lip. The lip of the lower cirque drops off to a northwest valley. Eight, small, end moraines (1-3 m high) occupy the valley ~1 km down-valley from the lip of the cirque at an altitude range of 1220 to 1110 m (4000 to 3650 ft).

Field relationships distinguish two age groups of moraines from south Swift Creek cirque (SSC) (Figure 3.2). The lower, older moraines are vegetated with mature subalpine vegetation and have impounded a number of small ponds and bogs. An extensive cover (within the soil) of Mazama ash on the lower moraines and bogs provides a minimum limiting age of ~ 6800 <sup>14</sup>C years for deposition. The upper moraines lack tephras, are bouldery, sparsely vegetated with only a few small trees growing on them, and are discontinuous but have matching right and left lateral crests and a few closely spaced end moraine crests (Figure 3.2). Upper moraines occur 120-180 m below the terminus of the small, present-day glacier. The oldest trees behind the right lateral moraine (~20 m to the west, growing on bedrock), on the end moraine, and on the left lateral moraine are 79, 77, and 70 years old, respectively (from 1998 A.D.). A number of factors favor or delay tree establishment on freshly exposed surfaces in this area. Established trees nearby provide abundant seed sources. However, this area has vegetation patterns and treelines controlled largely by lingering late summer snowpack, which also may inhibit tree establishment. The dated trees occur on relatively steep slopes (~30 degrees) where snow is less likely to stay late in the season and on topographic projections (moraine crests) where snow is likely to be shallower. But if the moraine crests are blown clear of snow in the winter, young trees may suffer from freeze kill.

North Swift Creek Cirque (NSC) (Figures 3.2 and 3.3 and 3.5) is a small (~0.25 km<sup>2</sup>), west-facing, well-developed cirque directly below Shuksan Arm at the extreme NE headwaters of Swift Creek. The average cirque floor altitude is 1390 m (4550 feet), similar to south Swift Creek cirque (SSC). North Swift Creek cirque is mostly bedrock-floored with scattered till cover and two substantial deposits of drift. Trail cuts reveal that Mazama ash mantles the lower deposit. Two discontinuous end moraine crests and a small



*Figure 3.4* South Swift Creek cirque (SSC) glacier in the late summer. The Lower Curtis Glacier on the west flank of Mt. Shuksan is in the background.

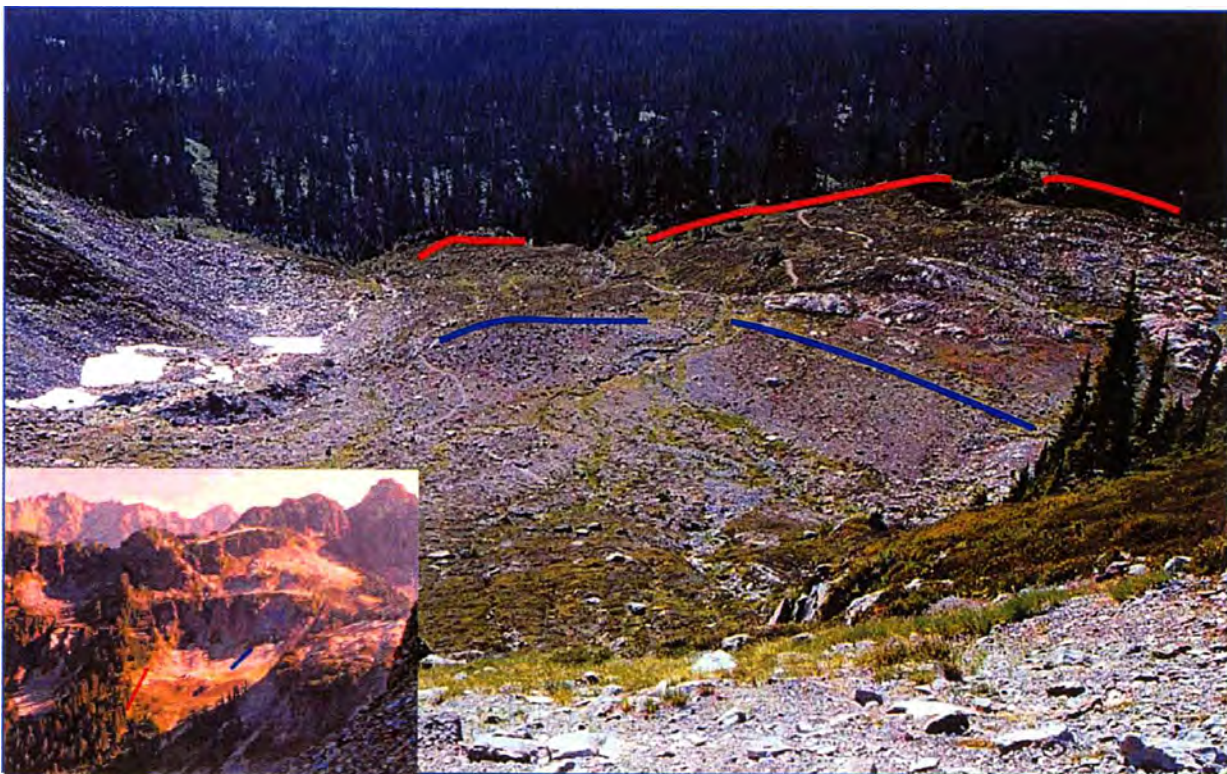


*Figure 3.5* North Swift Creek cirque (NSC). The inset is a view from south Swift Creek cirque looking NE. The larger view looks downvalley at the cirque floor. Blue lines delineate the upper limit of Mazama ash and red lines show pre-Mazama moraines at the edge of the cirque. Blue lines are also a possible post-Mazama moraine.

lateral moraine occur near the edge of north Swift Creek cirque (NSC) (Figure 3.5, red lines). Another moraine, sparsely vegetated with no trees, occurs near the head of the cirque (Figure 3.5, blue line). The upper moraine has no Mazama ash on it. Above the main cirque is a bench that may be considered a poorly developed cirque. The bench is scoured bedrock (Lake Ann Stock granodiorite) with striations pointing downslope (Figure 3.2).

The intervening area between south Swift Creek cirque (SSC) and north Swift Creek cirque (NSC) is extremely hummocky topography, dissected by small streams, and hosts a few small, discontinuous moraine crests (Figure 3.2). The bedrock at this location is granodiorite of the Lake Ann Stock, but erratic boulders of slightly metamorphosed ribbon chert (Figure 3.3) from the ridge of Shuksan Arm to the north occur in and on top of this drift and on the slopes and ridge above. These erratics indicate an ice source from the north (Shuksan Arm) rather than from the slopes and ridge above, as the topography would suggest. The north-to-south flowing Cordilleran Ice Sheet (CIS) transported these erratics and the hummocky topography is either stagnant ice drift or the remains of a post-CIS rock glacier. In either case, the erratics demonstrate that no substantial movement of ice downvalley occurred on the intervening slopes between south Swift Creek cirque (SSC) and north Swift Creek cirque (NSC) since the disappearance of the CIS. The erratics also demonstrate that the SSC and NSC glaciers did not coalesce on these slopes after the CIS left.

The high Swift Creek cirque (HSC) is west-facing, small (~0.125 km<sup>2</sup> area), and contains a permanent snowfield with two distinct end moraines at the edge of the snowfield at about 1585 m (5200 feet) altitude (Figure 3.2 and 3.6). The end moraines are bouldery and sparsely vegetated with no tephra on them (Figure 3.7). The upper moraine has a few small trees growing on it, the oldest of which is 85 years old (from 1998).

The head of Shuksan Creek is a compound cirque and has three sub-cirques at the head (Figure 3.1). The Lower Curtis Glacier on the southwest flank of Mt. Shuksan occupies the easternmost sub-cirque (not shown on Figure 3.1). At the northern head of the valley is north Shuksan Creek cirque and on the western side is Lake Ann Cirque. These three cirques are all at approximately the same elevation. They all have a lip at

approximately 1400 m (4600 feet) which drops off abruptly into a lower, larger cirque at the head of the main valley floor of Shuksan Creek. (Figure 3.1) South Shuksan Creek cirque is a small tributary valley/sub-cirque ~2 km south and west of Shuksan Creek headwaters. It also has a lip at approximately 1400 m.

Lake Ann lies at an altitude of 1430 m (4700 feet) and occupies Lake Ann cirque, a small, shallow, southeast-facing cirque (~0.125 km<sup>2</sup> area). The cirque floor is mostly exposed bedrock but contains five pre-Mazama moraines (Figure 3.8). The rounded, low pass between Lake Ann cirque and north Swift Creek cirque (NSC) suggests a common ice mass occurred here at the time of deposition, as does the large lateral moraine above and just northeast of the lake. The moraine at the distal edge of the cirque is sharp crested, is mantled with Mazama ash, and has large Mountain Hemlock trees growing on it (Figure 3.8). The mid-cirque moraines are bouldery, sparsely vegetated, and have a few small trees growing on them. They appear to be devoid of Mazama ash and Cathedral Crag tephra. However, both tephtras occur in the sediments of a small basin on the cirque floor up-valley from the moraines just north of the lake. Both tephtras are also found in the bottom sediments of Lake Ann. Lingering late summer snow cover explains the young appearance of these pre-Mazama moraines by preventing significant vegetation establishment and soil development. For example, during the summer of 1999, after a winter of record-setting snowfall, the lake and much of the basin never melted out.

The North Shuksan Creek cirque (NShC on Figure 3.1 and 3.2) is a small, poorly developed, south-facing cirque northeast of Lake Ann Cirque (~0.125 km<sup>2</sup>). Its floor altitude is the same as Lake Ann at 1430 m (4700 feet). Talus from the cliffs and gullies above occupy the east side. Till and a large, distinct, right lateral moraine high on the west slope cover the west side of the cirque. An esker occupies the floor of the cirque (Figures 3.1, 3.8, and 3.9). The esker is a low, sinuous ridge (~1 m high) and has gravel and cobbles exposed at the surface. A crested moraine occurs at the edge of the cirque downslope from the esker (Figure 3.1 and 3.8). The large amount of drift comprising the right lateral moraine of the cirque and the esker on the floor suggests a stagnant ice regime in this cirque.

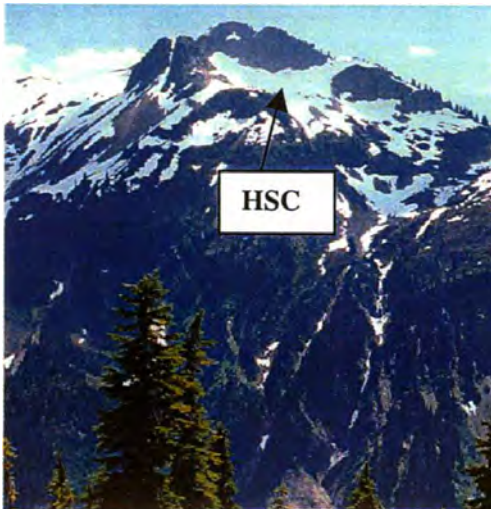


Figure 3.6 View looking SE to high Swift Creek cirque (HSC) from Huntoon Point.



Figure 3.7 This view is looking down at the high Swift Creek cirque moraines from the peak above.



Figure 3.8 View looking south at Lake Ann cirque and north Shuksan Creek cirque (NShC) from Shuksan Arm. Red lines are pre-Mazama moraines. The curving red line on the floor of NShC is an esker.



*Figure 3.9* The esker on the floor of north Shuksan Creek cirque. The esker is approximately 200 m long and 1-2 m high.



*Figure 3.10* The view southeast looking down South Shuksan Creek cirque (SShCC).

The south Shuksan Creek cirque (SShC on Figure 3.1) is a well developed, elongate, southeast-facing cirque just south of the Swift Creek headwaters (~0.6 km<sup>2</sup>) (Figure 3.10). This cirque is directly south of south Swift Creek cirque (SSC). The floor of the cirque (1490 m; 4900 ft) is sculpted bedrock covered with drift with little vegetation, and typically has a late summer snowpack. Three small paternoster lakes occupy the cirque floor. The deposits in the cirque were mapped only from air photos and field observations and from the north ridge of the cirque. Four sparsely vegetated, bouldery, moraine crests are apparent near the distal end of the cirque (Figure 3.1).

#### *Sediment Cores and Basal Radiocarbon Dates*

Sediment cores were collected from nine small ponds and bogs associated with the south Swift Creek cirque (SSC) moraines. The cores were obtained with a simple PVC, plastic-pipe, percussion-coring device. The pipes were driven to refusal, usually to till or rock.

Most of the south Swift Creek cirque (SSC) cores are from wet meadows/shallow bogs and small ponds and therefore subject to penetration from tree and plant roots, bioturbation (treethrow, burrowing animals, etc.), and other stratigraphic disturbance due to erosion, fire, and snow and pond ice freezing (Nichols, 1967). The lower Swift Creek cores (SC-2, 4, 6 and 7) come from a subalpine meadow/wetland environment in which small, shifting, streams erode and deposit sediment in the meadows. In places, abandoned channels of these small streams have eroded former bog sediments. The core sites were chosen to be as far away as possible from present and former channels of these streams.

Sampling results of the five most stratigraphically complete cores from south Swift Creek cirque (SSC) are presented in Figure 3.11. Cores SC-2, SC-4, SC-7, SC-8, and SC-9 from south Swift Creek cirque (SSC) all have the same basic stratigraphy (Figure 3.1 for locations and Figure 3.11 for stratigraphy). The general stratigraphy from bottom to top consists of basal inorganic sediment (mix of clay, silt, and sand) overlain by peat and/or

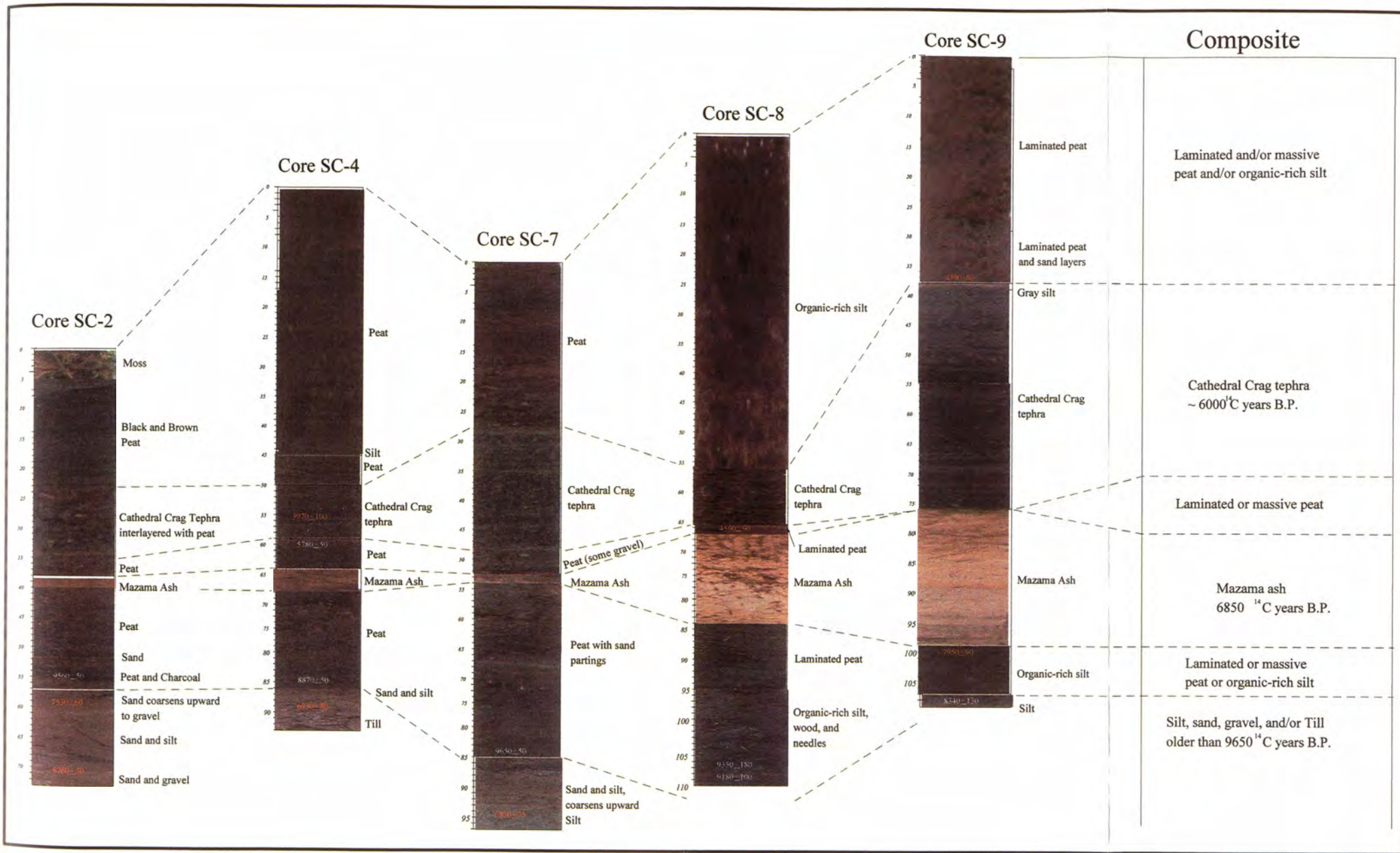


Figure 3.11 Swift Creek cores stratigraphy and fence diagram. See Figure 3.2 for locations of cores. All ages are radiocarbon dates with  $\pm 1$  sigma standard deviation. Radiocarbon dates in orange text have been deemed too young, see the discussion in the text. Depth units are in centimeters.

organic-rich silt, Mazama ash, peat or organic-rich silt, and Cathedral Crag tephra grading into a top layer of peat or organic-rich silt.

Incomplete cores were recovered from Lake Ann using a modified Livingstone piston sampler and a Reasoner corer. The best core from Lake Ann penetrated into Mazama ash, but the stratigraphy below the ash is unknown.

Interpreting basal sediments and radiocarbon dates from organic material in bog sediments can be problematic. Davis and Davis (1980) found that “piping” of fine sediments between large boulders can cause large time lags (800-9000  $^{14}\text{C}$  years) between deglaciation and onset of organic deposition. Bogs, from which cores SC-2, SC-4, and SC-7 were obtained, are dammed by moraines and rest on till. “Piping” may or may not occur in a moraine dammed depression since the till could have a fine or coarse matrix, inhibiting or allowing the “piping” process to occur. The basal radiocarbon ages from these bogs may be younger because earlier sediment was “piped” away. The sites of SC-8 and SC-9 have bedrock catchments and are not as susceptible to the “piping” process.

The two oldest radiocarbon dates are from near the base of two of the south Swift Creek cirque (SSC) cores and are associated with the lower-most moraines. The two dates are indistinguishable when calibrated (Table 3.1). The oldest date, from peat and plant fragments directly overlying basal sand and silt in core SC-7, is  $9650 \pm 50$   $^{14}\text{C}$  years B.P. (10,760-11,180 cal. years). The second oldest date, from a piece of charcoal in a layer of peat and charcoal just above basal gravel, sand, and silt in core SC-2, is  $9560 \pm 50$   $^{14}\text{C}$  years B.P. (10,690-11,110 calibrated (cal.) years). Core SC-7 was collected from a small bog just above the third moraine up-valley (Figures 3.1, 3.11 and 3.12 ). Core SC-2 was collected from a small bog between the two lowermost end moraines below south Swift Creek cirque (SSC) (Figures 3.1 and 3.11). These dates further limit the age of the moraines from the Mazama ash minimum limiting date.

Similar limiting ages as those discussed above constrain the uppermost lower moraine at the edge of lower south Swift Creek cirque (SSC) (Figures 3.1 and 3.13). Core SC-8 was collected from a small pond in a bedrock depression impounded by the uppermost lower moraine and a bedrock lip at the edge of the cirque. The basal sediment recovered in

Sample ID	C-14 Age	2 sigma ±	2 sigma (95.4 %) calibrated age range		area under probability curve	Sample Description	Lab ID
			max age	min age			
SC-2g	9560	100	11110	10694	1	charcoal above basal sand&silt	CAMS-59600
SC-2h	8760	100	10108 9919	10084 9553	0.024 0.976	organic-rich silt in basal sand	CAMS-59607
SC-2e	7530	120	8406 8274	8277 8194	0.679 0.321	roots at top of basal sand & silt	CAMS-59599
SC-4e	8870	100	10179 9854	9856 9755	0.878 0.122	charcoal near base of lower peat	CAMS-59603
SC4ae	6930	160	7932 7873	7893 7614	0.068 0.932	roots at base of core	AAMS-SC4a
SC-4h	5780	100	6719 6671	6700 6450	0.039 0.961	plant macrofossils at base of Cathedral Crag tephra	CAMS-59601
SC4de	3970	200	4813 4710 4655 4109	4755 4667 4146 4100	0.049 0.024 0.922 0.004	roots in Cathedral Crag tephra	AAMS-SC4d
SC-7a	9650	100	11178 11020 10963	11043 10993 10755	0.457 0.034 0.509	plant macrofossils at top of basal silt	CAMS-59606
SC7ae	6820	150	7791 7529	7565 7513	0.975 0.025	roots at base of core	AAMS-SC7a
SC6ae	6545	100	7565 7513 7397 7354	7529 7411 7364 7326	0.132 0.724 0.079 0.066	roots at base of core	AAMS-SC6a
SC6be	6230	240	7416 7370 7335 6832	7388 7347 6855 6802	0.022 0.016 0.942 0.021	plant macrofossils just below Cathedral Crag tephra	AAMS-SC6b
SC8a	9350	360	11132	10212	1	branch near base of core	BETA-124906
SC-8c	9180	200	10636 10582	10615 10178	0.011 0.989	single needle near base	CAMS-59604
SC8de	4560	180	5568 5472 4929 4901	5552 4962 4904 4880	0.006 0.974 0.01 0.01	peat bed between Mazama ash and Cathedral Crag tephra	BETA-SC8d
SC-9a	8340	260	9532	9029	1	small wood chunk in basal silt	CAMS-59605
SC9ae	7950	180	9026 8571	8583 8546	0.984 0.016	1-cm peat bed below Mazama ash	BETA-SC9a
SC9ce	4390	180	5293	4832	1	1-cm peat bed above Cathedral Crag tephra	BETA-SC9c

Table 3.1 Swift Creek cores radiocarbon dates. Lab codes: CAMS=Lawrence Livermore National Laboratory Center for Accelerator Mass Spectrometry; AAMS=Arizona AMS Radiocarbon Laboratory; BETA=Beta Analytic, Inc.



*Figure 3.12* Core SC-7 site. The moraine is the belt of trees in the background.



*Figure 3.13* Core SC-8 site. White PVC pipe is 1.5 m long for scale. Numerous macrofossils from trees (branches, twigs, needles) were recovered from the basal sediments of this pond. The environment at this site may have been very similar  $\sim 9350$   $^{14}\text{C}$  years ago as it is today.

this core consists of organic-rich silt with a high percentage of macrofossils (wood, needles, and plant fragments) (Figure 3.11). The corer hit refusal in a thin layer of sand or gravel (which was not recovered) and rock. Radiocarbon samples SC8a and SC-8c from the basal material are stratigraphically similar with mostly indistinguishable dates (Table 3.1). At the base of the core, a small branch with intact bark was dated at  $9350 \pm 180$   $^{14}\text{C}$  years B.P. (10,210 - 11,130 cal. years) (Table 3.1, sample SC8a). Just below the branch, a single mountain hemlock needle was dated at  $9180 \pm 100$   $^{14}\text{C}$  years B.P. (10,180-10,640 cal. years) (Table 3.1, sample SC8c).

The abundance of tree-related macrofossils at the SC8 core site indicates that by  $9350 \pm 180$   $^{14}\text{C}$  years B.P. (10,210 - 11,130 cal. years) trees were growing at the edge of the south Swift Creek cirque (SSC), perhaps similar to today (Figure 3.13).

In comparison to the basal dates for cores SC-2, SC-7, and SC-8, discussed above cores SC-4 and SC-9 show evidence of a lag between deglaciation and organic deposition. Near-basal radiocarbon samples from cores SC-4 and SC-9 are  $8870 \pm 50$  (9760-10,180 cal. years) and  $8340 \pm 130$   $^{14}\text{C}$  years B.P. (9030-9530 cal. years), respectively (Figure 3.11, Table 3.1). A similar basal date for core SC-4 would be expected to be close to those of SC-2 ( $9560 \pm 50$   $^{14}\text{C}$  years B.P.) and SC-7 ( $9650 \pm 50$   $^{14}\text{C}$  years B.P.). However, it is significantly younger. Organic deposition may have occurred later at the SC-4 site for any of the reasons discussed above, or is simply not the oldest part of the bog. The same applies for the basal date of core SC-9 ( $8340 \pm 130$   $^{14}\text{C}$  years B.P.) which should have a similar basal age as core SC-8 ( $9350 \pm 180$   $^{14}\text{C}$  years B.P.) (Figure 3.11).

### *Radiocarbon Date Inconsistencies*

A number of the dates from the south Swift Creek cirque (SSC) cores conflict with or are inconsistent with other dates and the age of Mazama ash. Figure 3.11 illustrates this problem. On the figure, dates in orange text are significantly younger compared to those in white text. Contrasting basal dates occur in cores SC-2, SC-4, and SC-7. Each pair of dates are from material sampled at stratigraphically equivalent positions in each core. The material that yielded the younger dates, originally interpreted as wood fibers, are most likely

instead penetrative root fibers. The dates from these contrast sharply with charcoal, peat, and plant macrofossil (heather needles) samples carefully scrutinized to eliminate root material. In all three cases, the roots are  $\sim 2000$   $^{14}\text{C}$  years younger (Table 3.2). The younger dates were a “first round” of samples sent to the Arizona Accelerator Mass Spectrometry facility (AAMS), while the older “second round” dates were done at Lawrence Livermore National Laboratory Center for Accelerator Mass Spectrometry (CAMS). The age discrepancy is not related to the facility where the material was dated, as these two labs calibrate against each other regularly.

Charcoal can be substantially older than the sediments in which it is encased. This situation is possible if the charcoal has been redeposited or if it is from old heartwood of an old growth tree. In the western Cascade Range, the oldest wood in a tree could be hundreds to a thousand years old. The fact that the two oldest radiocarbon dates, one of which is on charcoal (sample SC2g) and the other on macrofossils (sample SC7a), are basically the same age suggests that this particular piece of charcoal is not substantially older than the surrounding sediment.

The following discussion covers the radiocarbon date discrepancies in detail, based on Figure 3.11 and Table 3.1. Sample SC4ae is composed of wood fibers from the basal diamicton in core SC-4 with an age of  $6930 \pm 80$   $^{14}\text{C}$  years B.P. Above SC4ae is sample SC4e on charcoal at the base of the lower peat with an older age ( $8870 \pm 50$   $^{14}\text{C}$  years B.P.). Similarly, sample SC7ae, composed of wood fibers in the sand and silt at the base of the core has an age of  $6820 \pm 75$   $^{14}\text{C}$  years B.P. Sample SC7a, which is above SC7ae and composed of peat and identifiable heather needle macrofossils, is older ( $9650 \pm 50$   $^{14}\text{C}$  years B.P.) In addition, the SC7ae date is demonstrably too young because it is stratigraphically well below Mazama ash. Thus the ages of samples SC4ae and SC7ae are rejected on the basis of being far too young relative to older samples stratigraphically above them. These two samples were originally interpreted as wood fibers but are reinterpreted here as penetrative root fibers.

Samples SC-2e and SC-2g were collected in the “second round” of samples analyzed at CAMS as a direct test of this problem. Sample SC-2e, identified as stratigraphically

Sample ID	Age ( <sup>14</sup> C years)	1 sigma ±	Sample Description	Age Difference ( <sup>14</sup> C years)
SC-2g	9560	50	charcoal above basal sand&silt	2030
SC-2e	7530	60	roots at top of basal sand&silt	
SC-4e	8870	50	charcoal near base of lower peat	1940
SC4ae	6930	80	roots at base of core	
SC-4h	5780	50	plant macrofossils	1810
SC4de	3970	100	at base of Cathedral Crag tephra roots in Cathedral Crag tephra	
SC-7a	9650	50	plant macrofossils	2830
SC7ae	6820	75	at top of basal silt roots at base of core	

Table 3.2 Age differences between root fibers and those of charcoal and plant macrofossils.

transgressive roots, was sampled at the same location as sample SC-2g, which is a piece of charcoal. SC-2e, the roots, returned a date of  $7530 \pm 60$   $^{14}\text{C}$  years B.P. and SC-2g, the charcoal returned a date of  $9560 \pm 50$   $^{14}\text{C}$  years B.P. In addition, sample SC-2h, organic-rich silt, sampled stratigraphically below both SC-2e and SC-2g, yielded a date of  $8760 \pm 50$   $^{14}\text{C}$  years B.P. The younger date indicates probable contamination from younger material compared to SC-2g, the charcoal. Sample SC6ae ( $6545 \pm 50$   $^{14}\text{C}$  years B.P.) is probably too young as it is significantly below SC6be ( $6230 \pm 120$   $^{14}\text{C}$  years B.P.), but close to it in age.

Radiocarbon dates obtained from bulk peat samples are rejected as they may contain younger root material. These samples are SC8de ( $4560 \pm 50$   $^{14}\text{C}$  years B.P.), and SC9ce ( $4390 \pm 50$   $^{14}\text{C}$  years B.P.) (Figure 3.11 and Table 3.1). However sample SC9ae ( $7950 \pm 50$   $^{14}\text{C}$  years B.P.), a 1-cm thick peat bed below Mazama ash, is significantly older than the known age for the base of the ash and may indicate a hiatus of deposition prior to deposition of Mazama ash at this site.

#### *Limiting Dates for the Cathedral Crag Tephra.*

Two dates from the Swift Creek cores and one date from the Highwood Lake core (see Chapter 4) provide maximum limiting ages for the Cathedral Crag tephra (CCT) (for a discussion of origin and characteristics and other limiting dates see Easterbrook and Kovanen, in review-b). The youngest date of  $5780 \pm 50$   $^{14}\text{C}$  years B.P. (sample SC-4h) is composed of peat and plant macrofossils (heather needles) sampled from immediately below the CCT. Also immediately below the tephra, sample SC6be, on wood fibers, gives the oldest date of  $6230 \pm 120$   $^{14}\text{C}$  years B.P. Gyttja sampled from immediately below the CCT in the Highwood Lake core yielded an age of  $6210 \pm 40$   $^{14}\text{C}$  years B.P.

In comparison to the dates for the Cathedral Crag tephra discussed above, a date of  $3970 \pm 100$   $^{14}\text{C}$  years B.P. (sample SC4de) on wood fibers within the tephra, is too young and likely on roots.

## Chapter 4 Bagley Creek

Landforms were mapped on stereo air photos and topographic maps in Bagley Creek with special attention to moraines. Reconnaissance field mapping of deposits and landforms was done in September 1999. The Bagley Creek field area overlaps with the Ph.D. study area of Dori Kovanen, who is at the University of British Columbia. We are currently collaborating and jointly naming features. However, all work presented here is my own.

Bagley Creek basin is located ~ 5 km northwest of south Swift Creek cirque (Figure 1.2) and is comprised of a well-developed cirque and glacial trough with an area of ~1 km<sup>2</sup> (Figures 4.1, 4.2, and 4.3). The Bagley Creek valley is a hanging valley to the North Fork Nooksack River valley. The upper, northeast-facing slope, in the crook of the L-shaped Table Mountain, is a poorly developed cirque that hosts a small, unnamed glacier (0.05 km<sup>2</sup> area) at 1550-1710 m (5100-5600 feet) (Figures 4.1, 4.2, 4.4). This glacier was identified in the Post et al. (1971) glacier inventory as being 0.10 km<sup>2</sup> in area, but now appears to be little more than a permanent snowfield. The lower, well-developed, east-facing cirque has an average floor altitude of 1340 m (4400 feet). It is floored with sculpted bedrock, drift, talus, and rockfall deposits. The northeast-trending, U-shaped valley below the lower cirque (1160-1340 m; 3800-4400 ft) is floored with sculpted bedrock and littered with glacial drift. The upper of two glacially scoured tiers in the valley bottom is Heather Meadows. The lower tier of the valley has been incised by Bagley Creek. The creek also occupies the contact between Mt. Baker andesite and Mt. Herman greenstone of the Chilliwack Terrane. Cuts from roads and trails reveal subsurface stratigraphy of end moraines at the lower end of Bagley Creek valley (Figure 4.1, 4.2, 4.3, 4.5).

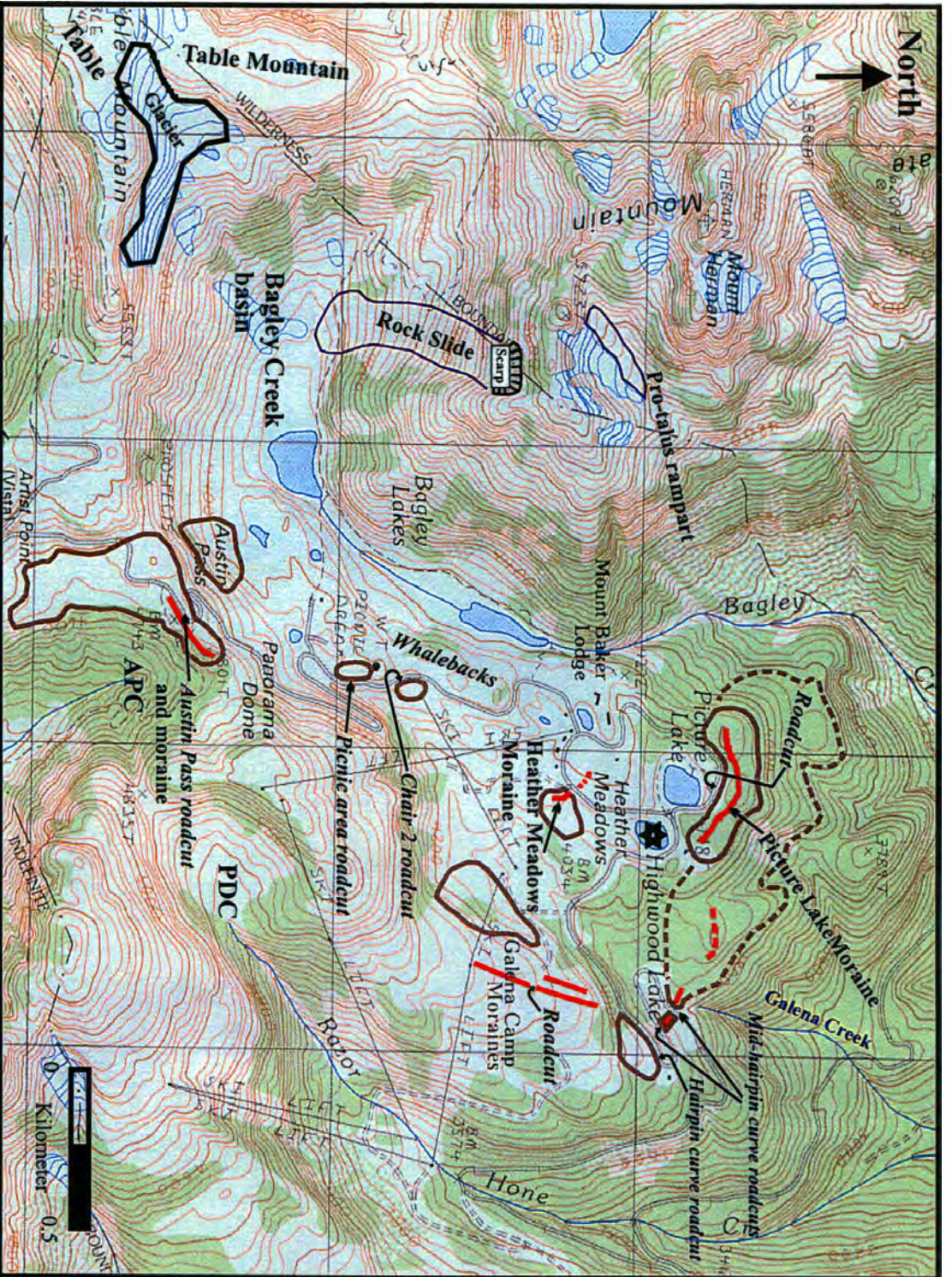


Figure 4.1 Glacial deposit and landform map of the Bagley Creek trough.

**Legend**

- ★ Core Location
  - Undifferentiated drift
  - Present Day Glacier
  - Pre-Mazama moraine crest
  - Dashed lines are inferred moraine boundaries
  - APC Austin Pass Cirque
  - PDC Panorama Dome Cirque
- Contour Interval:  
40 feet
- Source: Shuksan Arm,  
USGS 7.5 minute  
Quadrangle

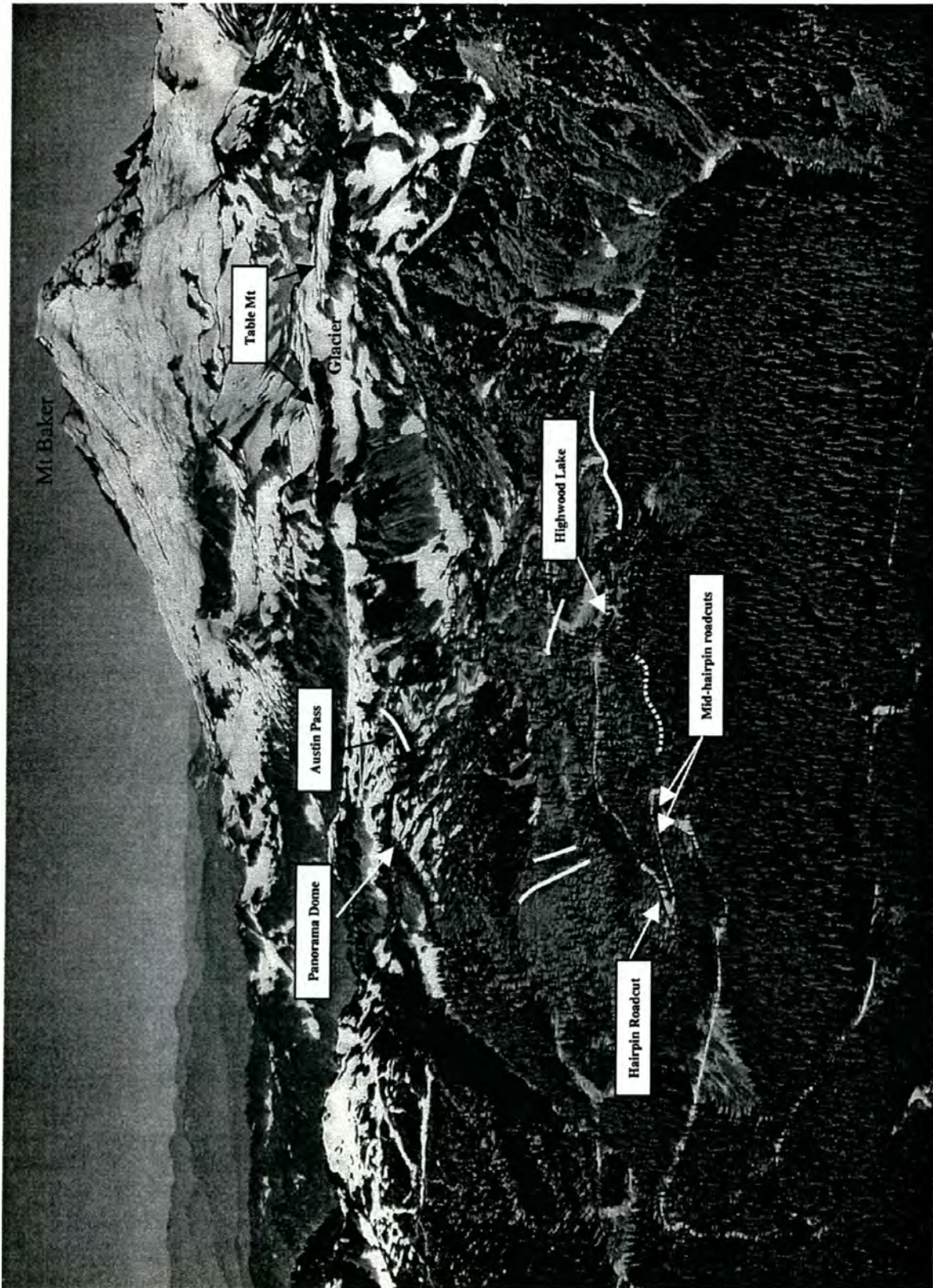


Figure 4.2 Aerial oblique view of Heather Meadows and Bagley Creek looking up the valley to the southwest. The white lines show moraine crests, dashed lines are inferred (compare with Figure 4.1 and 4.3). Photo courtesy USDA Forest Service. Photographed 09/04/72.

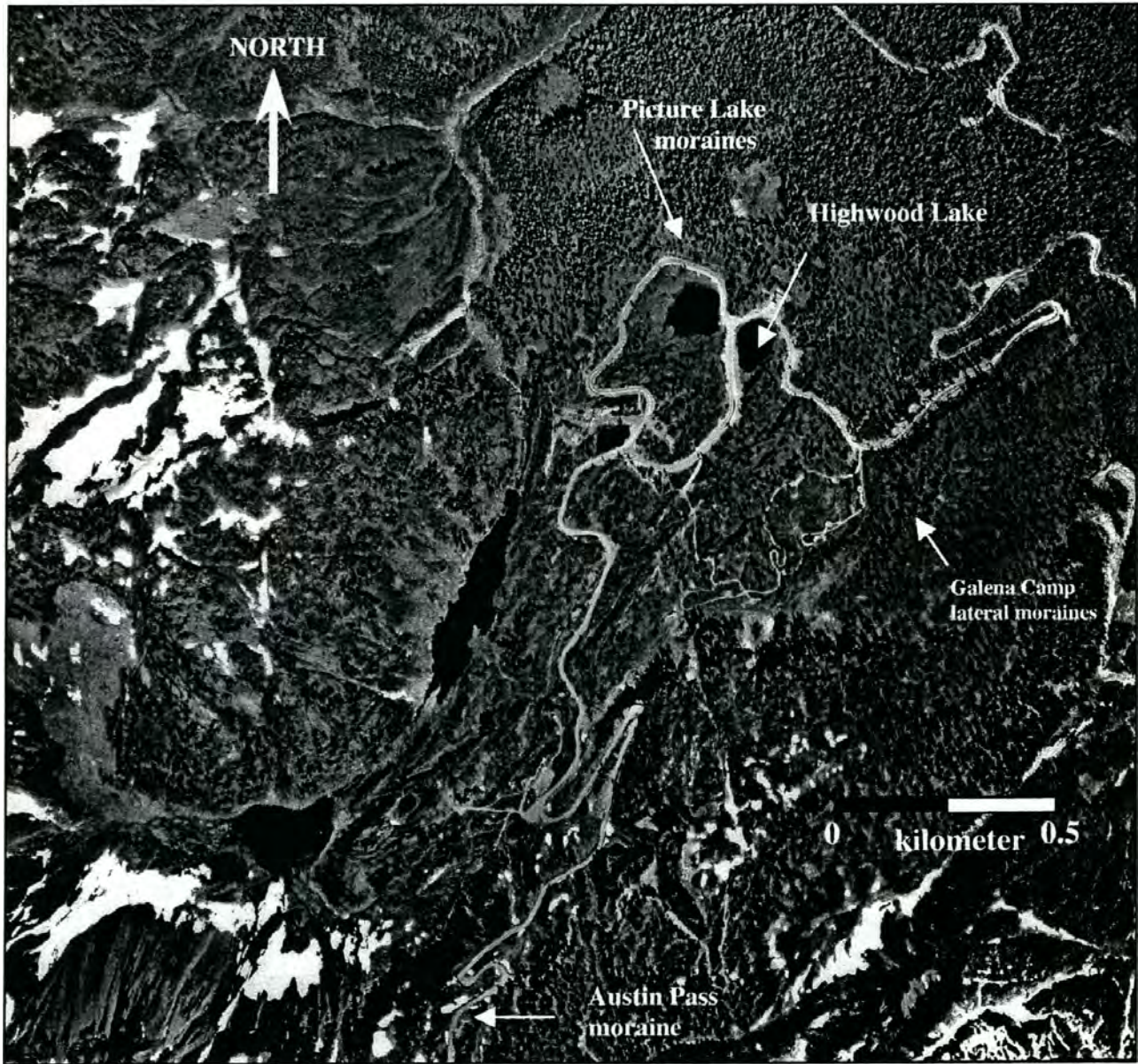
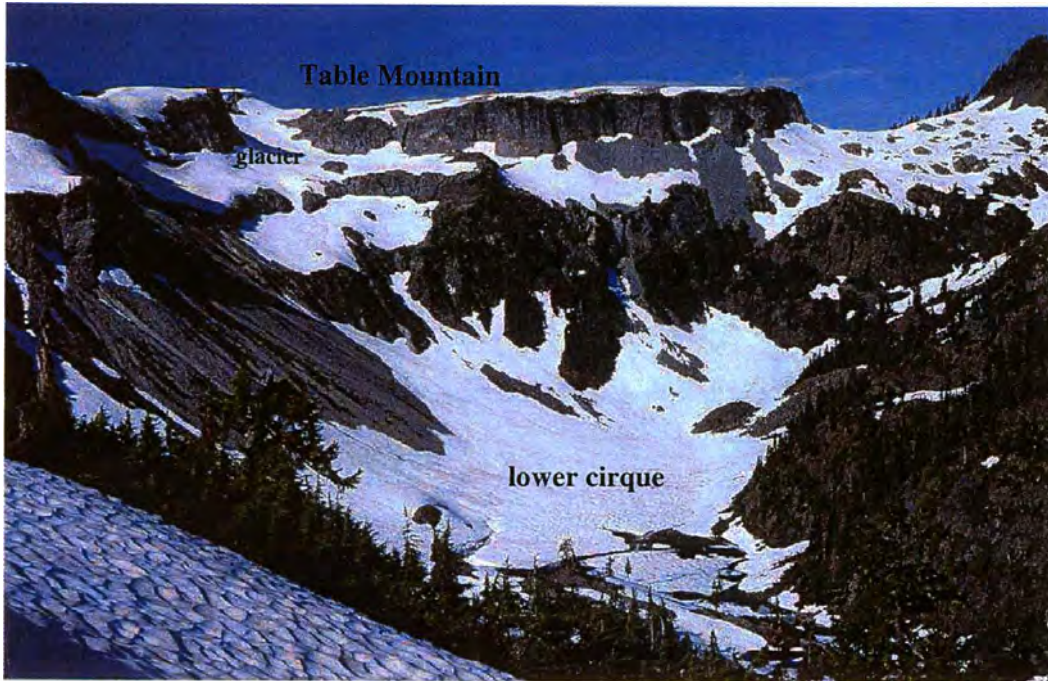
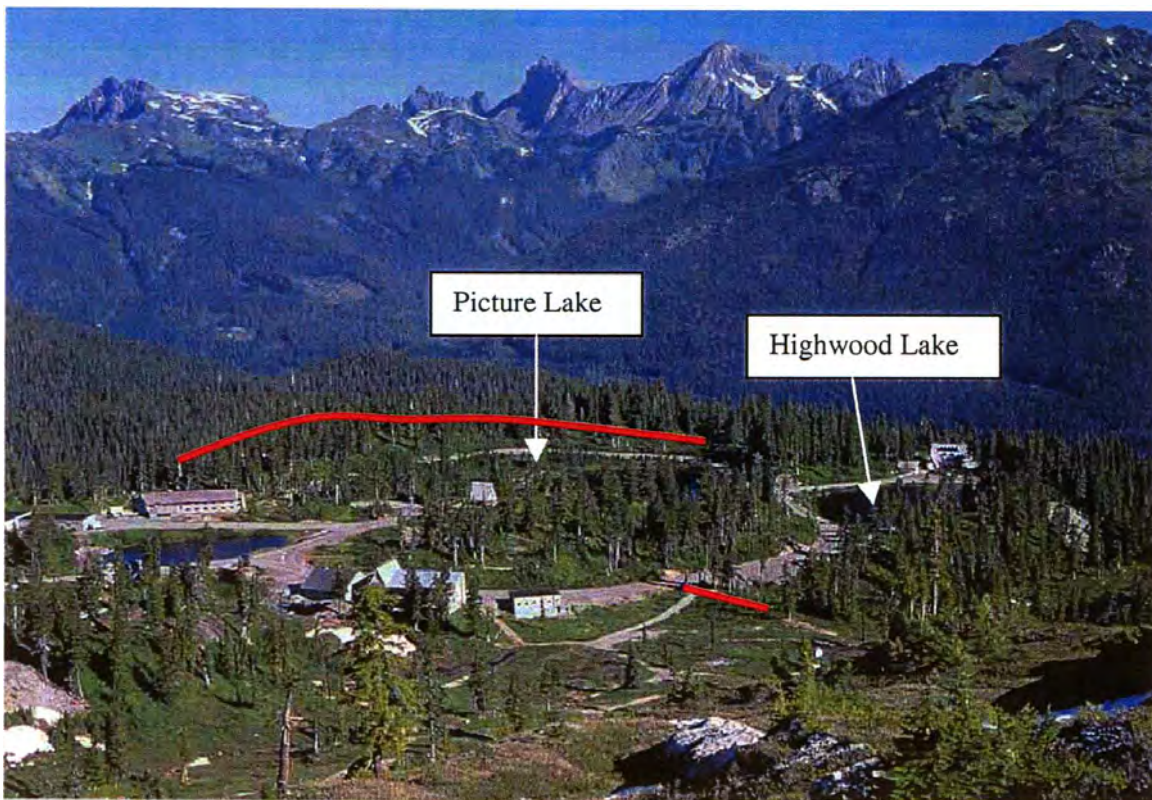


Figure 4.3 Vertical air photo showing lower Bagley Creek and Heather Meadows.



*Figure 4.4* The view looking west into Bagley Creek cirque from Austin Pass. The Bagley Creek glacier is on the upper right and upper Bagley Lake is in the lower left. Note large amount of snow accumulation on the cirque floor, due to avalanching during the winter. The photograph was taken in late September 1999.



*Figure 4.5* View looking northwest on lower Bagley Creek trench and end moraine complex. Heather Meadows moraine (short line) and Picture Lake moraine (long line) are both in red.

### *Moraine Morphology and Stratigraphy*

Much of the valley floor of Bagley Creek trough is littered with pockets of drift and lineated, sculpted, columnar andesite. Whalebacks, whose long axes trend down valley (northeast), are abundant (Figure 4.6). The Heather Meadows picnic area roadcut (Figure 4.1) is ~100 m long and 2-3 m high and is representative of the stratigraphy for much of the valley floor. It reveals a 1-2 m thick veneer of till overlying columnar andesite. The till consists of a clay, silt, and sand matrix surrounding cobbles and boulders of andesite and greenstone.

Two distinct lateral moraines that occupy the broad, flat rise of the Galena Camp locale are named the Galena Camp moraines (Figure 4.1) (Burrows and Kovanen, in progress). A road cut through the uppermost moraine reveals till with a silt-clay matrix and many andesite cobbles and boulders (Figure 4.7). The moraines are 2-3 m high and 3-5 m wide. A pocket of till, identified by a road cut and gullying, occurs topographically below but slightly up valley from the crested lateral moraines (Figure 4.8). Gullying indicates the extent of the till, and the road cut into the till reveals a composition similar to the moraine above it. Approximately 700 m to the west of this complex is a small end moraine, named the Heather Meadows moraine (Burrows and Kovanen, in progress) (Figure 4.1, 4.2, 4.3, and 4.5). This moraine, identified on the basis of morphology and gullying is ~1-2 m high by ~4-5 m wide, with a broad but distinct crest.

A hummocky end moraine complex occupies the edge of Bagley Creek trough to the north of Highwood and Picture Lakes (Figures 4.1, 4.2, 4.3, & 4.5). The morphology here consists of moraine crests and bedrock knobs. A distinct, sharp-crested, end moraine (named the Picture Lake moraine (Burrows and Kovanen, in progress)) occurs north of Picture Lake (Figures 4.1, 4.2, & 4.5). Roadcuts 1-3 m high on the north side of Picture Lake reveal a well-indurated diamicton with a silt and sand matrix, which contains pebbles and cobbles of andesite and greenstone (Figure 4.9).

A crested end moraine is transected in two places at the mid-hairpin curves of the Mt. Baker Highway (see Figure 4.1). These roadcuts are 3-4 m high and 5-6 m wide and reveal a diamicton similar to those in the Picture Lake road cuts. The 2-4 m high and ~200



*Figure 4.6* A whaleback on the valley floor of Bagley Creek trench. The long axis of the whaleback is ~ 40 m.

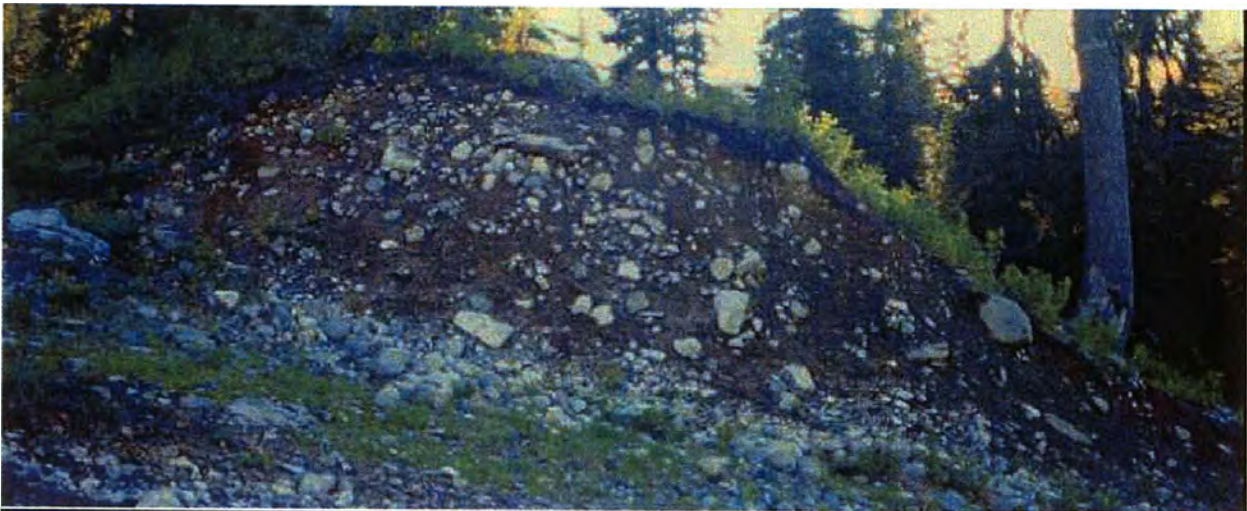


*Figure 4.7* Road cut of the upper Galena Camp lateral moraine. Cut is approximately 2.5 m in height.

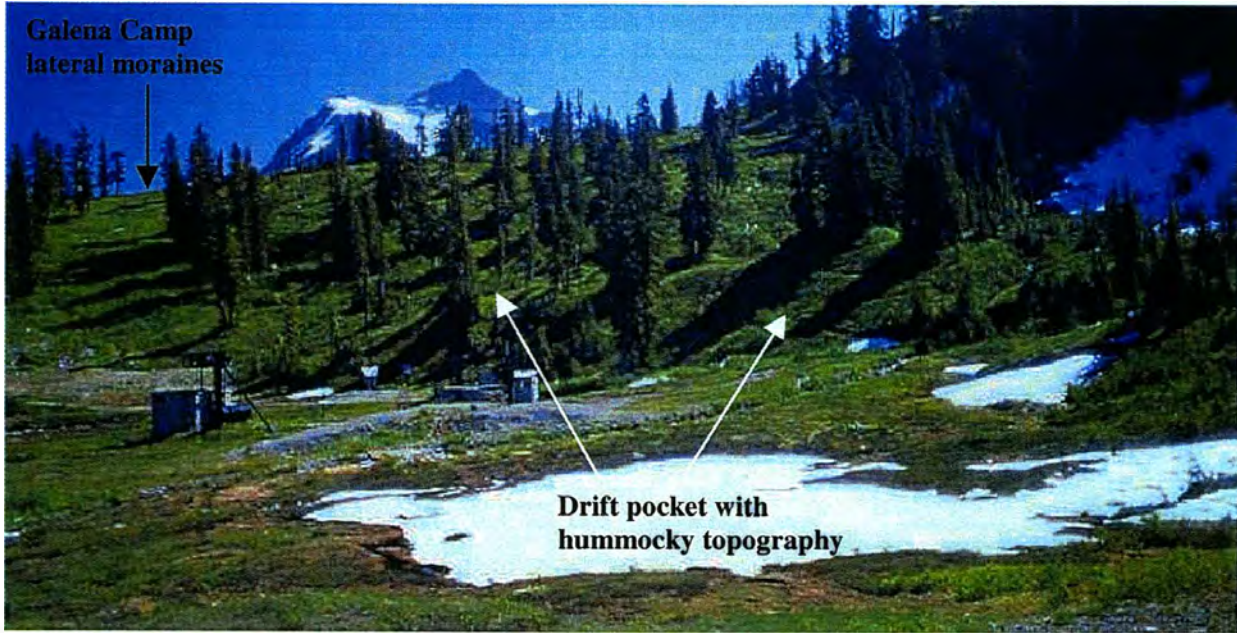


*Figure 4.8* The pocket of drift below the Galena Camp moraines is the hummocky topography at the base of the slope. The lateral moraines are on the crest of the ridge. This view is looking east with Mt. Shuksan in the background.

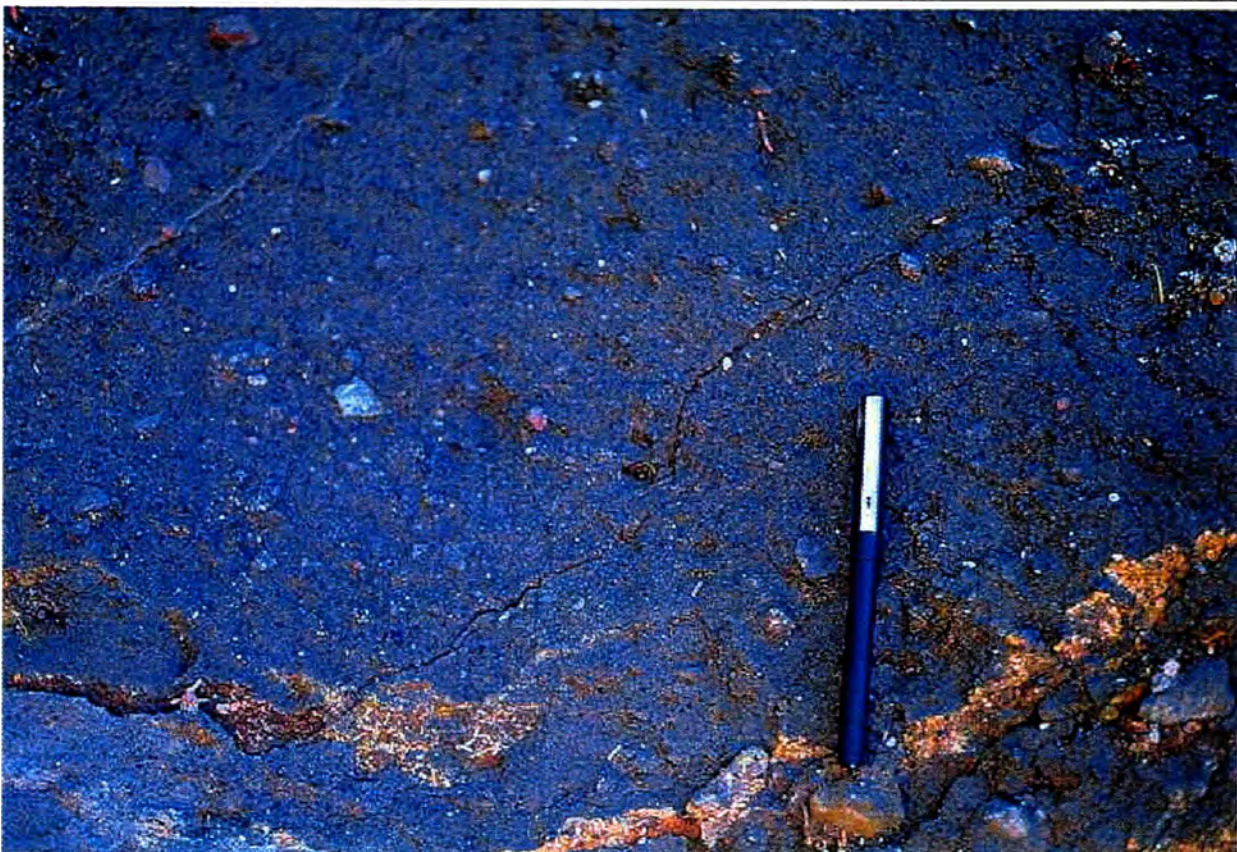


*Figure 4.9* The diamicton of the Picture Lake road cut. Pen for scale.

m long upper hairpin road cut is composed of till with many striated cobbles of andesite and greenstone (Figure 4.10). The gently sloping morphology upslope (southeast) from the cut indicates that this is a pocket of till rather than a distinct moraine crest.

Austin Pass is a notch in the southeast valley wall of the Bagley Creek trough (Figure 4.1). The pass is a low point (1430 m (4700 ft)) between the east rim of Table Mountain (1690 m (5550 ft)) and Panorama Dome (1520 m (5000 ft)). At the pass is a crested moraine with an excellent road cut revealing till (Figure 4.11), that contains cobbles and boulders of andesite from Table Mountain and Mt. Herman greenstone. A pocket of drift, with surface gullying characteristics of unconsolidated deposits (Figure 4.12), occurs below Austin Pass at the edge of the Bagley Creek valley floor (southeast side of the pass).

Austin Pass cirque (APC on Figure 4.1), southeast of Austin Pass, has a floor altitude of ~ 1280 m (4200 ft). A bench occurs at an altitude of ~ 1370 m (4500 ft) below Artist Point on the west side of the cirque headwall (Figure 4.1). The bench is mantled with drift, as indicated by hummocky topography and gullying. This debris may comprise a kame terrace that was formed as a result of ice below the bench in Austin Pass cirque. In addition, a substantial amount of drift with possible moraine crests lies where the cirque opens up into the greater Swift Creek basin (not shown).

Two post-Mazama depositional landforms occur on Mt. Herman (Figure 4.1 and 4.3). A pro-talus rampart at 1590 to 1650 m (5200-5400 ft) occupies a small northeast-facing cirque on the north side of Mt. Herman. The second deposit, a rockslide on the south-southwest flank of the mountain, is ~ 250 m wide and 600 m long from the scarp to the floor of the lower cirque (Figure 4.1 and 4.3).

### *Sediment Cores*

Six cores were collected from Highwood Lake with a modified Livingstone piston corer. The sediments were sampled at locations near the central, deepest part of the lake (Figure 4.1 and 4.13) in water 6.7 to 7.6 m (22-25 ft) deep. Results of analysis of three cores (HL-3, HL-6, and HL-7) are presented here. The stratigraphies of the overlapping sections of cores HL-6 and HL-7 are nearly identical. They have been combined into a single



*Figure 4.10* A road cut of till at the hairpin curve. Shovel on the right is ~0.5 m in height.

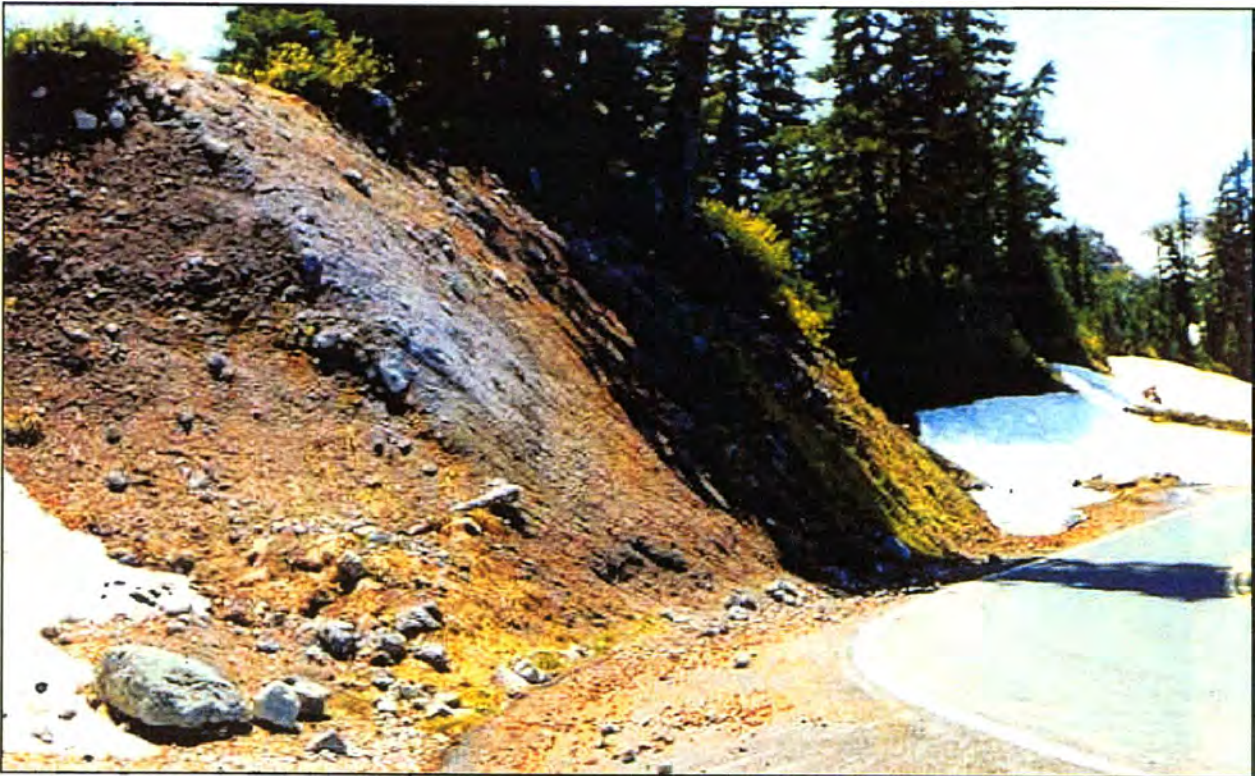


*Figure 4.11* The road cut of the Austin Pass moraine. The view is looking southwest and the cut is approximately 2.5 m high.

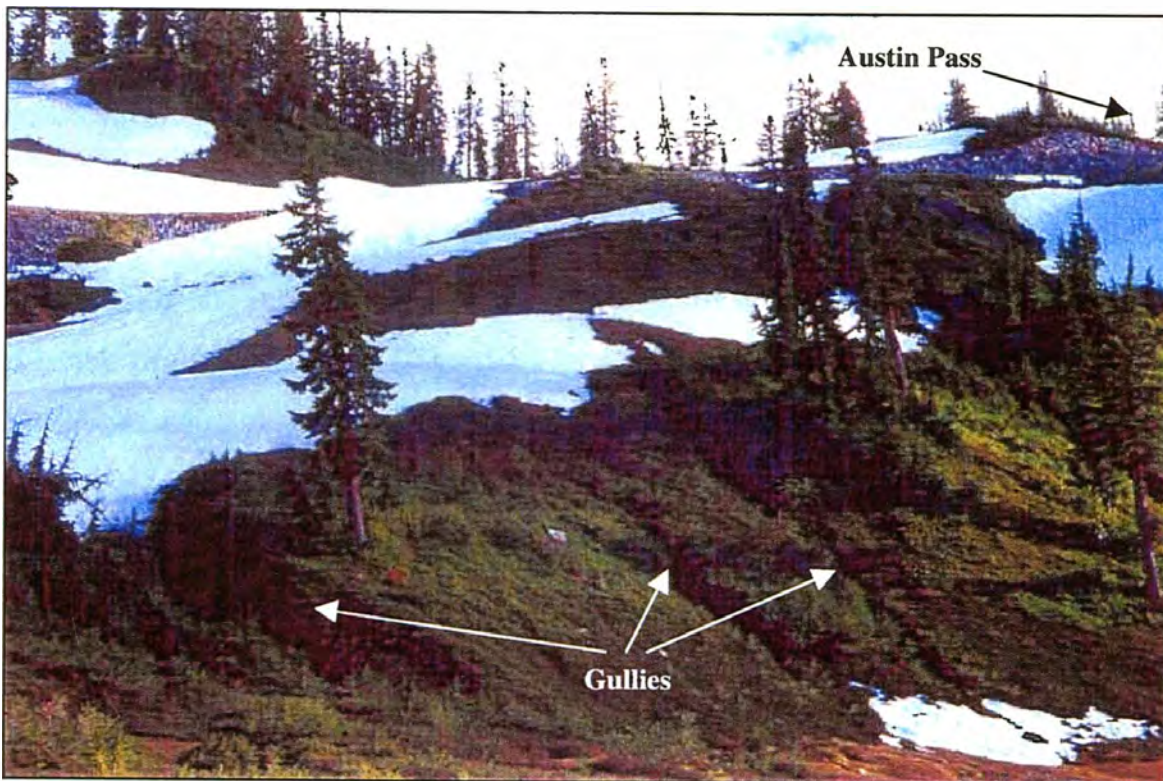


*Figure 4.12* The pocket of drift below Austin Pass. Note the gullies in the foreground. The trees in the foreground are 18-24 m tall for scale.



*Figure 4.13* Highwood Lake, looking to the north. Note the small fan/delta in the foreground.

composite section (Figure 4.14) to eliminate possible gaps in the core record resulting from the coring process. Radiocarbon dates on samples from cores HL-3, HL-4, and HL-7 are shown on equivalent horizons in Figure 4.14 (see also Table 4.1).

Magnetic susceptibility (MS) is used here as a general inverse proxy for organic content of lake sediment (high MS equates to low organic content). Here MS distinguishes between organic and inorganic sediment in the core and provides a quantified companion index to the visual stratigraphy (Figure 4.14). Loss-on-ignition (LOI) analysis is another excellent companion index to visual stratigraphy for a mountain lake sediment core. Loss-on-ignition measures the amount of combustible carbon within an 8 cm<sup>3</sup>-volume sample. Most carbon in shallow mountain lake sediments in the field area is organic so LOI approximates the amount of organic material present, although the technique can also dehydrate micas and clay minerals. Figure 4.15 compares LOI and MS from core HL-3. To the first order the LOI and MS curves are inversely related (Figure 4.15). Thus, samples with high organic content generally have a low magnetic susceptibility. However, in the sediment interval with high, variable MS at the bottom of the core (predominantly inorganic sediments), the abundance of magnetic minerals varies and this indicates changes not related to organic content. Generally, magnetic susceptibility is used as an inverse proxy for organic content of lake sediment. Thus since the first-order relationship was consistent in Highwood Lake, LOI was not conducted on other cores.

The top 43-cm of composite core HL-6 and 7 is massive dark brown, gelatinous gyttja with low MS, except for a small peak in the top 10 cm, which is probably related to historic clastic sedimentation during construction of the road that borders the lake (Figure 4.14). Below the gyttja, 15 cm of laminated Cathedral Crag tephra (CCT) displays the highest MS of the core sediments. Each lamination in the tephra consists of a layer of light brown silt and sand and a layer of black sand that appear to comprise a couplet. Approximately 27 couplets occur in the CCT in HL-6. A thin (~2 mm) light gray, silt parting underlies the tephra. Below the parting is 8 cm of dark brown gyttja with very low MS. Below the gyttja is 7 cm of Mazama ash with moderate MS. The top 2-cm of Mazama ash is transitional ash/gyttja. Forty-three centimeters of massive, dark brown, compact gyttja

with very low MS underlies Mazama ash. An inclined layer of dense, black, charcoal-like material occurs in the lower 5-10 cm of lowermost gyttja at ~ 100 cm core depth. The charcoal-like material is 2-4 mm thick with slickensided partings. The lowest 8 cm of gyttja grades into silt, with MS increasing downward to the basal silt of the core. The basal unit consists of 27 cm of yellow-gray laminated silt with high, generally increasing MS. Textural analysis indicates that 94-99 percent of the basal unit is silt and clay. The laminations appear to be couplets of yellow-gray-colored silt and clay and black very fine and fine sand. Approximately 115 couplets are present.

Analysis of the basal silt and clay shows that the peaks in the MS curve (Figure 4.14) correlate with better defined laminations, whereas less well defined laminations in the silt correlate with low MS values. Textural analysis of the silt with depth shows that the laminations are well defined because they contain distinct layers of black, very fine sand.

A radiocarbon date on gyttja at the base of the CCT (54 cm core depth in core HL-4) yielded  $6210 \pm 40$   $^{14}\text{C}$  years B.P. (6990-7250 cal. years B.P.) (Table 4.1, Figure 4.14). This date is the oldest, closely limiting, maximum age for the tephra found in this study. A twig stuck in both the base of Mazama ash and in the top of the gyttja at 69 cm depth in core HL-3 yielded a radiocarbon date of  $6850 \pm 50$   $^{14}\text{C}$  years B.P. (7590-7780 cal. years B.P.), confirming the Mazama ash designation. A small Y-shaped twig was recovered in gyttja at 80 cm depth in core HL-7. Radiocarbon dates from the twig and the surrounding gyttja are statistically indistinguishable within 1-sigma uncertainty at  $8160 \pm 50$   $^{14}\text{C}$  years B.P. (9010-9270 cal. years B.P.) and  $8230 \pm 60$   $^{14}\text{C}$  years B.P. (9030-9400 cal. years B.P.), respectively. The oldest radiocarbon date in core HL-7,  $9410 \pm 50$   $^{14}\text{C}$  years B.P. (10,430-11,040 cal. years B.P.) was obtained from the lowermost charcoal-like material, just above the gyttja-silt transition zone at 100 cm depth. The charcoal-like shear zone may be contaminated with younger material from above and/or older material from below. Despite this uncertainty the date is considered at face value.

Most of the stratigraphy of the core reflects organic sedimentation (gyttja). Inorganic sedimentation events include the two tephtras that were deposited from a combination of air fall and subsequent slope wash, and the basal laminated silt, the origin of which is discussed

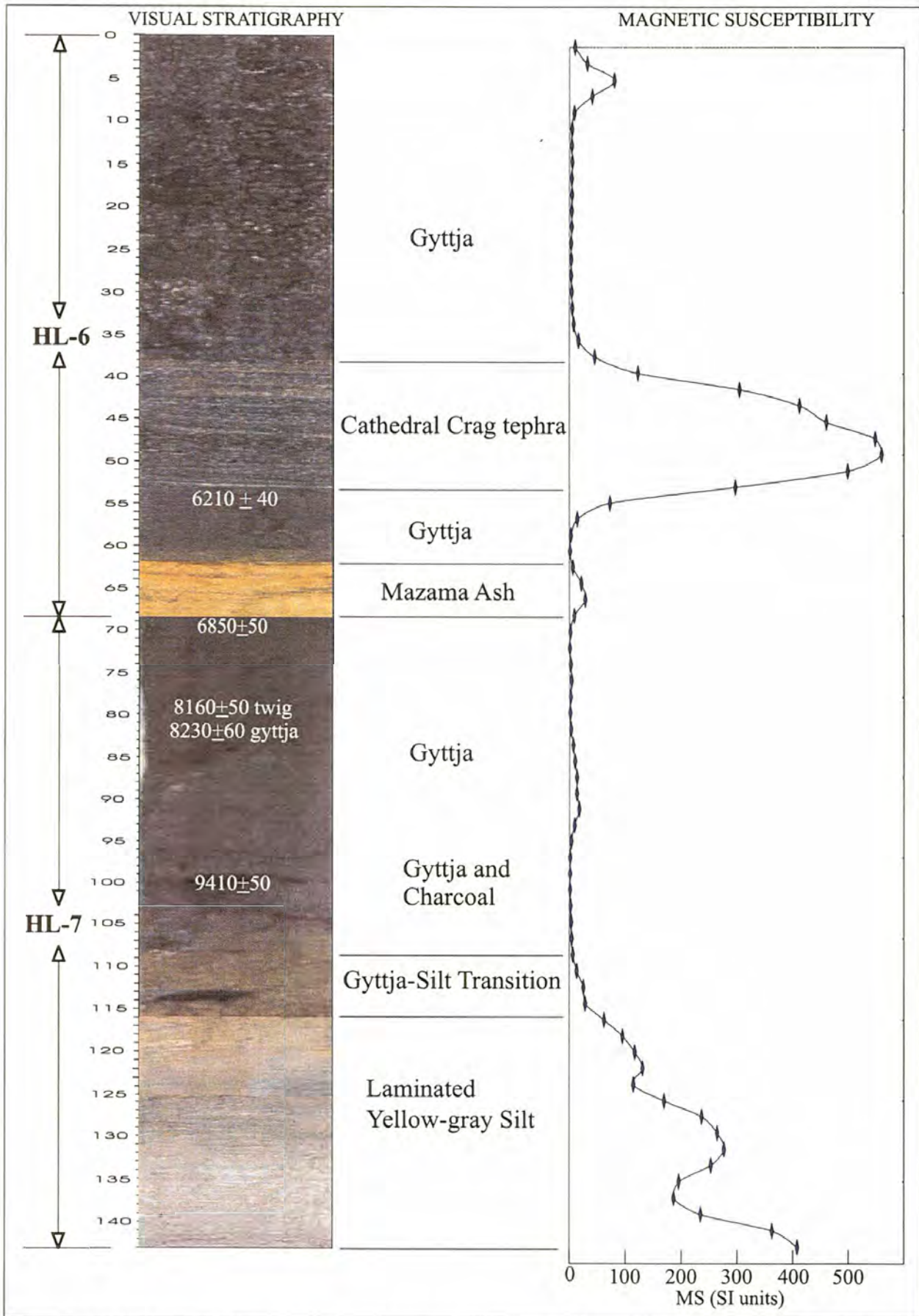
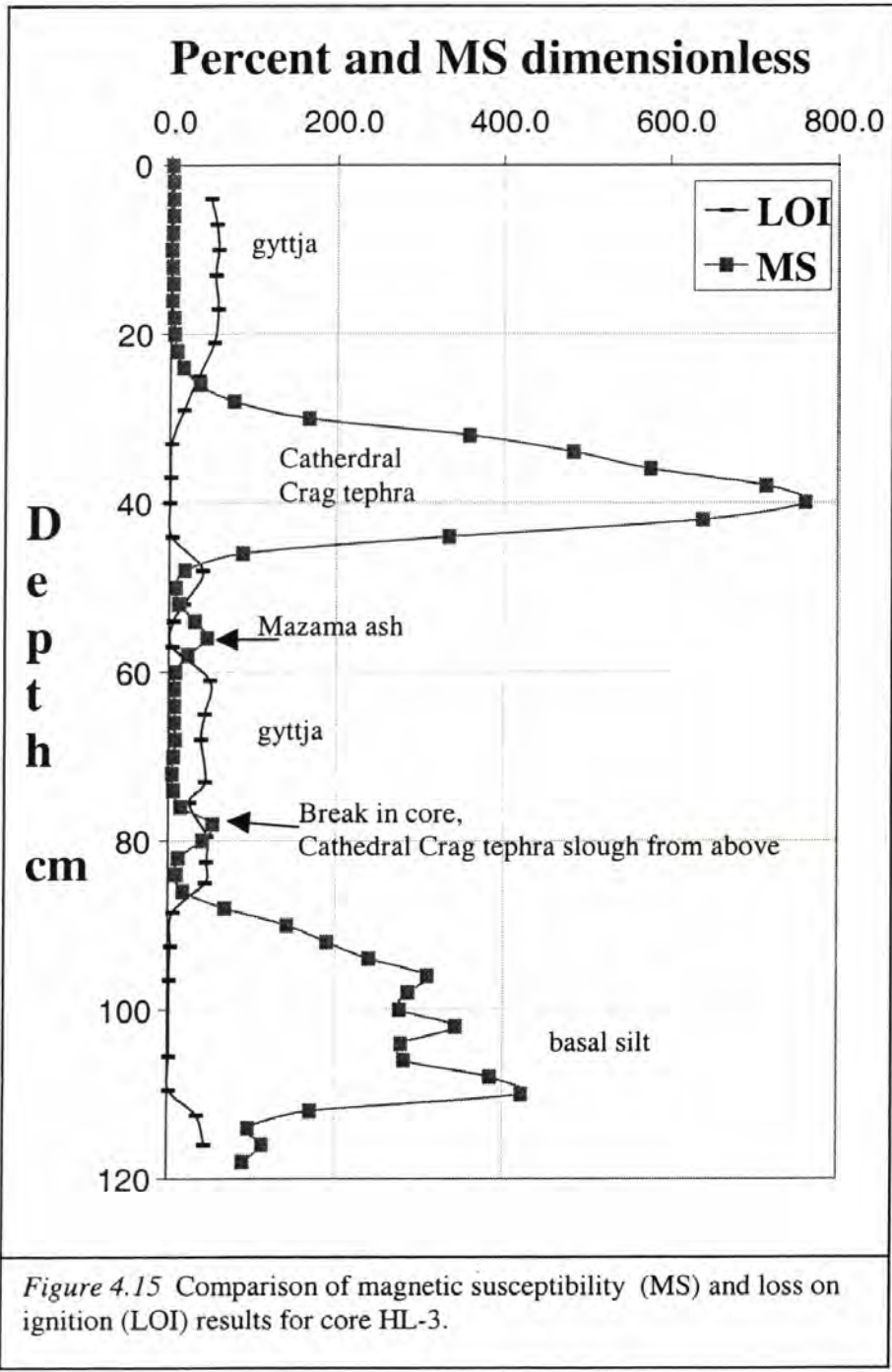


Figure 4.14 Highwood Lake core stratigraphy, magnetic susceptibility, and important radiocarbon dates from cores HL-6 and HL-7. Depth units are in centimeters.



Sample ID	C-14 Age	2 sig SD ±	2 sigma (95.4 %) calibrated age range		area under probability curve	Sample Description	Lab Code
			BP age max	BP age min			
HL7c1	9410	100	11040	11024	0.016	charcoal-like material in basal gyttja	CAMS-59594
			10992	10968	0.018		
			10753	10494	0.958		
			10436	10433	0.008		
HL7c3	8160	100	9267	9156	0.343	Twig in gyttja	CAMS-59595
HL7c4	8230	120	9399	9341	0.128	Gyttja around twig	CAMS-59596
			9324	9029	0.872		
HL4c4	6210	100	7250	6986	1	Gyttja at base of Cathedral Crag tephra	CAMS-59597
HL3c1	6850	100	7783	7775	0.025	Twig at base of Mazama ash	CAMS-59598
			7756	7588	0.975		

Table 4.1 Highwood Lake core radiocarbon dates.

below. Rythmites present in the CCT and basal silt suggest varves. Varves are likely because (1) each varve couplet consists of a layer of fine sediment and a layer of coarser sediment (Figures 4.10 and 4.11) and (2) Highwood Lake currently receives a persistent winter snow cover (it does not freeze over; rather it receives so much snowfall that a layer 2-4 m thick of snow, slush, and discontinuous ice covers the lake throughout most winters) that would have the same effect on reducing the depositional energy of the lake during the winter that lake ice would. Twenty-seven varves in the CCT would equate to 27-year period of deposition and 115 varves in the basal silt would equate to a 115-year period of deposition. Thus, relative to the gyttja intervals, these inorganic layers could be nearly instantaneous.

The most likely explanation for the origin of the basal silt is that it reflects deglaciation and subsequent pre-vegetation slopewash sedimentation. In this scenario, the Bagley Creek glacier retreated from the Picture Lake moraine rapidly, leaving only patchy ground moraine and bare bedrock in the surrounding lake basin. A small amount of water and sediment from the retreating glacier would have been shed into Highwood and Picture Lakes but most runoff would have been shed down Bagley and Galena Creeks (see Figure 4.1 for location of creeks). A small fan/delta at the head (south end) of Highwood Lake (Figure 4.13) could be a product of the rapid recession or simply post-glacial stream and slope wash. For a time after recession (years), abundant unvegetated till and rock flour would have been easily washed into the lake by slopewash, possibly on a seasonal cycle (if the couplets are varves). Gradually, as more vegetation became established and stabilized the slopes, lake sedimentation would have shifted from inorganic to organic (gyttja), as seen in the sediment cores (which the transition from silt to gyttja in the Highwood Lake core could be interpreted to indicate) (Figure 4.14).

Several lines of reasoning indicate that the basal silt of Highwood Lake is locally derived, rather than a distant source such as a tephra or eolian deposition related to the Cordilleran ice sheet. A volcanic glass microprobe analysis and database correlation shows that the basal silt has very altered glass (possibly from glacially scoured sediment in a basin

with volcanic bedrock) and does not correlate with any known tephras near in age to the basal limiting date of  $9410 \pm 50$   $^{14}\text{C}$  years B.P.

The mineralogy of the basal silt unit was compared to nearby till. The sand and clay fraction from one sample of till from the Picture Lake road cut and nine samples of the basal silt from the cores were dry sieved. Two samples from the basal silt and one sample of the till were analyzed for abundant minerals using standard packed powder X-ray diffraction techniques. Results yielded a very similar diffraction peak pattern for the lake silt and till. Diffraction peak patterns were clear for hypersthene and plagioclase in all cases but other minerals were difficult to identify. Other possible minerals include enstatite, chlorite, and actinolite (most diffraction peaks are present but not prominent). Most of the minerals compare to part of the local bedrock mineralogy of the Mt. Baker andesite (plagioclase, hypersthene, clinopyroxene, olivine, and hornblende (Coombs, 1939; Stavert, 1971)) and Mt. Herman greenstone (chlorite, actinolite, and epidote).

Two additional points lend support to a local source. First is that the silt is the basal-most sediment in the lake and directly overlies bedrock or coarse till (coring efforts always bottomed on rock). Thus, one would expect the basal sediment in an obviously deglaciated lake basin to be inorganic fine sediment. Second, the silt is biologically sterile, that is no macrofossils were recovered and LOI shows virtually no organic material present, also typical of a recently deglaciated basin.

## Chapter 5 Interpretation and Chronology

Past glaciers in the study area are reconstructed by combining information from moraines, erratic location and provenance, trimlines, topography, and patterns of modern glacier surfaces and margins. For this study, the glacier reconstructions are drawn to approximate glaciers at a neutral mass balance. They are subjective but are based on the best available information.

### *Swift Creek and Shuksan Creek Glacial Chronology*

The uppermost moraines in south Swift Creek cirque (SSC) demonstrate characteristics of deposition in the late Little Ice Age by the absence of tephras, lack of soil and vegetation development, and bouldery surfaces (Figures 3.5 and 3.7). The oldest tree associated with these moraines grows on bedrock inside the right lateral moraine (see Figure 5.1 for location). The tree is 79 years old from A.D. 1998. The addition of 15 - 35 years ecesis time for the establishment of the tree (Long 1953, Miller 1969, Leonard 1974, Heikkinen 1984), places the minimum age of deposition of the moraine sometime between A.D. 1884 and 1904. Because the oldest trees on the end and left lateral moraines are of similar age (77 and 70 years old, respectively) and a coherent continuous margin can be drawn to connect them, all the uppermost moraines in south Swift Creek cirque appear to be contemporaneous.

Surface characteristics of the uppermost moraines in high Swift Creek cirque (HSC) closely resemble those of south Swift Creek cirque. In high Swift Creek cirque, an 85 year-old (from A.D. 1998) tree grows on the upper of the two highest moraines. The age of this tree with the addition of 15- 35 years ecesis time places the minimum age of deposition of the moraine sometime between A.D. 1878 and 1898. This moraine thus appears to be contemporaneous with the uppermost moraines of south Swift Creek cirque. The lower high Swift Creek cirque moraine has virtually identical surface characteristics to the upper moraine (except no trees grow on the lower). The two upper moraines in high Swift Creek

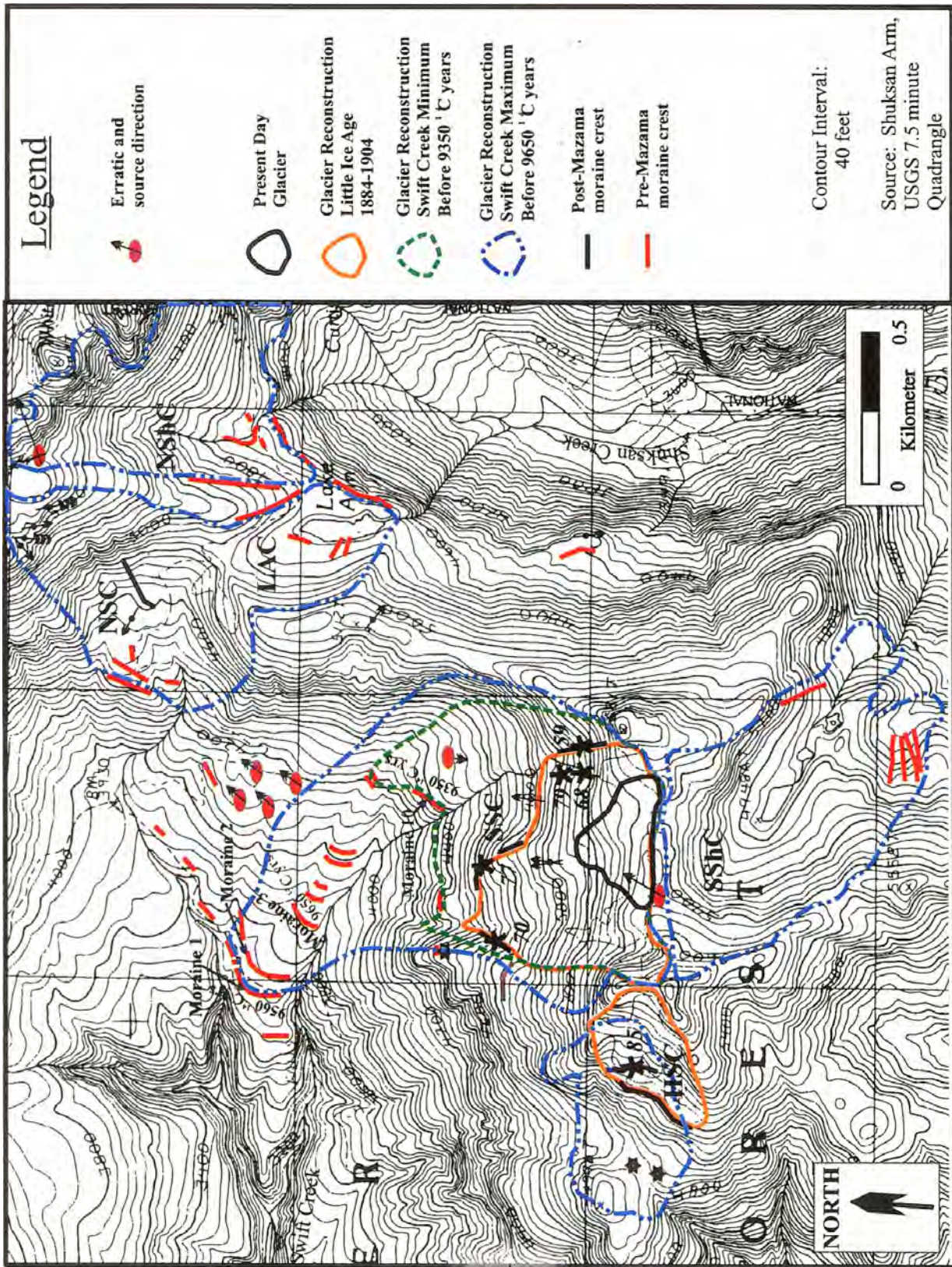


Figure 5.1 Swift Creek and Shuksan Creek glacier reconstructions. NSC = North Swift Creek Cirque; SSC = South Swift Creek Cirque; HSC = High Swift Creek Cirque; NShC = North Shuksan Creek Cirque; SShC = South Shuksan Creek Cirque; LAC = Lake Ann Cirque.

cirque were therefore most likely deposited within decades of each other rather than being separated by hundreds or thousands of years. All of the upper moraines in Swift Creek were deposited late in the Little Ice Age (LIA) and are hereafter referred to collectively as the Swift Creek LIA moraines.

The small area, distinct moraine extent, trimlines, and cirque topography, made reconstruction of Little Ice Age glacier margins relatively straightforward. However, reconstruction of the pre-Mazama extents are more subjective. All of the maximum reconstructions in Figure 5.1 are based on the outermost pre-Mazama moraines, whereas the minimum reconstructions are based on the innermost. The moraines from cirque to cirque may or may not be contemporaneous, but the maximum reconstruction lines for all cirques are designated the same line-type and color in Figure 5.1. The minimum limiting ages are also indicated on the figure.

Radiometric minimum ages on pre-Mazama moraines in the Swift Creek and Shuksan Creek area were obtained only for the south Swift Creek cirque moraines from the Swift Creek cores. The two oldest bog bottom dates from Swift creek cores constrain the three lowermost south Swift Creek cirque moraines with close minimum ages (moraines 1-3, Figure 5.1). The oldest date,  $9650 \pm 50$   $^{14}\text{C}$  years B.P. (10,760 - 10,960, 10,990 - 11,020, 11,040 - 11,180 cal. years B.P.) from charcoal near the base of core SC-7 (Figure 5.2), is from a bog just upvalley from moraine 3 (Figure 5.1). The second oldest radiocarbon date,  $9560 \pm 50$   $^{14}\text{C}$  years B. P. (10,690 - 11,110 cal. years B.P.) from peat near the base of core SC-2 (at a depth of 55 cm) (Figure 5.2) was obtained from a small bog a few meters downvalley from moraine 1 (Figure 5.1). The radiocarbon ages of these two dates overlap at 1-sigma, making them statistically indistinguishable.

The oldest minimum age for moraine 10 (Figure 5.1) of  $9350 \pm 180$   $^{14}\text{C}$  years B. P. (10,210 - 11,130 cal. years B. P.) is not significantly different from the two dates discussed above. This date is on a tree branch from the base of core SC-8 at ~106 cm depth. The lowermost 15-cm (95-110 cm depth) of core SC-8 is organic-rich silt with abundant conifer needles and wood (Figure 5.2). Abundant wood at the base of the core suggests that trees

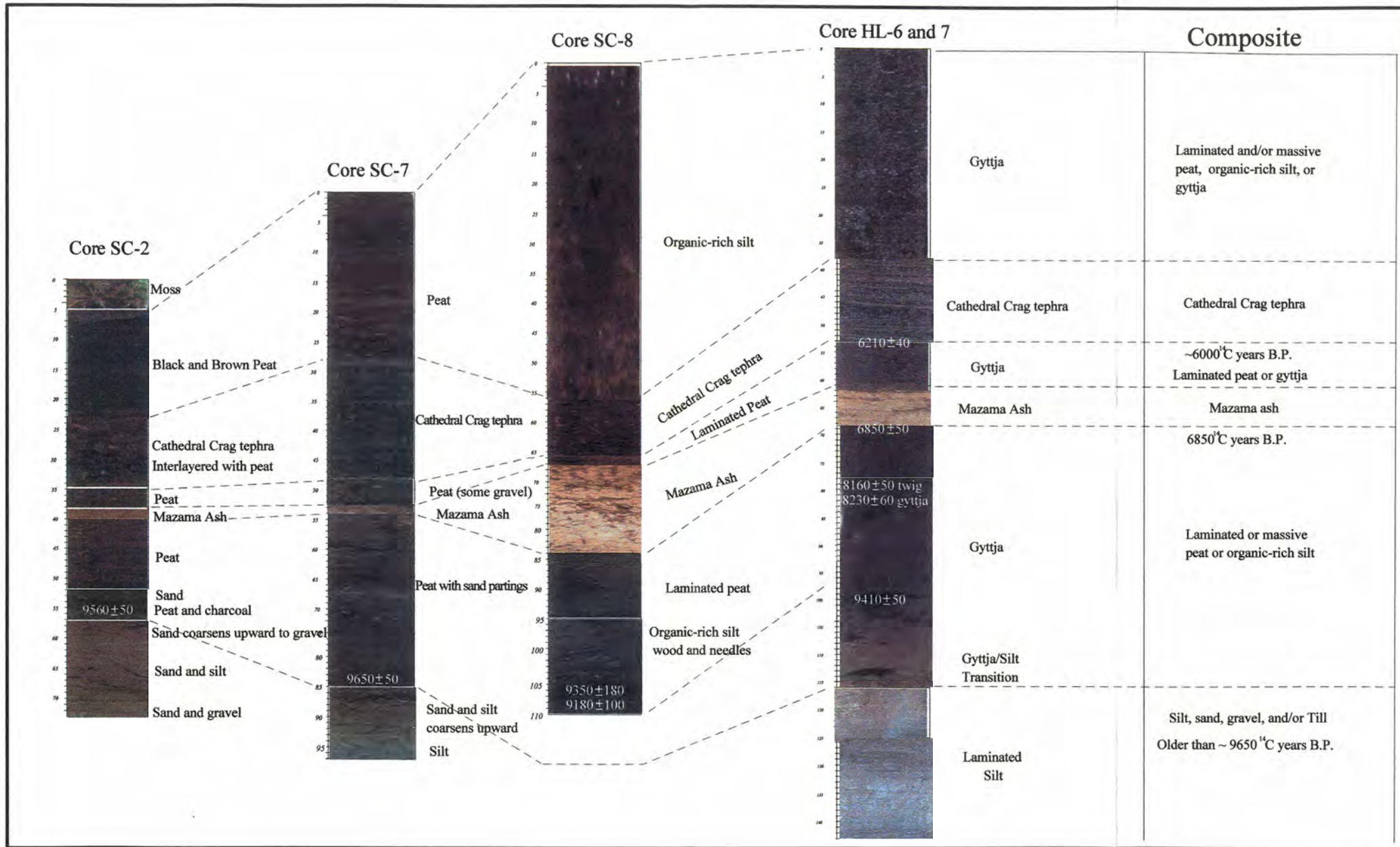


Figure 5.2 Correlation of Swift Creek cores and Highwood Lake core. See Figures 3.2 and 4.1 for locations of cores. All ages are radiocarbon dates with  $\pm 1$  sigma standard deviation. Depth units are in cm.

were growing next to the pond at the time of deposition, perhaps similar to the modern environment (See Figure 3.15).

The south Swift Creek cirque moraines are small (1-3 m in height) and thus probably do not represent much time for deposition. This inference is supported by the coherence of the limiting radiocarbon dates discussed above. The ten oldest lower moraines are named the Swift Creek moraines (Burrows and Kovanen, in progress) and are older than 9350 to 9650  $^{14}\text{C}$  years B. P.

### *Bagley Creek Glacial Chronology*

The glacier reconstruction for the Picture Lake moraine (Burrows and Kovanen, in progress), is closely constrained only by the headwall and moraines. The upper left margin (north side of valley) of the glacier is reconstructed ~ 60 m lower than the upper right margin (south side of the valley), because of its south-facing exposure. The terminus position is based on moraines, topography, and patterns of modern glacier margins (Figure 5.3).

A near-basal radiocarbon date from the Highwood Lake sediments of  $9410 \pm 50$   $^{14}\text{C}$  years B. P. (10,430-10,440; 10,490-10,750; 10,970-10,990; 11,020-11040 cal. years B. P.) (Figure 4.14) provides a minimum limiting age for the Picture Lake moraine. This date is only slightly younger than the oldest limiting ages of the south Swift Creek cirque moraines.

Analysis of remnant magnetism in the core sediments provides a means to correlate inclination and declination of the sediments with those of a known chronology at Fish Lake, Oregon (Verosub et al., 1986). Matching inclination and declination curves with those from the Fish Lake core indicates a basal age of ~9450  $^{14}\text{C}$  years B. P. (11,060-10950 cal. years B.P.) (Housen, personal communication, 2000). This analysis appears to contradict the near-basal radiocarbon date in the core. The calibrated Highwood Lake inclination curve suggests an 8900  $^{14}\text{C}$  years B. P. at a tie point that is stratigraphically below the  $9410 \pm 50$   $^{14}\text{C}$  years B. P. date from Highwood Lake. More information is needed to reconcile this discrepancy. The paleomagnetic comparison suggests that the age for the base of the Highwood Lake silt may be within a couple of hundred years of the lowest radiocarbon date. The possible varves (only 115 years represented) in the basal silt suggests this as well.



### *Summary of Morainal Evidence*

Trees growing on and behind the upper moraines of two cirques in Swift Creek (south Swift Creek cirque and high Swift Creek cirque) provide a close (within 15-35 years) minimum limiting age of 96 to 122 years old or deposition sometime from 1878 to 1904 A.D. Bouldery surfaces, sparse vegetation, small trees, and the absence of any tephras also support recent deposition of these moraines at late Little Ice Age.

Minimum limiting radiocarbon ages from bog and lake cores constrain the oldest cirque moraines in south Swift Creek cirque and Bagley Creek cirque. The Swift Creek moraines and Picture Lake moraines appear to be contemporaneous, based on similar geomorphic positions, extent, reconstructed equilibrium line altitudes (~ 1400 m; see Chapter 6), and similar stratigraphies of the Swift Creek cores and the Highwood Lake core (Figure 5.2), and relatively close basal ages. Radiocarbon minimum limiting ages constrain the Swift Creek moraines as older than  $9650 \pm 50$   $^{14}\text{C}$  years B. P. (10,760 - 10,960, 10,990 - 11,020, 11,040 - 11,180 cal. years B.P.). In Bagley Creek basin, the Picture Lake moraines are constrained by a minimum limiting radiocarbon date of  $9410 \pm 50$   $^{14}\text{C}$  years B. P. (10,430-10,440; 10,490-10,750; 10,970-10,990; 11,020-11040). Near-basal sediment core radiocarbon ages from both Swift Creek and Bagley Creek are very close and when calibrated at the 2-sigma uncertainty level have ages that overlap from 10,760 to 11,040 cal. years.

The only maximum age limit for the Swift Creek moraines and Picture Lake moraines is from two dates of  $10,788 \pm 77$  (13,112 – 12,442 cal. years B. P.) and  $10,603 \pm 69$  (12,944 – 12,176 cal. years B. P.)  $^{14}\text{C}$  years B. P. on charcoal layers in outwash from a tongue of the Nooksack alpine glacier system that flowed ~40 km down the North Fork of the Nooksack valley (Easterbrook and Kovanen, 1996; Kovanen, 1996; Kovanen and Easterbrook, 2001). When calibrated, these dates are statistically indistinguishable so the mean of ~ 10,700 years will be referred to as the maximum limiting age. Bagley Creek cirque was possibly a part of the source area for the Nooksack alpine glacier system. Although Swift Creek is not part of the Nooksack drainage system, a contemporaneous

alpine valley glacier of greater extent than outlined in this study would likely have occupied the Swift Creek drainage.

Moraine sets of two ages were deposited in Swift Creek during the late Holocene and the late-Pleistocene/earliest Holocene, whereas only the older set of the late-Pleistocene/earliest Holocene age moraines are preserved in Bagley Creek trough. Swift Creek Little Ice Age moraines were deposited sometime between about 1878 and 1904 A.D. in south Swift Creek cirque (SSC) and high Swift Creek cirque (HSC). The Swift Creek and Picture Lake moraines were deposited sometime between 10,700 and 9600 <sup>14</sup>C years B. P.

## Chapter 6 Equilibrium Line Altitudes (ELAs) and Paleoclimatic Reconstructions

The Equilibrium line altitude (ELA) of a glacier is the hypothetical contour across the glacier that has a zero net mass balance at the end of an annual ablation season. In actuality, the contour that defines the ELA is an average of the irregular end-of-summer snowline. The ELA and mass balance of a glacier are dependent on the balance between snow and ice accumulation (closely dependent on winter precipitation/accumulation) and snow, firn, and ice ablation (closely dependent on summer temperature). Winter precipitation/accumulation and summer temperature are dependent on the influence, interaction, and feedback of many climatic and topographic factors especially for cirque glaciers (Graf, 1976).

ELAs on modern glaciers typically vary widely from year to year and so to gain a sense for the cumulative effect of this variation on the response of a glacier, the ELAs must be averaged for several years in a row, appropriate to the response time of the particular glacier. A calculated ELA attempts to approximate the averaged ELA that would keep the glacier at a neutral mass balance and hence a stillstand. Calculating the ELA at a stillstand is significant because it relates back to a climate during the period of stillstand that is marked by a moraine building event. If the moraine building event is an advance, then the climate estimate is a minimum. If the event is a recession then the climate estimate is only a snapshot of ameliorating conditions.

Glacier response and moraine deposition are not necessarily simple climate relations. The interaction of glacier mass balance with topography (affecting glacier geometry and flow dynamics) further filters the climate signal (Furbish and Andrews, 1984). These relationships explain different glacier responses in the same mountain range to the same climate regime and make correlation of moraines from cirque to cirque without solid dating control impossible. However, to expect at least a few moraines to correlate in age from cirque to cirque in a mountain range is reasonable.

Equilibrium Line Altitudes for the Little Ice Age and early Holocene/late Pleistocene glacier reconstructions from Chapter 5 were calculated using the standard accumulation area

ratio (AAR) method (Meier and Post, 1962) with an assumed error of  $\pm 50$  m. The AAR is the area above the equilibrium line (accumulation area) divided by the total area of the glacier. Meier and Post (1962) observed that most mountain glaciers with a neutral mass balance, along the Northwest coast of North America and the western U.S. have an AAR between 0.5 and 0.8. Porter (1975) was one of the first to apply AAR to calculate ELA and used 0.6 AAR. Values of 0.6 or 0.65 are now commonly in use (i.e. Meierding, 1982; Thomas, 1997; Heine, 1998). Then, by estimating modern climate at the calculated ELAs for the reconstructed glaciers and comparing those climates to the range of climates on modern glaciers, the range of deviation from modern climate can be estimated. Ablation season temperature and accumulation season precipitation are the climate parameters used. This follows Leonard (1989) who applied this method to Pleistocene ELAs in the Colorado Front Range. This is assuming that climate at ELAs of modern glaciers in the Pacific Northwest and Canadian Rockies are valid models for past glaciers in the study area.

Estimating climatic conditions associated with past glacier extents in Swift Creek and Bagley Creek is important in assessing regional climate changes. Although Equilibrium Line Altitude (ELA) reconstructions and associated climate conditions provide only a snapshot of past conditions, they are important to compare with modern conditions and with other paleoclimate proxies.

### *The Modern ELA*

Equilibrium line altitudes of modern glaciers in the Cascades are primarily controlled by winter precipitation, summer temperature, and local topography (Porter, 1977; Clark et al., 1994). Important topographic factors are aspect, cirque geometry and topography, and locations of passes, ridges, and peaks (Graf, 1976). Typically, as the size of a glacier decreases (to the point it is confined to a cirque), the more it is dependent on the surrounding topography in order to continue to maintain enough mass balance to exist under marginal climate conditions. Assuming marginal climate conditions, an optimum location to maintain a small cirque glacier (referred to as a glacieret) in the northern hemisphere is in a large cirque with a northeast aspect, width greater than length, high steep walls, a pass located to

the windward, and a peak to the southwest (Graf, 1976). This situation would also tend to result in a lower ELA than larger, more exposed glaciers in the surrounding area. As the size of a glacier increases and becomes valley glacier size, the mass balance and ELA become less dependent on the local topographic situation. The effect of regional winter precipitation and summer temperature would more strongly control the mass balance and ELA. Topography is still important, but especially the area-altitude distribution (Tangborn, 1999). The area-altitude distribution is dependent on the size, shape, and altitude range of the valley in which the glacier resides.

Glaciers in and near the study area are excellent illustrations of the relationship between size, topography, and the ELA. Based on these relationships two modern ELA values are used in this study. The regional ELA (1890 m) is from substantial north-facing glaciers that exist on higher peaks in the area (Baker, Shuksan, Ruth, Icy, Hadley, and Ptarmigan Ridge) (Table 6.1). The mean from these represents the mean ELA of some of the larger, meteorologically exposed, N-facing glaciers in the area. The local ELA (1640 m) is from the two glacierets in Bagley Creek and Swift Creek (Table 6.1). The local and the regional ELA are related in that they are both subject to the same climate conditions, but the local ELA is more subject to local topographic conditions.

The two glacierets in the study area owe their continued existence to their northerly aspect and having favorable topographic conditions for collecting wind-blown snow. Wind-blown snow from prevailing winter storm winds (from the south and southwest) deposits snow through the pass at the head of Swift Creek glacier (Figure 3.1). The calculated modern ELA for Swift Creek Glacier is 1625 m (5330 ft). The Bagley Creek glacier sits in a depression in the northeast-facing crook of L-shaped Table Mountain (and is also probably significantly shaded) (Figure 4.1). Storm winds redeposit snow in this depression from the flat tops of the mountain. The calculated modern ELA of Bagley Creek glacier is 1650 m (5410 ft). Both of these calculated ELAs are within the ELA error margins ( $\pm 50$  m) of the other. The rounded average ELA from Swift Creek and Bagley Creek of 1640 m is used as the local ELA.

In the vicinity of the study area, winter precipitation and summer temperature

probably more strongly influence ELAs of glaciers on the large peaks of Mt. Baker (Harper, 1992) and others than in the study area itself. To approximate the modern ELA in the vicinity of the study area, I calculated ELAs from the most recent 7.5' topographic quadrangles (1989) for several modern glaciers on Mt. Baker, Mt. Shuksan, Icy Peak, Ruth Mt., Hadley Peak, and Ptarmigan Ridge (see Figure 1.1 for locations). These values varied from 1795 to 1990 m for northwest to northeast facing glaciers with a mean of 1890 m (Table 6.1). The mean of 1890 m is referred to from here on as the regional ELA. The large difference of ~250 m between the mean regional ELA and the local ELA demonstrates how strongly an influence topography is for preserving the glacierets in Swift Creek and Bagley Creek.

Two ELAs were calculated for south-facing, modern glaciers to compare the affect of aspect and to compare with ELAs of south-facing reconstructed glaciers in the study area. The south-southeast-facing Crystal glacier on Mt. Shuksan has a calculated ELA (0.65 AAR method) of 2200 m. This compares well with 2015 m (0.65 AAR method) for the south-southwest-facing Easton glacier on Mt. Baker (Thomas 1997). The mean for these two south-facing glaciers is 2110 m. The Crystal glacier ELA may be higher than the Easton because of its hypsometry and/or because the Crystal has a calving margin over a cliff.

Noisy Creek glacier, several kilometers to the southeast of the study area, is a small cirque glacier (0.6 km<sup>2</sup> area), with little vertical relief, and has a calculated ELA of 1820 m with a field-measured ELA of 1765 m for 1995-96, a near-neutral mass balance year (Riedel, pers. comm., 2000). The Noisy Creek Glacier ELA is probably below the regional ELA mean because it sits in a relatively flat basin that likely collects avalanched snow from the slopes above. In comparison, the South Cascade glacier, a larger valley glacier (~ 2 km<sup>2</sup> area) several km to the south of Noisy Creek with significant vertical relief (~400 m), had a field-measured ELA at 1900 m during the same year (Krimmel, 1997). The contrast between measured ELAs on these two glaciers that have a similar climate further illustrates the importance of local topographic effects on the ELA of small cirque glaciers.

Glacier	Location	Aspect	Calculated		Measured ELA (m)
			ELA (m)	ELA (ft)	
Crystal	Mt. Shuksan	S	2200	7220	
Easton	Mt. Baker	S	2015	6610	
unnamed	Ruth Mt.	N	1925	6310	
unnamed	Icy Peak.	NW	1845	6050	
Mazama	Mt. Baker	N-NE	1940	6360	
Hadley	Hadley Peak	N	1990	6530	
Sholes	Ptarmigan Ridge	NE	1795	5890	
Noisy Creek	Bacon Peak	N	1820	5970	1765
Swift Creek	upper SSC	N	1625	5330	
Bagley Creek	upper Bagley Cr.	NE	1650	5410	
	North-facing Regional mean:	1890			
	Local mean:	1640			

Table 6.1 Modern ELAs of glaciers in the vicinity of the study area, calculated from 0.65 AAR. The regional ELA is 1890 m from north facing glaciers

Name	Phase	Aspect	ELA (m)	ELA (ft)
Bagley Creek	Picture Lake	E-NE	1390	4560
SSC	Swift Creek	N-NW	1415	4640
SSC	Swift Creek Minimum	N-NW	1475	4840
SSC	LIA	N	1550	5080
HSC	LIA	W-NW	1645	5400
HSC	pre-Mazama unknown	W-NW	1565	5130
SShC	pre-Mazama unknown	SE	1595	5230
NSC	pre-Mazama unknown	W-NW	1470	4820
LAC	pre-Mazama unknown	SE	1460	4790

Table 6.2 Calculated past ELAs for the study area.

Glacier Name	local ELA	regional ELA	Local $\Delta$ ELA		Regional $\Delta$ ELA	
			LIA	Swift Cr.	LIA	Swift Cr.
Swift Cr.	1625	1890	75	210	340	475
Bagley Cr.	1650	1890	NA	260	NA	500
S. Shuksan Cr.	unknown	1890	NA	NA	NA	515

Table 6.3  $\Delta$ ELAs for Swift Creek, Bagley Creek, and south Shuksan Creek Glaciers.

### *ELA Reconstructions*

Past glacier surface contours were drawn based on the reconstructed glacier margins outlined in Chapter 5, (Figures 6.1 through 6.4). Paleo-ELAs based on these reconstructions were calculated using a 0.65 AAR (Table 6.2).

The Little Ice Age ELA for south Swift Creek cirque (SSC) (1550 m) (Figure 6.1) is nearly 100 m lower than for high Swift Creek cirque (HSC) (1645 m), reflecting the more northerly aspect and greater potential for snow drifting at SSC.

The reconstructed ELAs for the Swift Creek (1415 m) and Picture Lake (1390) moraines are not significantly different (Table 6.2). Considering the similar aspect and elevation of the cirques, the correspondence in ELAs further support correlation of these two sets of moraines along with minimum limiting radiocarbon dates (see Chapter 5).

ELAs from maximum moraine reconstructions in Lake Ann cirque and north Swift Creek cirque (NSC) (Table 6.2) are not significantly different at 1460 m and 1470 m, respectively, suggesting the maximum moraines in these cirques are contemporaneous. This inference is further supported because the glaciers shared a common source area across the dividing ridge (Figure 6.2). The SSC pre-Mazama minimum extent (from the highest moraines) ELA (1475 m) (Figure 6.3) closely compares with those of Lake Ann cirque and NSC, suggesting a similar age. However, without more precise dating control the age and correlations of SSC, Lake Ann cirque and NSC moraines is impossible to confirm.

### *$\Delta$ ELAs*

The ELA depression or  $\Delta$ ELA ( $\Delta$ ELA will be used from here on) is the difference between the modern ELA and the calculated ELA for a reconstructed past glacier. Two sets of  $\Delta$ ELAs were calculated for the Swift Creek LIA and Swift Creek and Picture Lake moraine reconstructions; one depression each from the modern regional ELA (1890 m) and the other from the local Swift Creek/Bagley Creek ELAs (1640 m) (Table 6.3). Comparison of the paleo-ELAs with the modern local ELA is useful if the paleo-glacier was subject to the same localized conditions that preserves the modern glaciers (probably increased accumulation due to wind drifting). This is most likely the case for the Little Ice Age extent

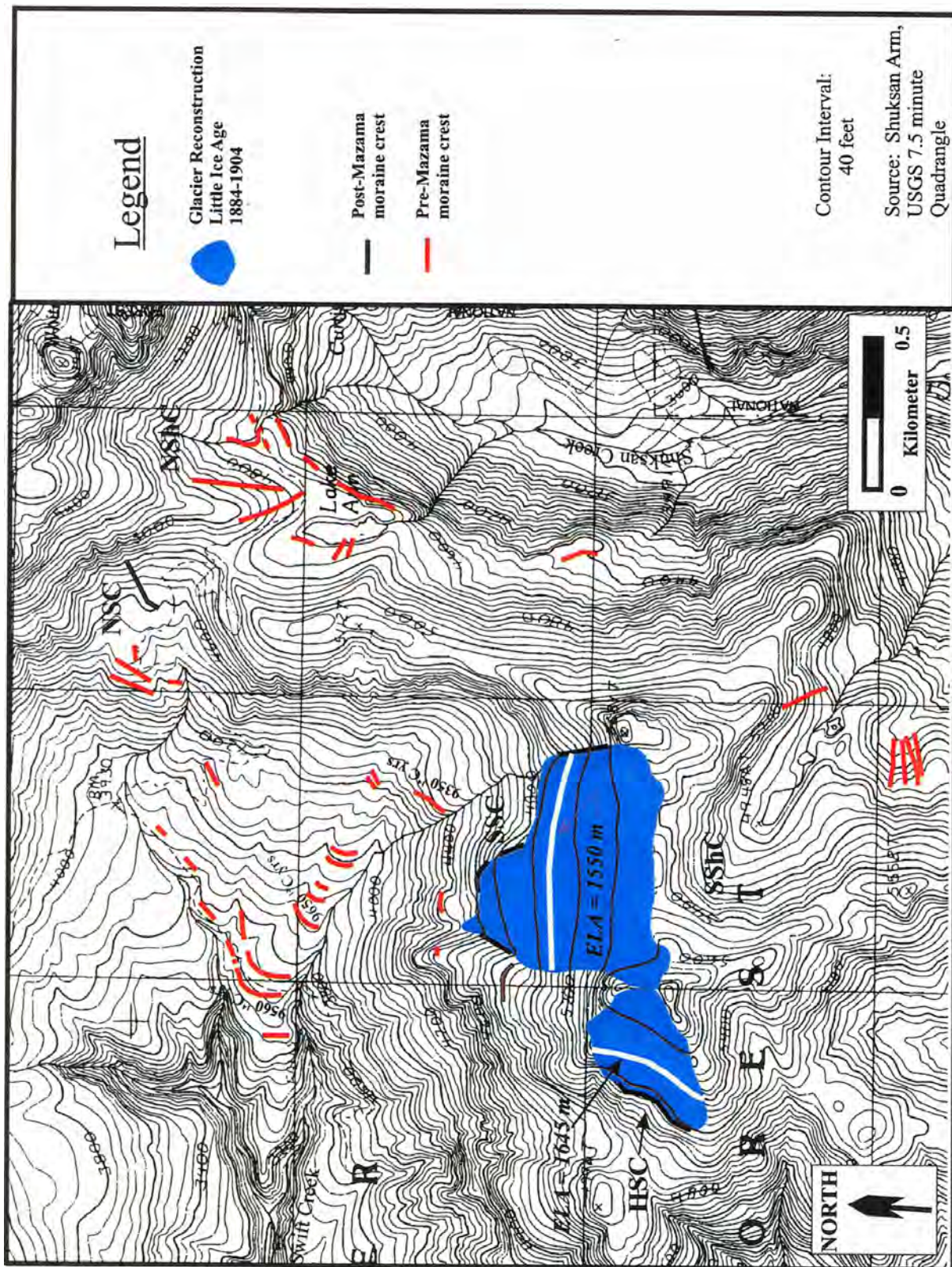


Figure 6.1 Swift Creek Little Ice Age glacier reconstruction. The south Swift Creek glacier and the now extinct high Swift Creek glacier may have reached the Little Ice Age maximum sometime between 1884 and 1904 A.D. NSC=north Swift Creek cirque; SSC = south Swift Creek cirque; HSC = high Swift Creek cirque; NShC = north Shuksan Creek cirque; SShC = south Shuksan Creek cirque.

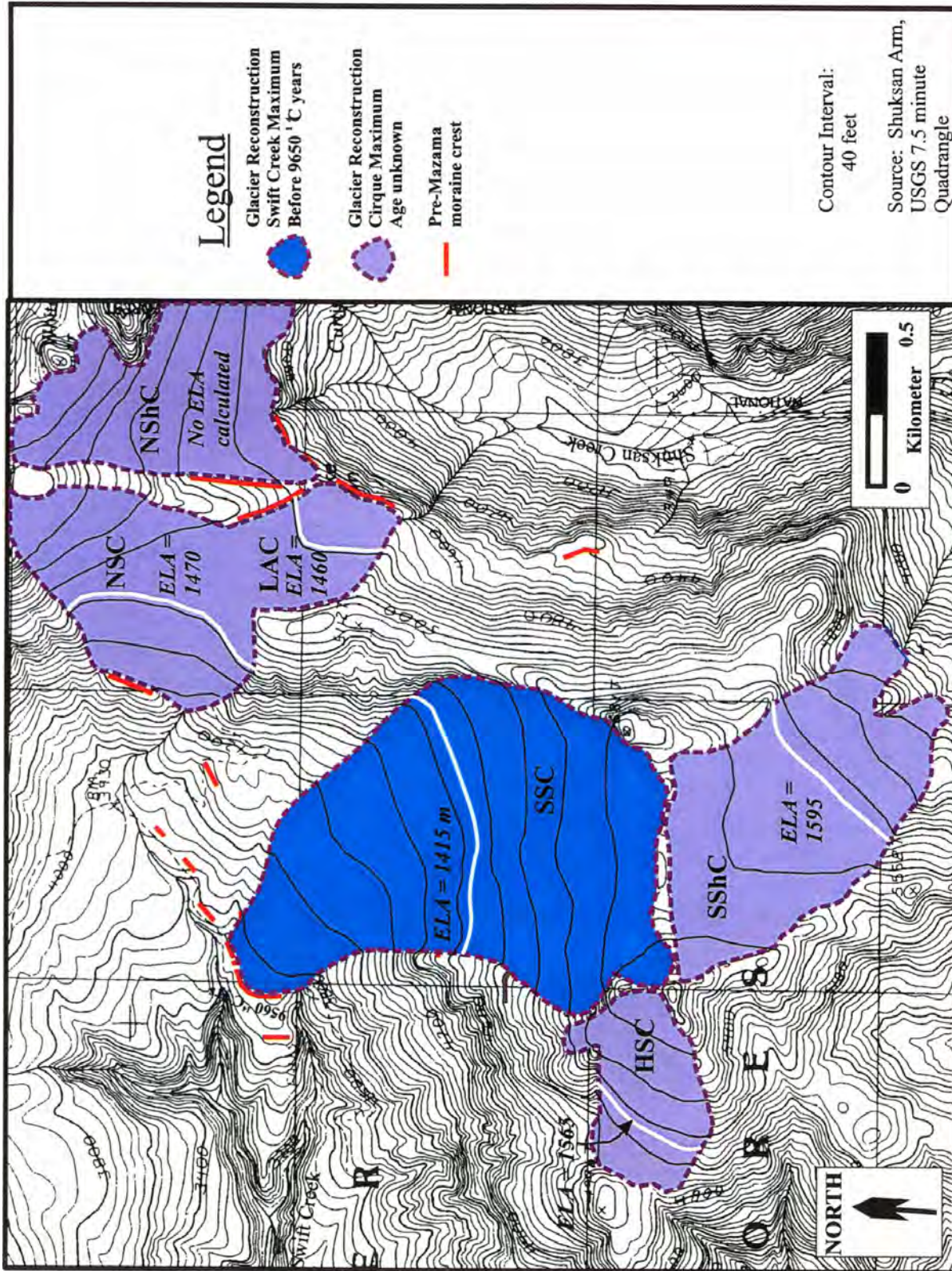


Figure 6.2 Swift Creek and Shuksan Creek glacier reconstructions based on the outermost moraines. This position of the Swift Creek Glacier (in SSC) is the early Holocene/late Pleistocene extent. NSC = North Swift Creek Cirque; SSC = South Swift Creek Cirque; HSC = High Swift Creek Cirque; NShC = North Shuksan Creek Cirque; SShC = South Shuksan Creek Cirque; LAC = Lake Ann Cirque.

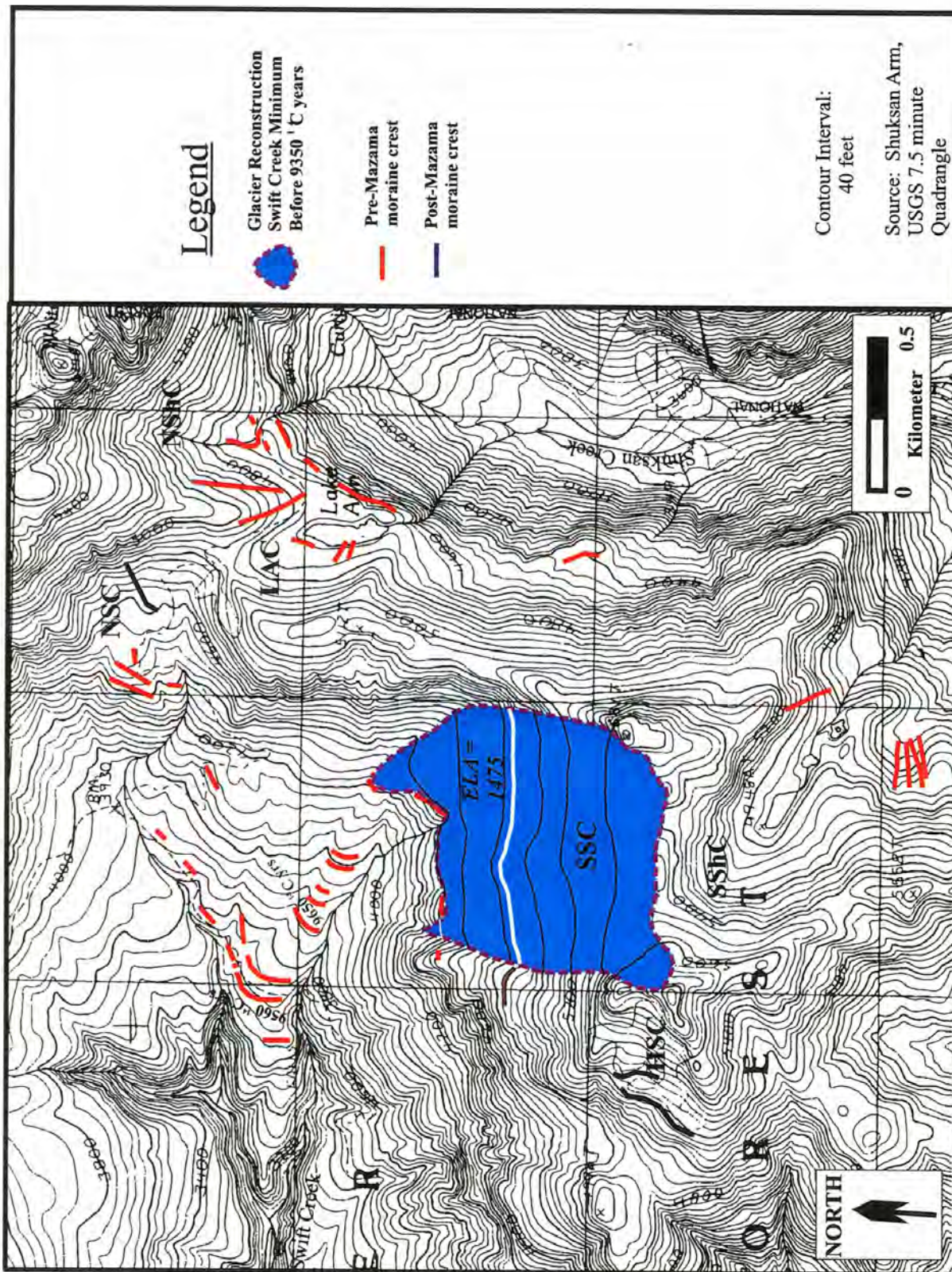


Figure 6.3 South Swift Creek early Holocene/late Pleistocene minimum glacier reconstruction. This glacier has a minimum limiting age of 9350 <sup>1</sup>C years B.P. NSC = North Swift Creek Cirque; SSC = South Swift Creek Cirque; HSC = High Swift Creek Cirque; NSHC = North Shuksan Creek Cirque; SshC = South Shuksan Creek Cirque; LAC = Lake Ann Cirque.

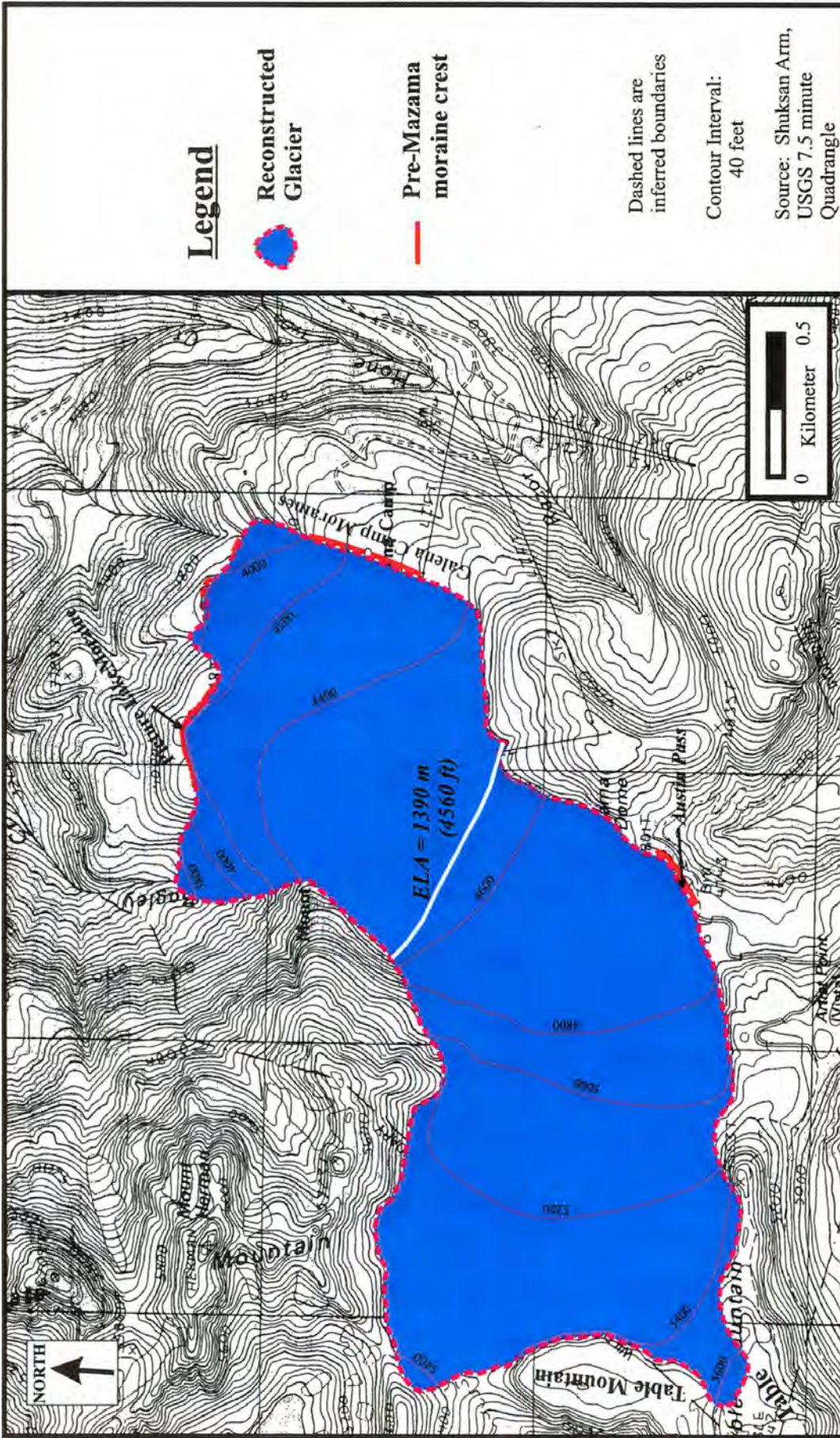


Figure 6.4 Bagley Creek Glacier reconstruction for the early Holocene/late Pleistocene Picture Lake end moraine with a minimum limiting radiocarbon age of 9410 years B.P.

because the glacier was only slightly larger than it is now. The  $\Delta$ ELA from the modern Swift Creek glacier for the south Swift Creek LIA moraines is 75 m. The  $\Delta$ ELA from the regional ELA for the south Swift Creek LIA moraines is 340 m. The  $\Delta$ ELA for the late Pleistocene/early Holocene extents of Swift Creek and Bagley Creek from the modern regional ELA is ~490 m. This comparison is probably more valid because both glaciers were significantly larger (Bagley Creek was over 3 km<sup>2</sup> and Swift Creek was ~ 1 km<sup>2</sup>) and more dependent on winter precipitation and summer temperature. For example, a modern analog is the South Cascade Glacier (~ 2 km<sup>2</sup> in area), which is similar in size and geomorphic position to the late Pleistocene/early Holocene Bagley Creek Glacier. The modern, near-neutral, mass balance ELA (1900 m) for the South Cascade Glacier (Krimmel, 1997) is very close to the regional ELA (1890 m). Therefore, the late Pleistocene/early Holocene ELAs of Swift Creek and Bagley Creek were probably in the same range as the larger glaciers on Mts. Baker and Shuksan, hence the  $\Delta$ ELA from the regional mean ELA.

In addition, the  $\Delta$ ELA for south-facing south Shuksan Creek cirque (SShC) from the south-facing regional mean ELA (2110 m) is 515 m. This value is in the same range as the early Holocene/late Pleistocene reconstructions in Swift Creek and Bagley Creek, suggesting a correlation.

Using the  $\Delta$ ELA from the regional mean for the late Pleistocene/early Holocene extents of Swift Creek and Bagley Creek is probably a simplification. The relative change in ELA between the study area glaciers and higher-altitude, larger-extent glaciers in the region was probably not linear between today and the late Pleistocene/early Holocene, so the  $\Delta$ ELA of 490 m should be considered a maximum.

### *Climate at Modern Glacier ELAs*

Comparing modern climate conditions at the ELAs of the reconstructed glaciers in the study area with climate at modern glacier ELAs in the North American Cordillera can provide a measure of how summer temperatures and winter precipitation have changed since the Little Ice Age and the early Holocene/late Pleistocene. These deviations from modern temperature and precipitation indicate what change was necessary (from present) to

glacierize the basins of the study area. This approach follows Leonard (1989) who plotted a global distribution of accumulation-season precipitation and ablation-season temperature at ELAs of modern glaciers and then developed two envelope equations to encompass the data. Ohmura et al. (1992) published an expanded data set and more rigorous treatment of the climate at glacier ELAs (takes the radiation balance into account). However, for the sake of simplicity only precipitation and temperature are considered here.

Kotlyakov and Krenke (1982) proposed a “tabulated global formula” to encompass ELA climates at modern glaciers:

$$A = 1.33 (T_{vi-viii} + 9.66)^{2.85} \quad (1)$$

Where A is accumulation season precipitation (October through May) in mm water equivalent and  $T_{vi-viii}$  is mean summer temperature in degrees C (June, July, and August). This curve fits one extreme of their data very well, but to encompass the other extreme of the data, Leonard (1989) developed a curve in the same form:

$$A = 1.33 (T_{vi-viii} + 6.66)^{2.85} \quad (2)$$

Likewise, I used variations on the same function to generate an envelope for those glaciers that may serve as better modern analogs to reconstructed glaciers in the study area. These glaciers are in the North Cascades, British Columbia Coast Ranges, and Canadian Rockies and I used climate data for these glaciers tabulated in Ohmura et al., 1992) (Table 6.4; Figure 6.5). The function to fit the left-hand side of this envelope is:

$$A = (T_{vi-viii} + 8.5)^{2.85} \quad (3)$$

The function to fit the right-hand side of the envelope is:

$$A = (T_{vi-viii} + 5.2)^{2.85} \quad (4)$$

Equation (4) is the right hand side of the envelope and the minimum combination of accumulation season precipitation and summer mean temperature needed to sustain a glacier. Values generated from equation (4) are compared with modern climate (developed in the next section below) at reconstructed ELAs in the study area.

Modern Glacier	ELA	ablation season temp, deg. C	winter mass balance, mm w.e.	ablation months	Location	Regime	source
South Cascade	1965	6.9	2650	Jun-Aug	N. Cascades, WA	maritime	Ohmura et al. 1992
Nisqually	2080	9.5	4900	Jun-Aug	Cascades, WA	maritime	Ohmura et al. 1992
Place	2155	6.8	2100	Jun-Aug	BC Coast Ranges	maritime	Ohmura et al. 1992
Sentinal	1805	8.7	3500	Jun-Aug	BC Coast Ranges	maritime	Ohmura et al. 1992
Tiedemann	1890	6.2	2300	Jun-Aug	BC Coast Ranges	maritime	Ohmura et al. 1992
Bench	1860	6.4	2000	Jun-Aug	BC Coast Ranges	maritime	Ohmura et al. 1992
Helm	2090	5	2100	Jun-Aug	BC Coast Ranges	maritime	Ohmura et al. 1992
Zabisha	2280	4.1	1750	Jun-Aug	BC Coast Ranges	maritime	Ohmura et al. 1992
Bridge	2200	4.5	1950	Jun-Aug	BC Coast Ranges	maritime	Ohmura et al. 1992
Sykora	2200	4.5	1900	Jun-Aug	BC Coast Ranges	maritime	Ohmura et al. 1992
Woolsey	2270	8.9	2700	Jun-Aug	BC Coast Ranges	maritime	Ohmura et al. 1992
Ram River	2860	4.7	1000	Jun-Aug	Canadian Rockies	continental	Ohmura et al. 1992
Peyto	2670	6.1	1400	Jun-Aug	Canadian Rockies	continental	Ohmura et al. 1992

Table 6.4 Some ELAs and climatic parameters of glaciers that may serve as models for the reconstructed glaciers of this study.

Station or ELA	UBD	MBL	Picture Lake moraine ELA	Swift Creek Max. ELA	Swift Creek LIA ELA	local modern ELA	regional modern ELA
Altitude (m)	150	1324	1390	1415	1550	1640	1890
Mean Summer Temperature (deg. C)	16	10.1	9.8	9.7	9.0	8.6	7.3
Winter Precip. (mm)	2100	2150	2153	2154	2160	2163	2174
Summer Dry Lapse Rate =	0.50 deg.C/100m						
Winter Precipitation lapse rate =	4.26 mm/100m						

Table 6.5 Table showing modern climate conditions for various altitudes, which correspond to calculated past and modern ELAs. The summer lapse rate was determined by finding the lapse rate between Upper Baker Dam (UBD) and Mount Baker Lodge (MBL) for the ablation season (May-Sept) mean temperature. Mount Baker lodge data is from that reported in Porter (1977), Upper Baker dam data is from the Western Regional Climate Center website: <http://www.wrc.dri.edu/>

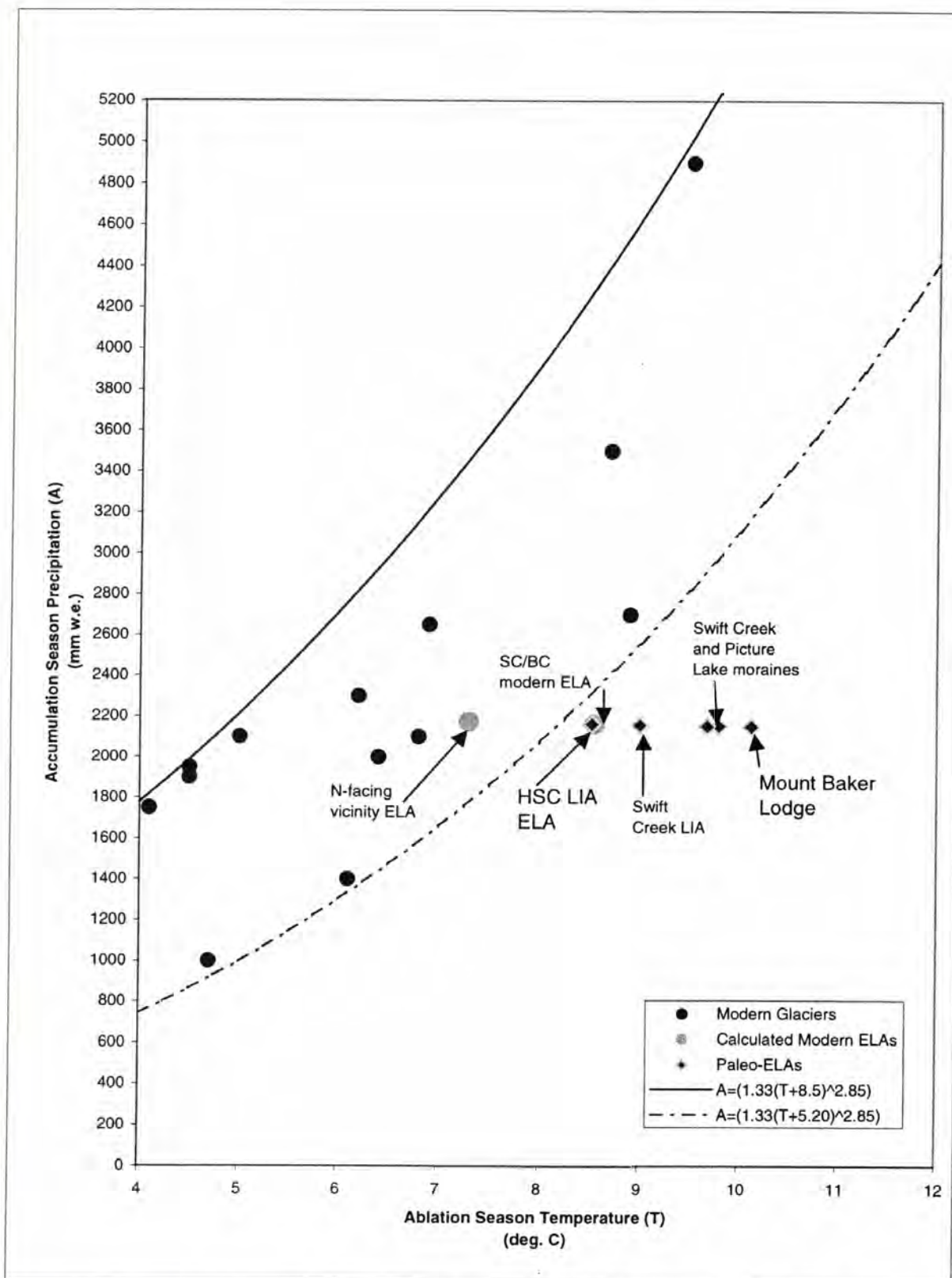


Figure 6.5 A comparison of modern glacier ELA climates (measured and estimated) with modern climates at past ELAs of this study. The envelope curves (solid and dashed lines) are modified from Kotlyakov and Krenke (1982) and Leonard (1989). The estimated regional ELA climate estimates fit well within the envelope. See text for deviations of modern climates at past ELAs from modern glacier ELA climates. These data are from Table 6.4 and Table 6.5.

### *Modern Climate at Calculated ELAs for Past Glaciers in the Study Area*

Modern ablation-season temperatures at the reconstructed ELAs are estimated by generating and interpolating from mean summer temperature lapse rates in the study area. The mean summer temperature lapse rate between the study area at Mt. Baker Lodge (MBL) and Upper Baker Dam (UBD) ~ 15 km to the southwest is 0.5 deg. C/100 m (Figure 1.1 and 1.2 for locations).

Winter precipitation at Mt. Baker Lodge (MBL) and Upper Baker Dam (UBD) are similar and the winter precipitation lapse rate is low at 4.26 mm/100m. Porter (1977) recognized that precipitation values above weather stations in the Cascades probably are not significantly different and the low precipitation lapse rate value is congruent with this. The interaction of topography and wind and the altitude of the freezing level are probably stronger controls on the winter snowfall in this region than altitude (D. Burrows, personal comm., 2000), but the lapse rate is used anyway. In the Cascades, a strong west to east decreasing precipitation gradient exists across the range. However, the distance between Mt. Baker and Mt. Shuksan of the study area does not cover enough west-east distance to be significant (Porter, 1977).

Mean temperatures and precipitation for Mt. Baker Lodge at 1320 m altitude in Heather Meadows are reported in Porter (1977) from 1931 to 1960. Climate data for Upper Baker Dam is from the period 1960-1990. Unfortunately the earlier 30-year mean from Upper Baker Dam is not available. Thus, they are assumed to be reasonably close for this comparison.

The mean accumulation-season precipitation is 2150 mm, whereas the mean annual is 2790 mm. Upper Baker Dam is at 150 m altitude and has a mean accumulation-season precipitation of 2100 mm.

At Mt. Baker Lodge, the mean annual temperature is 4.5 deg. C, the mean ablation-season (May-September) temperature is 10.1 deg. C, and mean July temperature is 12.2 deg. C (Porter, 1977). Taking the difference between ablation season temperatures of Upper Baker Dam and Mt. Baker Lodge and dividing by the difference in altitude yields a lapse rate of 0.50 deg. C/100m.

The lapse rate was applied to the various altitudes corresponding to modern and paleo-ELAs. These results are reported in Table 6.5 and compared graphically to the modern glacier data from Ohmura et al. (1992) in Figure 6.5. The calculated north-facing mean regional ELA climate parameters fall within the envelope as would be expected. The climate conditions that exist today at paleo-ELAs fall outside of the envelope as would be expected. Climate conditions for the local Swift Creek/Bagley Creek ELA fall outside of the envelope, showing topography/weather interactions must be at work to keep glaciers at these locations. In actuality, this point is probably shifted into the envelope by increased accumulation due to wind drifting and decreased summer temperature due to a north-facing aspect.

#### *Climate Shifts to Reestablish Reconstructed Glaciers*

The differences between the reconstructed ELA climate conditions (Table 6.5) and the envelope for glacier existence (Figure 6.5) are tabulated on Table 6.6. The maximum temperature depression is the difference with no change in precipitation and the maximum precipitation increase is the difference with no change in temperature. These are the extremes that would be necessary to create glacier ELA climatic conditions. The maximum temperature depression for the Swift Creek and Picture Lake moraines would be ~ 1.6 deg. C. and the maximum precipitation increase would be 870 mm. For the Swift Creek Little Ice Age ELA a maximum temperature depression of 0.85 deg. C or a maximum precipitation increase of 440 mm would be needed. Probably some combination of a decrease in temperature and increase in precipitation from modern conditions occurred because modern climate trends show increased precipitation with cooler periods and decreased precipitation with warmer periods. Such conditions could persist for a short period (a few years) and cause a stillstand or small advance and moraine deposition by a retreating glacier. A larger advance from growth of an originally smaller glacier would probably require a climate change favorable for growth to last at least a few decades. The decrease in temperature for the Little Ice Age seems plausible as Graumlich and Brubaker (1986) approximate a 1 deg. C decrease in mean annual temperature based on tree-ring correlations for the Little Ice Age.

Glacier Phase	Max Temp Decrease (deg. C)	Max Precip Increase (mm)
Early Holocene/l. Pleistocene	1.6	870
Swift Creek Little Ice Age	0.85	440

Table 6.6 Ablation season temperature and accumulation season precipitation shifts from modern climate at past ELAs to a glacial climate.

## Chapter 7 Comparison with other studies

No previous work in glacial geology in the study area has been published, but numerous studies of historical glacier fluctuations and glacial geology have been conducted in the North Cascades. Several studies have investigated Holocene and historical glacier fluctuations on Mt. Baker (Bengston, 1956; Burke, 1972; Easterbrook and Burke, 1972; Fuller, 1980; Heikkinen, 1984; Harper, 1993; Thomas, 1997; Thomas et al., 2000), and in nearby cirques (Easterbrook and Burke, 1972; Easterbrook and Kovanen, 1999; Thomas, 1997; Thomas et al., 2000). Leonard (1974) studied Neoglacial moraines from the Price Glacier on the north side of Mt. Shuksan. Other Neoglacial and Little Ice Age moraine studies in the North Cascades include the Dome Peak area (Miller, 1969), and Depot Creek (Riedel, 1987). Holocene glaciation has been quite extensively studied on and around Mt. Rainier (Burbank, 1981; Crandell and Miller, 1964; Harrison, 1956; Heine, 1998; Porter and Burbank, 1979; Sigafos and Hendricks, 1961, 1972; Veatch, 1969). Ryder and Thomson (1985) and Souch (1994) report on timing of Neoglacial advances in the British Columbia Coast Range. This chapter compares the results from Swift Creek and Bagley Creek to glacier records around the western United States.

### *Little Ice Age*

The Swift Creek LIA moraines correlate with many Little Ice Age moraines in the Cascade Range. The Swift Creek LIA moraines delimit a maximum at the end of the Little Ice Age. In contrast, many glaciers in the North Cascades reached their maximum earlier in the Little Ice Age and have younger nested moraines upvalley from the maximum that may correlate with the Swift Creek moraines. The outermost Little Ice Age moraines are typically within 0.5 km of the inner moraines at these other sites and don't represent a large change in ELA. The following modern glaciers and cirques have Little Ice Age moraines that may have formed at the same time as and are within the range of dates possible for those at Swift Creek (1878-1904 A.D.): on nearby Mt. Baker the Boulder Glacier (Burke, 1972; Easterbrook and Burke, 1972), Coleman/Roosevelt Glacier (Heikkinen, 1984), the Easton Glacier (Thomas 1997), and possibly the Deming Glacier (Fuller, 1980); on Mt. Shuksan, just a few kilometers to the east of the study area, the Price Glacier (Leonard, 1974); the Dome Peak area, ~ 30 km

south and east of the study area, which includes the South Cascade, the LeConte, the Dana, and the Chickamin glaciers (Miller, 1969); and Mt. Rainier, on the Carbon, Emmons, Ohanapecosh, Winthrop, and Cowlitz Glaciers (Sigafos and Hendricks, 1972; Burbank, 1981). A similar Little Ice Age pattern occurs in the Canadian Cordillera as well (Osborn and Luckman, 1988).

Two of the north-facing glaciers on Mt. Rainier have similar  $\Delta$ ELAs as the south Swift Creek LIA moraines (Burbank, 1981). The Winthrop Glacier has a  $\Delta$ ELA of 99 m and the Carbon Glacier a  $\Delta$ ELA of 60 m. The Winthrop glacier  $\Delta$ ELA is from the Little Ice Age maximum extent and so the inner moraines that correlate with Swift Creek may be closer to the Swift Creek LIA  $\Delta$ ELA of 75 m. The lower Carbon Glacier is heavily debris-covered and thus is not comparable with the others.

#### *Early Holocene/late Pleistocene*

The Swift Creek and Picture Lake moraines do not appear to correlate to the early Holocene moraines (7700-8400  $^{14}\text{C}$  years B. P.) of the Easton shelf glacier on the south flank of Mt. Baker or a cirque moraine nearby (Easterbrook and Kovanen, 1999; Thomas, 1997; Thomas et al., 2000). The 2-sigma calibrated age ranges for Thomas' maximum, 9270-9535 cal years, and the oldest minimum for the Swift Creek moraines, 10,760-11,180 cal years, do not overlap; therefore these appear to be two separate events. However, lateral moraines on the Easton shelf, just below those discussed above, appear to be older than Thomas' maximum and may correlate to the Swift Creek and Picture Lake moraines. Dates on charcoal in a nearby cirque moraine (not part of the Mt. Baker glacier system) suggest an age of  $\sim 8500$   $^{14}\text{C}$  years B. P. (Easterbrook and Kovanen, 1999).

If  $9650 \pm 50$   $^{14}\text{C}$  years B. P. is a close minimum limiting age for the Swift Creek moraines then they may correlate with McNeely II cirque moraines near Mt. Rainier (Heine, 1998). Radiocarbon and tephrochronologic analyses on lake sediments associated with the McNeely moraines demonstrate that McNeely II moraines are bracketed between 9800 and 8950  $^{14}\text{C}$  years B.P. Indeed, the  $\Delta$ ELA (from the modern ELA on Mt. Rainier) of 400-500 m for the McNeely advances compare closely with the 475-500 m  $\Delta$ ELA (from the regional ELA) for the Swift Creek and Picture Lake moraines. However, if the constraining date for the Swift

Creek and Picture Lake moraines is not closely limiting (not within  $\sim 200$   $^{14}\text{C}$  years), then they would not correlate with McNeely II moraines.

As discussed in Chapter 5 moraines of the North Fork of the Nooksack alpine glacier system (NAGS) provides a maximum limiting age of  $\sim 10,700$   $^{14}\text{C}$  years B. P. for the Swift Creek and Picture Lake moraines. In addition, lateral moraines of the Middle Fork Nooksack alpine glacier contains logs which were dated at  $\sim 10,700$  and  $\sim 10,500$   $^{14}\text{C}$  years B.P. that are the result of the readvance of alpine ice in the Middle Fork Nooksack valley (Kovanen and Easterbrook, 2001). These moraine building events in the Nooksack may correlate to inner moraines of the Sumas Stade on the Fraser Lowland (the last remnant of the CIS), bracketed between  $\sim 11,000$  and  $10,250$   $^{14}\text{C}$  years B. P (Kovanen and Easterbrook, 2001). The innermost Sumas moraine has a maximum limiting age of  $10,250$   $^{14}\text{C}$  years B. P. (Easterbrook and Kovanen, in review-a). The Swift Creek and Picture Lake moraines, could correlate with the youngest Sumas moraines.

The number of alpine moraines of different ages in the Pacific Northwest suggests variable climates during the late-Pleistocene/earliest Holocene (and different responses of glaciers to unique climate changes for each period because of different area-altitude relationships). Several authors have attempted to correlate late-Pleistocene and Holocene alpine moraines throughout the North American Cordillera (e.g. Burke and Birkeland, 1983; Davis and Osborn, 1987; Davis, 1988; Osborn and Luckman, 1988; Luckman 1998). Although many studies identified "pre-Neoglacial moraines" of possible early Holocene and/or late-Pleistocene age, relatively few moraines have rigorous numeric age control. However, in recent years, some "pre-Neoglacial moraines" in the North American Cordillera have been shown to be latest Pleistocene in age. Alpine cirque moraines in the Canadian Rockies (Reasoner et al., 1994), Colorado Rockies (Menounos and Reasoner, 1997), and Wyoming Wind River Range (Gosse et al., 1994) that are of slightly greater extent than Little Ice age moraines. The moraines from these studies correlate with the North Atlantic Younger Dryas event ( $11,000$  to  $10,000$   $^{14}\text{C}$  years B. P.). In the Sierra Nevada, Clark and Gillespie (1997) demonstrated that "Recess Peak" moraines (also of slightly greater extent) previously thought to be late Holocene ( $\sim 2500$   $^{14}\text{C}$  years B. P.), are pre-Younger Dryas (older than  $11,200$   $^{14}\text{C}$  years B.P.).

## Chapter 8 Summary

### *The Moraine Record and Limiting Ages*

Two distinct sets of post-Vashon moraines occupy several cirques of the study area in northwestern Washington between Mt. Baker and Mt. Shuksan. Younger (upper) and older (lower) sets of moraines were deposited in Swift Creek, whereas only the older set is preserved in Bagley Creek basin. The upper moraines lack tephra, are bouldery, sparsely vegetated with only a few small trees growing on them. From dendrochronology, the Swift Creek LIA moraines were deposited sometime between about 1878 and 1904 A.D. in south Swift Creek cirque and high Swift Creek cirque. The lower, older moraines in south Swift Creek cirque are vegetated with mature subalpine vegetation and have impounded a number of small ponds and bogs. An extensive cover of Mazama ash on the lower moraines and bogs provides a minimum limiting age of 6800  $^{14}\text{C}$  years for deposition. Minimum limiting radiocarbon ages from bog and lake cores constrain the oldest cirque moraines in south Swift Creek cirque and Bagley Creek basin. The Swift Creek moraines and Picture Lake moraines appear to be contemporaneous, based on similar geomorphic positions, extent, reconstructed equilibrium line altitudes, and relatively close basal ages from the Swift Creek cores and the Highwood Lake core. Radiocarbon minimum limiting ages constrain the Swift Creek moraines as older than  $9650 \pm 50$   $^{14}\text{C}$  years B. P. (10,760 - 10,960, 10,990 - 11,020, 11,040 - 11,180 cal. years B.P.). In Bagley Creek trough, the Picture Lake moraines are constrained by a minimum limiting radiocarbon date of  $9410 \pm 50$   $^{14}\text{C}$  years B. P. (10,430-10,440; 10,490-10,750; 10,970-10,990; 11,020-11,040). Near-basal sediment core radiocarbon ages from both Swift Creek and Bagley Creek are very close to each other and when calibrated at the 2-sigma uncertainty level have ages that overlap from 10,760 to 11,040 cal. years. The primary uncertainties with interpreting the closeness of the minimum limiting ages are: (1) possible piping of older sediments through porous till (in the cases of Swift Creek core sites); (2) unknown sedimentation rates below the radiocarbon dates; (3) an unknown hiatus time between deglaciation and establishment of vegetation and organic sedimentation; and (4) coring the deepest, oldest part of the bog or lake.

Moraines are preserved in other sub-cirques of Swift Creek and Shuksan Creek that

are of similar extent to the lower south Swift Creek cirque moraines. Moraines in north Swift Creek cirque, Lake Ann cirque, north Shuksan Creek cirque, and south Shuksan Creek cirque are constrained by Mazama ash as a minimum limiting age. However, without further age constraints, whether these moraines correlate to the late Pleistocene/early Holocene moraines in Swift Creek and Bagley Creek is unknown.

The only maximum age limit for the cirque moraines in Swift Creek and Bagley Creek is 10,700  $^{14}\text{C}$  years B. P. from charcoal layers in outwash from the Nooksack alpine glacial system of the North Fork of the Nooksack valley (in which Bagley Creek is a tributary) (Kovanen, 1996; Easterbrook and Kovanen, 1996; Kovanen and Easterbrook, 2001). Although Swift Creek is not part of the Nooksack drainage system, a contemporaneous alpine valley glacier of greater extent than outlined in this study probably occupied Swift Creek.

Two dates from the Swift Creek cores and one date from the Highwood Lake provide maximum limiting ages of ~ 5800 to 6200  $^{14}\text{C}$  years B.P. (~ 6800 cal. years B. P.) for the Cathedral Crag tephra. These dates contribute to a suite of similar limiting ages for the tephra (Kovanen and Easterbrook, in review-b).

Discordant radiocarbon dates were observed on different materials at stratigraphically similar locations within the Swift Creek sediment cores. The wood fibers that yielded the younger dates, are most likely penetrative root fibers. The dates from this material contrast sharply with charcoal, peat, and plant macrofossil (heather needles) samples carefully scrutinized to eliminate root material. In all cases the roots are ~ 2000  $^{14}\text{C}$  years younger.

### *ELA Reconstructions and $\Delta\text{ELAs}$*

Two sets of  $\Delta\text{ELAs}$  were calculated for the south Swift Creek cirque LIA and Swift Creek and Picture Lake moraines reconstructions; one depression each from the modern regional ELA (1890 m for north-facing glaciers) and the other from the modern local ELA (~ 1640 m). Comparison of the paleo-ELAs with the local ELA is useful if the paleo-glacier was subject to the same localized conditions that preserves the modern glaciers (probably increased accumulation due to wind drifting). This is most likely the case for the Little Ice

Age extent because the glacier was only slightly larger than it is now. The  $\Delta$ ELA from the local ELA for the south Swift Creek LIA moraines is 75 m. This is similar to the Little Ice Age  $\Delta$ ELA from north facing Winthrop Glacier on Mt. Rainier.

During the late Pleistocene/early Holocene extents of Swift Creek and Bagley Creek glaciers the  $\Delta$ ELA from the regional ELA is ~490 m. This  $\Delta$ ELA is very similar to the McNeely II moraines  $\Delta$ ELA of 400 to 500 m from the modern ELA on Mt. Rainier.

### *Paleoclimate Significance of Moraines*

By comparing the range of climate conditions (ablation season temperature and accumulation season precipitation) at ELAs of modern glaciers with the modern climate at a reconstructed ELA the range of possible climate change is quantified. Two cases of change are the endpoints for the range of change. These are (1) the maximum ablation season temperature depression with no change in accumulation season precipitation and (2) the maximum increase in accumulation season precipitation with no change in ablation season temperature. The maximum temperature depression (case 1) for the Swift Creek Moraines would be ~ 1.6 deg. C, and the maximum precipitation increase (case 2) would be 870 mm. For the Swift Creek Little Ice Age ELA a maximum temperature depression (case 1) of 0.85 deg. C or a maximum precipitation increase (case 2) of 440 mm would need to have occurred. Probably some combination of a decrease in temperature or increase in precipitation from modern conditions occurred because modern climate trends show increased precipitation with cooler periods and decreased precipitation with warmer periods. The decrease in temperature for the Little Ice Age seems plausible as Graumlich and Brubaker (1986) approximate a 1 deg. C decrease in mean annual temperature for that period.

### *Comparison with Other Studies*

The Swift Creek LIA moraines appear to correlate with numerous LIA moraines in the Cascade Range. However, many glaciers in the North Cascades reached their maximum

extent earlier in the LIA and have younger nested moraines upvalley from the maximum that appear to correlate with the Swift Creek moraines.

The Swift Creek and Picture Lake moraines do not appear correlate to the early Holocene moraines (7700-8400 <sup>14</sup>C years B. P.) of the Easton Shelf Glacier on the south flank of Mt. Baker (Thomas, 1997; Thomas, et al., 2000) or to small cirque moraines (~ 8500 <sup>14</sup>C years B. P.) nearby to the Easton Glacier (Easterbrook and Kovanen, 1999). The 2-sigma calibrated age ranges for Thomas' maximum, 9270-9535 cal. years, and the oldest minimum for the Swift Creek moraines, 10,760-11,180 cal. years, do not overlap. Therefore these appear to be two separate events. In addition the 2-sigma age range of 8500 ± 100 <sup>14</sup>C years B. P. is 9724 - 9149 cal. years and does not overlap with the moraines of this study. However, lateral moraines on the Easton shelf just below the Thomas et al. (2000) early Holocene moraines appear to be older and may correlate with the Swift Creek and Picture Lake moraines.

Given the uncertainty of the minimum ages to timing of deglaciation of Swift Creek and Bagley Creek and the large limiting age range (10,700 – 9600 <sup>14</sup>C years B.P.), two correlations from the Pacific Northwest are possible for the Swift Creek and Picture Lake moraines. These possibilities are (1) correlation with McNeely II moraines near Mt. Ranier, which is probably the most likely when also considering ΔELAs, or (2) correlation with the last stillstand of the Sumas Stade sometime after 10,250 <sup>14</sup>C years B.P. In this case, the Swift Creek and Picture Lake moraines could correlate with the very end of the Younger Dryas Chronozone after recession of the Nooksack alpine glacial system.

In conjunction, two possibilities exist for the glacial regime of the Swift Creek and Picture Lake moraines: (1) the moraines mark a short-lived readvance after a full or near disappearance of alpine ice in the study area, or (2) the moraines are recessional moraines deposited by brief stillstands of disappearing alpine ice in the study area. . A readvance is probably more likely if the moraines correlate with McNeely II. Recessional moraines are probably more likely if these moraines correlate with the youngest Sumas and end of the Nooksack alpine glacial system. However, the possibility exists in which the Swift Creek and Picture Lake moraines do not correlate with either McNeely II or Sumas. Future studies in the study area and the North Cascades may illuminate these uncertainties.

## References

- Ahrens, D. C., 1994, *Meteorology Today; An Introduction to Weather, Climate, and the Environment*, Fifth Edition, West Publishing Company, St. Paul, MN, 198 p.
- Armstrong, J. E., 1981, Post-Vashon Wisconsin glaciation, Fraser Lowland, British Columbia: *Geological Survey of Canada Bulletin*, vol. 322, p. 34.
- Armstrong, J. E., Crandell, D. R., Easterbrook, D. J., Noble, J.B., 1965, Late Pleistocene stratigraphy and chronology in southwestern British Columbia and northwestern Washington: *Geological Survey of Canada Bulletin*, vol. 76, p. 321-330.
- Bacon, C. R., 1983, Eruptive history of Mount Mazama and Crater Lake Caldera, Cascade Range, U.S.A.: *Journal of Volcanology and Geothermal Research*, vol. 18, p. 57-115.
- Beget, J. E., 1981, Early Holocene glacier advance in the North Cascade Range, Washington: *Geology*, vol. 9, p. 409-413.
- Beget, J. E., 1988, Comment on "Age of pre-Neoglacial cirque moraines in the central North American Cordillera", by P.T. Davis and G. Osborn: *Geographie physique et Quaternaire*, vol. 42, p. 331-336.
- Bender, M., and others., 1994, Climate correlations between Greenland and Antarctica during the past 100,000 years: *Nature*, vol. 372, p. 663-666.
- Bengston, K. B., 1956, Activity of the Coleman Glacier, Mt Baker, WA, USA, 1949-1955: *Journal of Glaciology*, vol. 2, no. 20, p. 708-713.
- Blaise, B., Clague, J. J., and R. W. Mathewes, 1990, Time of maximum late Wisconsin glaciation, west coast of Canada: *Quaternary Research*, vol. 34, p. 282-295.
- Brown, E.H., and others, 1987, Geologic map of the northwest Cascades, Washington: Geological Society of America Map and Chart Series, MC-61, 1:15840.
- Burbank, D. W., 1981, A chronology of late Holocene glacier fluctuations on Mount Rainier, Washington: *Arctic and Alpine Research*, vol. 13 no. 4, p. 369-386.
- Burke, R. M., 1972, Neoglaciation of Boulder Valley, Mt. Baker, WA. M.S. Thesis, Western Washington University, Bellingham, Washington 47 p.
- Burke, R. M., and Birkeland, P. W., 1983, Holocene glaciation in the mountain ranges of the western United States: *The Holocene; Late Quaternary environments of the United States*, Editor: Wright, H. E., Jr: vol.2, p.3-11.

Burrows, R. B., and Kovanen, D. J., In Progress, Chronology and significance of alpine cirque moraines near Mt. Baker, North Cascade Range, WA: journal undetermined.

Clague, J. J. and Mathewes, R. W., 1989, Early Holocene thermal maximum in western North America: New evidence from Castle Peak, British Columbia: *Geology*, vol. 17, p. 277-280.

Clague, J. J., Mathewes, R. W., Guilbault, J. P., Hutchinson, I., Ricketts, B. D., 1997, Pre-Younger Dryas resurgence of the southwestern margin of the Cordilleran ice sheet, British Columbia, Canada: *Boreas*, vol. 26, p. 261-277.

Clague, J. J., Mathewes, R. W., Guilbault, J. P., Hutchinson, I., Ricketts, B. D., 1998, 'Pre-Younger Dryas resurgence of the southwestern margin of the Cordilleran Ice Sheet, British Columbia, Canada': Reply to comments: *Boreas*, vol. 27, p. 229-230.

Clark, D. H., Clark, M. M., Gillespie, A. R., 1994, Debris-covered glaciers in the Sierra Nevada, California, and their implications for snowline reconstructions: *Quaternary Research*, vol.41, no.2, p.139-153.

Clark, D. H. and Gillespie, A.R., 1997, Timing and significance of late-glacial and Holocene cirque glaciation in the Sierra Nevada, California: *Quaternary International*, vols. 38/39, p. 21-38.

Coombs, H. A., 1939, Mount Baker, a Cascade volcano: *Geological Society of America Bulletin*, vol.50, no.10, p.1493-1509.

Cooper, W. S., 1958, Terminology of post-Valders time: *Geological Society of America Bulletin*, vol. 69, p. 941-945.

Crandell, D. R. and Miller, R. D., 1964, Post-Hypsithermal glacier advances at Mt. Ranier, Washington: U.S. Geological Survey Professional Paper 501-D, p. D110-D114.

Davis, P. T. and Davis, R. B., 1980, The interpretation of minimum-limiting radiocarbon dates for deglaciation of Mount Katahdin area, Maine, *Geology*, vol. 8, p. 396-400.

Davis, P. T. and Osborn G., 1987, Age of pre-Neoglacial cirque moraines in the central North America Cordillera: *Geographie physique et Quaternaire*, vol. 41, p. 365-375.

Davis, P. T., Upson, S. and Waterman, S. E., 1979, Lacustrine sediment variations as an indicator of late Holocene climatic fluctuations, Arapaho Cirque, Colorado Front Range: *Geological Society of America Abstracts with Programs*, vol. 11, p. 410.

Denton, G. H. and Porter, S. C., 1970, Neoglaciation: *Scientific American*, vol. 222, p. 100-110.

Deevy, E. S. and Flint, R. F., 1957, Postglacial hypsithermal interval: *Science*, vol. 125, p. 182-184.

Douglas, B. W., 1969, Subalpine plant communities of the western North Cascades, Washington: *Arctic and Alpine Research*, vol. 4, no. 2, p. 147-166.

Easterbrook, D. J., 1963, Late Pleistocene glacial events and relative sea-level changes in the northern Puget Lowland, Washington: *Geological Society of America Bulletin*, vol. 74, p. 1465-1483.

Easterbrook, D. J., 1975, Mt. Baker Eruptions: *Geology*, vol. 3, p. 679-682.

Easterbrook, D. J., 1986, Stratigraphy and chronology of Quaternary deposits of the Puget Lowland and Olympic Mountains of Washington and the Cascade Mountains of Washington and Oregon: *Quaternary Science Reviews*, vol. 5, p. 145-159.

Easterbrook, D. J., 1992, Advance and retreat of the Cordilleran Ice Sheets, USA: *Geographie et Quaternaire*, vol. 46, p. 51-68.

Easterbrook, D. J., and Burke, R. M., 1972, Glaciation of the northern Cascades, Washington: *Geological Society of America Abstracts with program*, vol. 4, p.152.

Easterbrook, D.J., and Kovanen, D. J., 1998, 'Pre-Younger Dryas resurgence of the southwestern margin of the Cordilleran Ice Sheet, British Columbia, Canada': *Comments: Boreas*, vol. 27, p. 225-228.

Easterbrook, D. J., and Kovanen, D. J., 1999, Early Holocene glaciation in the North Cascades near Mt. Baker, Washington: *Geological Society of America Abstracts with Program*, vol. 31, no. 7, p. A367.

Fuller, S. R., 1980, Neoglaciation of Avalanche Gorge and the Middle Fork Nooksack River valley, Mt. Baker, WA: M.S. Thesis, Western Washington University, Bellingham, Washington, 68 p.

Furbish D. J., and Andrews, J. T., 1984, The use of hypsometry to indicate long-term stability and response of valley glaciers to changes in mass transfer: *Journal of Glaciology*, vol. 30, no. 105, p. 199-211.

Gosse J. C., Evenson, E. B., Klein, J., Lawn, B., Middleton, R., 1995, Precise cosmogenic <sup>10</sup>Be measurements in western North America: Support for a global Younger Dryas cooling event: *Geology*, vol. 23, p. 877-880.

- Graf, W. L., 1976, Cirques as glacier locations: *Arctic and Alpine Research*, vol. 8, no. 1, p.79-90.
- Graumlich, L. J., and Brubaker, L. B., 1986, Reconstruction of annual temperature (1590-1979) for Longmire, Washington, derived from tree rings: *Quaternary Research*, vol. 25, p. 223-234.
- Hallet, D. J., Hills, L. V., Clague, J. J., 1997, New accelerator mass spectrometry radiocarbon dates for the Mazama tephra layer from Kootenay National Park, British Columbia, Canada: *Canadian Journal of Earth Science*, vol. 34, p. 1202-1209.
- Harper, J. T., 1993, Glacier terminus fluctuations on Mt. Baker, WA, USA, 1940-1990, and climatic fluctuations: *Arctic and Alpine Research*, vol. 25, p. 332-340.
- Harrison, A. E., 1956, Fluctuations of the Nisqually Glacier, Mount Rainier, Washington, since 1750: *Journal of Glaciology*, vol. 2, p. 675-683.
- Heikkinen, O., 1984, Dendrochronological evidence of variations of Coleman Glacier, Mount Baker, WA, USA: *Arctic and Alpine Research*, vol. 16, p. 53-64.
- Heine, J. T., 1998, Extent, timing, and climatic implications of glacier advances, Mount Rainier, Washington, USA, at the Pleistocene/Holocene transition: *Quaternary Science Reviews*, vol. 17, p. 1139-1148.
- Heller, P. L., 1980, Multiple ice flow directions during the Fraser Glaciation in the lower Skagit River drainage, Northern Cascade Range, Washington: *Arctic and Alpine Research*, vol. 12, no. 3, p. 299-308.
- Hyde, J. H., and Crandell, D. R., 1978, Post-glacial volcanic deposits at Mount Baker, Washington, and potential hazards from future eruptions: U.S. Geological Survey Professional paper 1022-C, 18 p.
- Johnsen, S. J., 1997, The delta-<sup>18</sup>O record along the Greenland Ice Core Project deep ice core and the problem of possible Eemian climatic instability: *Journal of Geophysical Research*, vol. C12, p. 26,397-26,410.
- Karlen, W., 1976, Lacustrine sediments and tree-line variations as indicators of climatic fluctuations in Lapland, northern Sweden: *Geografiska Annaler*, vol. 58A, p. 1-34.
- Kotlyakov, V. M., and Krenke, A. N., 1982, Investigations of the hydrological conditions of alpine regions by glaciological methods: International Association of Hydrological Sciences Publication, vol. 138, p. 31-42.

- Kovanen, D.J., 1996, Extensive late-Pleistocene alpine glaciation in the Nooksack River Valley, North Cascades, Washington: M.S. Thesis, Western Washington University, Bellingham, Washington, 186 p.
- Kovanen, D. J., in review, Spatial and Morphostratigraphic Evidence for Multiple Phases of the Sumas Stade, in the Fraser Lowland of Western North America: Quaternary Research.
- Kovanen, D. J. and Easterbrook, D. J., 1996, New evidence for a late-glacial, post-Cordilleran ice sheet, readvance of alpine glaciers in the North Cascades, Washington: Geological Society of America Cordilleran Section Meeting, Portland, Abstracts with Program, p. 83.
- Kovanen, D. J. and Easterbrook, D. J., 2001, Late Pleistocene alpine glaciation of the Nooksack Valley, North Cascades, Washington: Geological Society of America, Bulletin.
- Kovanen, D. J. and Easterbrook, D. J., in review-a, Chronology of the Sumas Stade in the Fraser Lowland of Western North America: Quaternary Research
- Kovanen, D. J. and Easterbrook, D. J., in review-b, Quaternary tephtras and lahars at Mount Baker, Washington: Geological Society of America, Bulletin.
- Krimmel, R. M., 1997, Water, ice, and meteorological measurements at South Cascade Glacier, Washington, 1996 balance year: USGS Water-Resources Investigations Report 97-4143, 40 p.
- Lawrence, D. B., 1950, Estimating Dates of recent glacial advances and recession rates with dendrochronology: American Geophysical Union Transactions, vol. 32, 243-248.
- Leonard, E. M., 1974, Price Lake moraines: Neoglacial chronology and lichenometry study: M.A. thesis, Simon Fraser University, Vancouver, BC, 102 p.
- Leonard, E. M., 1986a, Varve studies at Hector Lake, Alberta, Canada and the relationship between glacial activity and sedimentation: Quaternary Research, vol. 25, p. 199-214.
- Leonard, E.M., 1986b, Use of lacustrine sedimentary sequences as indicators of Holocene glacial history, Banff National Park, Alberta, Canada: Quaternary Research, vol. 26, 218-231.
- Leonard, E. M., 1989, Climatic change in the Colorado Rocky Mountains: estimates based on modern climate at late Pleistocene equilibrium lines: Arctic and Alpine Research, vol. 21, no. 3, p. 245-255.
- Livingstone, D. A., 1955, A lightweight piston sampler for lake deposits: Ecology vol. 36, 139-141.

Long, W. A., 1953, Recession of Easton and Deming glaciers, Mount Baker, Washington: *Scientific Monthly*, vol. 64, 241-247.

Luckman, B. H., 1998, Holocene glacier history of the North American Cordillera: AMQUA Program and Abstracts of the 15<sup>th</sup> Biennial Meeting, vol. 15, p. 34-36.

Madsen, D. B. and Currey, D. R., 1979, Late Quaternary glacial and vegetational changes, Little Cottonwood Canyon area, Wasatch Mountains, Utah: *Quaternary Research*, vol. 12, p. 254-270.

Mathes, F. E., 1939, Report of Committee on Glaciers, 1935-1936: *Transactions, American Geophysical Union*, p. 283-294.

Mathewes, R. W., Heusser, L. E., and R. T. Patterson, 1993, Evidence for a Younger Dryas-like cooling event on the British Columbia coast: *Geology*, vol. 21, p. 101-104.

McCabe, G.J. and Fountain, A. G., 1995, Relations between atmospheric circulation and mass balance of South Cascade Glacier, Washington, U.S.A.: *Arctic and Alpine Research*, vol. 27, no. 3, p. 226-233.

Meese, D. A., and others, 1994, The accumulation record from the GISP2 Core as an indicator of climate change throughout the Holocene: *Science*, vol. 266, p. 1680-1682.

Meier, M. F., and Post, A. S., 1962, Recent variations in mass net budgets in western North America: IUGG/IASH Committee on Snow and Ice, General Assembly, Obergurl, International Association of Science and Hydrology, vol. 58, p. 63-77.

Meierding, T. C., 1982, Late Pleistocene glacial equilibrium-line altitudes in the Colorado Front Range: A comparison of methods: *Quaternary Research*, vol. 18, p. 289-310.

Menounos, B. and Reasoner, M. A., 1997, Evidence for cirque glaciation in the Colorado Front Range during the Younger Dryas Chronozone: *Quaternary Research*, vol. 18, p. 38-47.

Miller, C. D., 1969, Chronology of Neoglacial moraines in the Dome Peak area, North Cascade Range, Washington: *Arctic and Alpine Research*, vol. 1, p. 49-66.

Mullineaux, D. R., Waldron, H. H., and Meyer, R., 1965, Stratigraphy and chronology of late interglacial and early Vashon time in Seattle area, Washington: *U.S. Geological Survey Bulletin* 1194-O, 10 p.

Nichols, H., 1967, The disturbance of arctic lake sediments by "bottom ice": A hazard for palynology, *Arctic*, vol. 20, p.213-214.

- Oldfield, F., 1977, Lakes and their drainage basins as units of sediment based ecological study: *Progress in Physical Geography*, vol. 1, p. 460-504.
- Ohmura, A., Kasser, P., and Funk, M., 1992, Climate at the equilibrium line of glaciers: *Journal of Glaciology*, vol. 38, no. 130, p. 397-411.
- Osborn, G., Luckman, B. H., 1988, Holocene glacier fluctuations in the Canadian Cordillera (Alberta and British Columbia): *Quaternary Science Reviews*, vol. 7, p. 115-128.
- Porter, S. C., 1975, Equilibrium-line altitudes of late Quaternary glaciers in the southern Alps, New Zealand: *Quaternary Research*, vol. 5, p. 27-47.
- Porter, S. C., 1976, Pleistocene glaciation in the southern part of the North Cascade Range, Washington: *Geological Society of America Bulletin*, vol. 87, p. 61-75.
- Porter S.C., 1977, Present and past glaciation threshold in the Cascade Range, Washington, U.S.A.: topographic and climatic controls, and paleoclimatic implications: *Journal of Glaciology*, vol. 18, no. 78, p. 101-116.
- Porter, S. C. and Burbank, D. W., 1979, Lichenometric studies of Holocene moraines at Mount Rainier, Washington: *Rhizocarpon geographicum* growth curves and preliminary results: *Geological Society of America Abstracts with Programs*, vol. 11, no.4, p. 122.
- Porter, S. C. and Denton, G. H., 1967, Chronology of Neoglaciation in the North American Cordillera: *American Journal of Science*, vol. 265, p. 177-210.
- Porter, S. C., and Swanson, T. W., 1998, Radiocarbon age constraints on rates of advance and retreat of the Puget Lobe of the Cordilleran Ice Sheet, during the last glaciation: *Quaternary Research*, vol. 50, p. 205-213.
- Post, A., Richardson, D., Tangborn, W. V., Rosselot, F. L., 1971, Inventory of glaciers in the North Cascades, Washington: U. S. Geological Survey Professional Paper P 0705-A, 26 p.
- Reasoner, M. A., 1993, Equipment and procedure improvements for a lightweight, inexpensive, percussion core sampling system: *Journal of Paleolimnology*, vol. 8, p. 273-281.
- Reasoner, M. A., Osborn, G., Rutter, N. W., 1994, Age of the Crowfoot advance in the Canadian Rocky Mountains: A glacial event coeval with the Younger Dryas oscillation: *Geology*, vol. 22, p. 439-442.

- Riedel, J. L., 1987, Chronology of late Holocene glacier recessions in the Cascade Range and deposition of a recent esker in a cirque basin, North Cascade Range, Washington: M. S. Thesis, University of Wisconsin-Madison, 91 p.
- Rowley, J. R., and Dahl, A. O., 1956, Modifications in design and use of the Livingstone piston sampler: *Ecology*, vol. 37, p. 849-851.
- Rutter, N. W., Weaver, A. J., Rokosh, D., Fanning, A. F., Wright, D. G., 2000, Data model comparison of the Younger Dryas event: *Canadian Journal of Earth Science* vol. 37, p. 811-830.
- Ryder, J. M., and Thomson, B., 1985, Neoglaciation in the southern Coast Mountains of British Columbia: chronology prior to the late Neoglacial maximum: *Canadian Journal of Earth Science*, vol. 23, p. 273-287.
- Saunders, I. R., Clague, J. J., Roberts, M. C., 1987, Deglaciation of Chilliwack River valley, British Columbia. *Canadian Journal of Earth Science*, vol. 24, p. 915-923.
- Sigafoos, R. S. and Hendricks, E. L., 1961, Botanical evidence of the modern history of Nisqually Glacier, Washington: U.S. Geological Survey Professional Paper, 387-A, 20 p.
- Sigafoos, R. S. and Hendricks, E. L., 1972, Recent activity of glaciers of Mount Rainier, Washington: U.S. Geological Survey Professional Paper, 387-B, 24 p.
- Souch, C., 1994, A methodology to interpret downvalley lake sediments as records of neoglacial activity: Coast Mountains, British Columbia, Canada: *Geografiska Annaler*, vol. 76A, p. 169-185.
- Stavert, L. W., 1971, A geochemical reconnaissance investigation of Mount Baker andesites: M.S. Thesis, Western Washington University, Bellingham, Washington, 60 p.
- Stuiver, M., and Reimer, P. J., 1993, Extended 14C database and revised CALIB radiocarbon calibration program: *Radiocarbon*, vol. 35, p. 215-230.
- Stuiver, M., Reimer, P. J., Bard, E., Beck, J. W., Burr, G. S., Hughen, K. A., Kromer, B., McCormac, F. G., V. D. Plicht, J., and Spurk, M., 1998, INTCAL98 Radiocarbon age calibration 24,000 - 0 cal BP: *Radiocarbon*, vol. 40, p. 1041-1083.
- Surgenor, J. W., 1978, Lacustrine sediments as indicators of fluctuations of Riukojietha Glacier, Lappland, Sweden: unpubl. M. A. thesis, University of Maine, 54 p.
- Tabor, R. and Haugerud, R., 1999, Geology of the North Cascades; A mountain mosaic: *The Mountaineers*, Seattle, Washington, 143 p.

Tangborn, W., 1999, A mass balance model that uses low-altitude meteorological observations and the area-altitude distribution of a glacier: *Geografiska Annaler*, vol. 81A, p. 753-765.

Thomas, P. A., 1997, Late Quaternary glaciation and volcanism on the south flank of Mount Baker, WA: M.S. Thesis, Western Washington University, Bellingham, Washington, 98 p.

Thomas, P. A., Easterbrook, D. J., and Clark, P. U., 2000, Early Holocene glaciation on Mount Baker, Washington State, USA: *Quaternary Science Reviews*, vol. 19, p. 1043-1046.

Vallentyne, J. R., 1955, A modification of the Livingstone piston sampler for lake deposits: *Ecology*, vol. 36, p. 139-141.

Veatch, F. M., 1969, Analysis of a 24-year photographic record of Nisqually Glacier, Mount Rainier National Park, Washington. U. S. Geological Survey Professional Paper 631, 52 p.

Verosub, K. L., Mehringer, P. J., and P. Waterstraat, 1986, Holocene secular variation in western North America: Paleomagnetic record from Fish Lake, Harney County, Oregon: *Journal of Geophysical Research*, vol. 91, no. B3, p. 3609-3623.

Waite, R. B. Jr., 1972, Geomorphology and glacial geology of the Methow drainage basin, eastern North Cascade Range, Washington: Doctoral dissertation, University of Washington, Seattle, Washington, 154 p.

Waite, R. B., J. C. Yount, and P. T. Davis, 1982, Regional Significance of an early Holocene moraine in Enchantment Lakes Basin, North Cascade Range, Washington: *Quaternary Research*, vol. 17, p. 191-210.

Walker, M. J. C., and others, 1999, Isotopic 'events' in the GRIP ice core: a stratotype for the late Pleistocene: *Quaternary Science Reviews*, vol. 18, p. 1143-1150.

White, J. W. C., and others, 1997, The climate signal in the stable isotopes of snow from Summit, Greenland: Results of comparisons with modern climate observations: *Journal of Geophysical Research*, vol. C12, p. 26,425-26,439.

Whitlock, C. W., 1992, Vegetational and climatic history of the Pacific Northwest during the last 20,000 years: Implications for understanding present-day biodiversity: *Northwest Environmental Journal*, vol. 8, p. 5-28.

Wright, H. E., Mann, D. H., Glaser, P. H., 1984, Piston corers for peat and lake sediments: *Ecology*, vol. 65, p. 657-659.